ABSTRACT

Title of Thesis: MIXED COMPLEMENTARITY MODELING IN THE GLOBAL NATURAL GAS MARKET

Justin C. Huemme
Department of Mechanical Engineering
University of Maryland, College Park, MD

Thesis directed by: Professor Steven A. Gabriel
Department of Mechanical Engineering
University of Maryland, College Park, MD

This thesis describes the development and capabilities of the 2020 World Gas Model (WGM), an updated mixed complementarity problem model of the global natural gas market derived from the 2014 World Gas Model [18]. The significance of this research applies to industry professionals and academics alike as the developed processes and analysis further expands the capabilities and flexibility of equilibrium modeling. Through an understanding of the current state of the natural gas market, the WGM determines the economic behavior of various market players with the deployment of Karush-Kuhn-Tucker (KKT) optimality conditions in conjunction with market-clearing conditions. The capabilities of the World Gas Model are highlighted through two case studies that are of varying international importance. The case studies are specifically selected from different issues that face the natural gas market such as a United States and China trade war and U.S. Coast Guard liquefied natural gas (LNG) inspection workforce forecasting. The goal of

the United States and China Trade War case study is to analyze the potential long- and short-term affects of a prolonged trade war under several different possible scenarios. Results from the study indicate that while increased tariffs on LNG trade from the U.S. to China greatly reduce the amount of trade volume between the two countries, the overall economic effect is negligible and of greater concern to other affected nations. Another found result, is that if the potential geopolitical consequence of China increasing their domestic production of natural gas in an effort to reduce reliance on imports, this will cause a global natural gas market effect. The U.S. Coast Guard LNG inspection workforce forecasting case study utilizes the WGM to provide the future workforce demand for U.S. regulatory personnel and the associated costs based on the growth of the U.S. LNG industry. The results from the study indicate that in order to avoid future costs and restriction on the U.S. LNG industry, the USCG must increase its LNG inspection workforce by a factor of .3 to 1 from current forecasts.

MIXED COMPLEMENTARITY MODELING IN THE GLOBAL NATURAL GASMARKET

by

Justin C. Huemme

Thesis submitted to the Faculty of the Graduate School of the
University of Maryland, College Park in partial fulfillment
of the requirements for the degree of
Master of Science
2020

Advisory Committee:
Professor Steven A. Gabriel, Chair/Advisor
Professor Shapour Azarm
Associate Professor Qingbin Cui

Acknowledgments

This thesis would not have been made possible without the contributions, encouragement and insight from professors and fellow students during my time at the University of Maryland.

To my advisor, Dr. Steven Gabriel, thank you for your selfless time and effort given towards the development of myself both academically and professionally throughout the course of this research.

To the thesis committee members, Dr. Shapour Azarm and Dr. Qingbin Cui, thank you for your invaluable advice and willingness to provide necessary feedback and guidance towards the further development of this document.

To my colleagues, Pattanun Chanpiwat and Tony Shu, thank you for your friendship and support throughout graduate school and the research process.

Lastly, a special thank you to my wife Sierra, for her undying love and support throughout graduate school and beyond.

Table of Contents

List of Tables

List of Figures

List of Abbreviations[1]

ABM	Agent-based Model
BCM	Billion Cubic Meters
BIWGTM	Baker Institute World Gas Trade Model
CFR	Code of Federal Regulations
CM	Cubic Meters
EIA	United States Energy Information Agency
EWI	Institute of Energy Economics at the University of Cologne
FERC	United States Federal Energy Regulatory Commission
GFIT	Global Fossil Infrastructure Tracker
IEA	International Energy Agency
INGM	International Natural Gas Model
KKT	Karush-Kuhn-Tucker
LGCNCOE	Liquefied Gas Carrier National Center of Expertise
LNG	Liquefied Natural Gas
LP	Linear Program
MCM	Million Cubic Meters
MCP	Mixed Complementarity Problem
PCA	Panama Canal Authority
TSO	Transmission System Operator
USCG	United States Coast Guard
USCG	United States Geological Survey
WGM	World Gas Model

[1] Mathematical nomenclature is found in Appendix C and Appendix D.

Chapter 1: Introduction and Motivation

Natural gas has become a globalized market in which distribution extends beyond country lines and the capacities of existing pipelines. By understanding the natural gas processes and current market dynamics, coupled with equilibrium modeling, the interactions and relationships amongst leading players can be analyzed in order to draw conclusions about the future implications of various factors and policy in an ever-growing dynamic global market.

1.1 Significance of The Global Natural Gas Market

In the past two decades the natural gas market has undergone several technological advances such as horizontal drilling and fracking that have reshaped the world's international natural gas market. The global market dynamics have shifted significantly as a result of these advancements as countries re-position themselves through their ability to produce, consume and distribute gas on both a domestic and global scale. For example, since 2000, the United States of America has seen a 62.5% increase in the total amount of domestic natural gas marketed production from 572 BCM in 2000 to 930 BCM in 2018, visually represented in Fig. 1.1 [61]. Current predictions by the International Energy Agency in their 2018 World Energy

Outlook suggest that natural gas will overtake coal by 2030 to become the world's second largest energy source after oil.

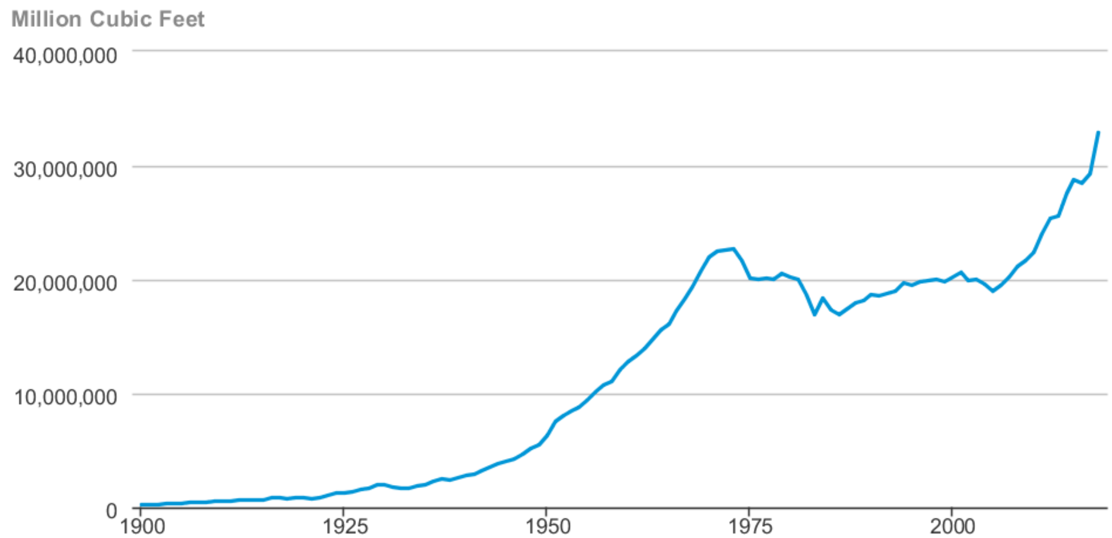

Figure 1.1: U.S. Natural Gas Marketed Production [61]

This drastic shift in natural gas production levels has enabled the United States to change position from being one of the largest importers of gas to becoming energy self-sufficient over a 10 year period, as well as a world leader in natural gas exports and reserve capacity. As seen, in Fig. 1.2, the United States is one of many countries who have, within the past decade, redefined their role in the global market. Indicated by the different colors in Fig. 1.2, an individual country such as the United States can be seen to change market behavior through a rapid transition from 2007 to 2017 by becoming one of the world's largest net-exporters of natural gas. Similar transitions are observed in areas such as central Asia and China.

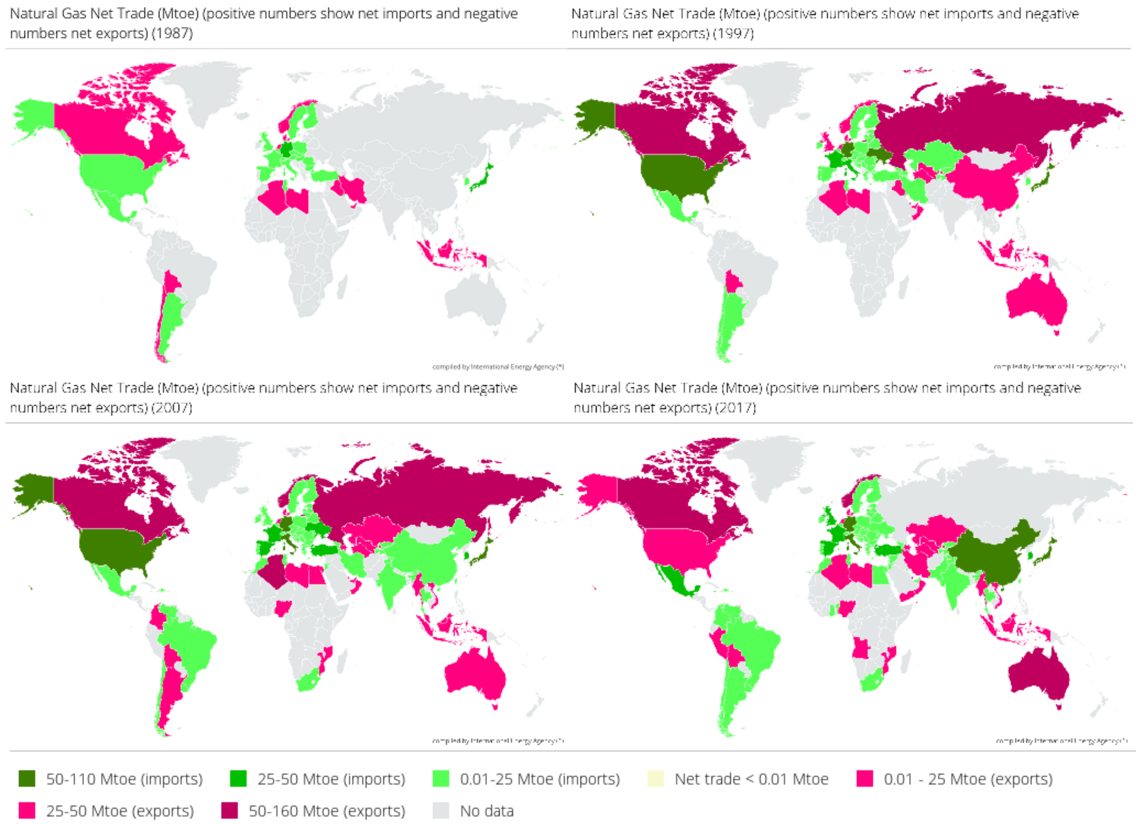

Figure 1.2: Global Natural Gas Net Trade - (a) Top Left: Natural Gas Net Trade 1987 (b) Top Right: Natural Gas Net Trade 1997 (c) Bottom Left: Natural Gas Net Trade 2007 (d) Bottom Right: Natural Gas Net Trade 2017 [32]

1.1.1 Shale Gas Revolution

One of the advancements that has brought upon the reshaping of the global gas market has been the deployment of horizontal drilling and fracking. These techniques have enabled producers to extract massive quantities of natural gas from the once inaccessible underground shale formations. Prior to the shale gas revolution it was thought that this process was uneconomic. However, since being proved otherwise by hydraulic drilling and fracking, over the past two decades the effective extraction of shale gas has shifted the gas market. For example, in Fig. 1.3, Southwestern Energy, a natural gas exploration and production company incorporated in Delaware and headquartered in Spring, Texas, was able to significantly reduce the number of days to drill, well-finding and development costs while rapidly increasing production from 2007 to 2010 through the use of hydraulic fracking.

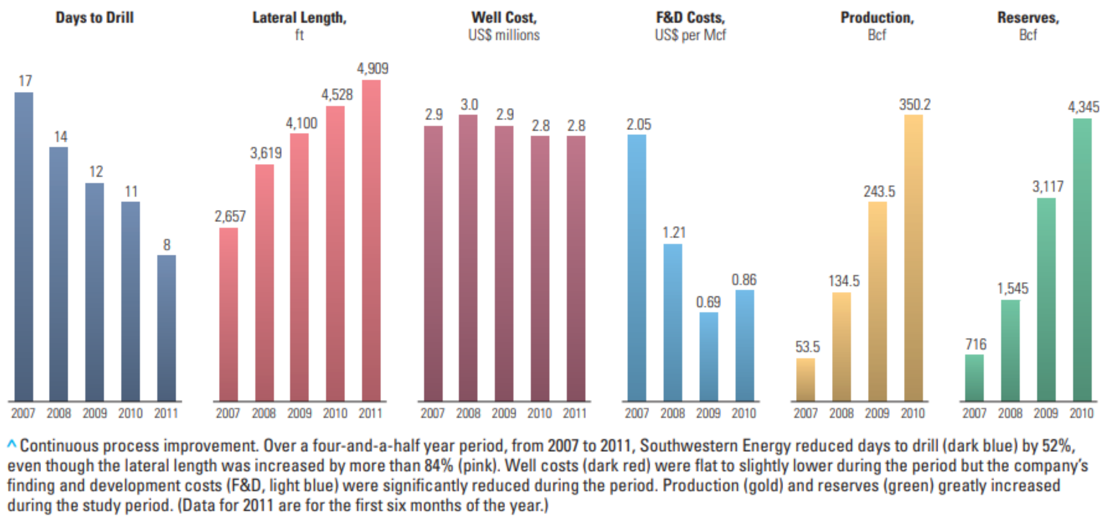

Figure 1.3: Southwestern Energy Production Cost [1]

Countries around the world have evaluated their shale gas resources and have sought to rapidly meet their domestic energy demand through the implementation of shale gas fracking. Most notably, China sits on one of the worlds largest shale gas reserves, estimated in 2015, by China's Ministry of Land Resources, as 21.8 trillion cubic meters[1] worth of technically recoverable natural gas [8], and seeks to meet their ever-energy demand through increased domestic production. In September

[1] 770 MMCF

2018, the Chinese State Council set an aggressive plan to produce 200 billion cubic meters (BCM)/year of domestic natural gas by 2020, which, as of 2018, China produced 155 BCM of domestic natural gas and accounted for 45% of China's gas supply [61][8].

1.1.2 Liquefied Natural Gas

The transportation of liquefied natural gas has enabled countries with the requisite infrastructure to reach markets that would otherwise be uneconomical or infeasible to reach via pipeline. When considering the demand for natural gas, many countries, most notably those in Asia and Europe, have been able to meet their growing energy consumption through the import of LNG and the globalization of this abundant resource. In the International Energy Agency's 2019 World Energy Outlook, Stated Policies Scenario, Liquefied Natural Gas is projected to overtake pipelines as the main way of trading gas between countries "by the late 2020s" [33]. In Fig. 1.4 the major trade flows as analyzed by BP's Statistical Review [48], can be seen and the elevated significance of LNG's ability to reach foreign markets can be visually interpreted when considering what the trade flows would look like in the absence of LNG. Where blue trade arcs represent LNG flow and red arcs represent pipeline trade flow, it can be seen that LNG enables a globalized natural gas market; however, LNG trade retains a degree of localization where significant flows are found between countries of relative close proximity, i.e., Australia and the Philippine's LNG export destinations.

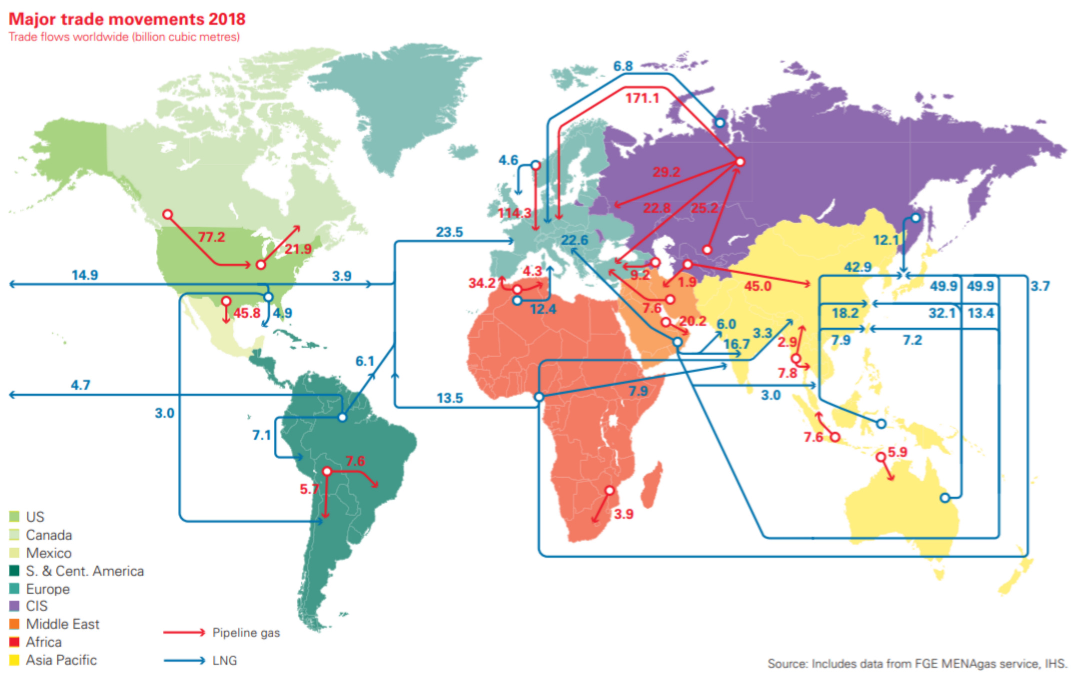

Figure 1.4: Major Trade Flows [33]

Wood Mackenzie's Chairman and Chief Analyst Simon Flowers states that "The LNG market will more than double in size to over 1000 BCM by 2040, a growth rate eclipsed only by renewables. A niche market not long ago, shipped LNG volumes will exceed global pipeline exports within six years."[14] However, the increased volume of global LNG flow will also increase diversity and competition as different countries compete for markets of high demand and utilizing their geographical advantage to that extent. In concurrence with Wood Mackenzie, the IEA forecasts similar LNG growth by 2040;however, the heightened geographical competition between markets can be seen in results from IEA's 2018 World Energy Outlook New Policies Scenario Fig 1.5 [33]. In Fig. 1.5 it can be seen that LNG trade (green) is forecasted, by the IEA, to grow at a rate much greater than pipeline trade(purple) from 2017 to 2040. The growth in LNG is seen to be mostly attributed to Asian natural gas demand where countries from around the world seek to meet the growing demand.

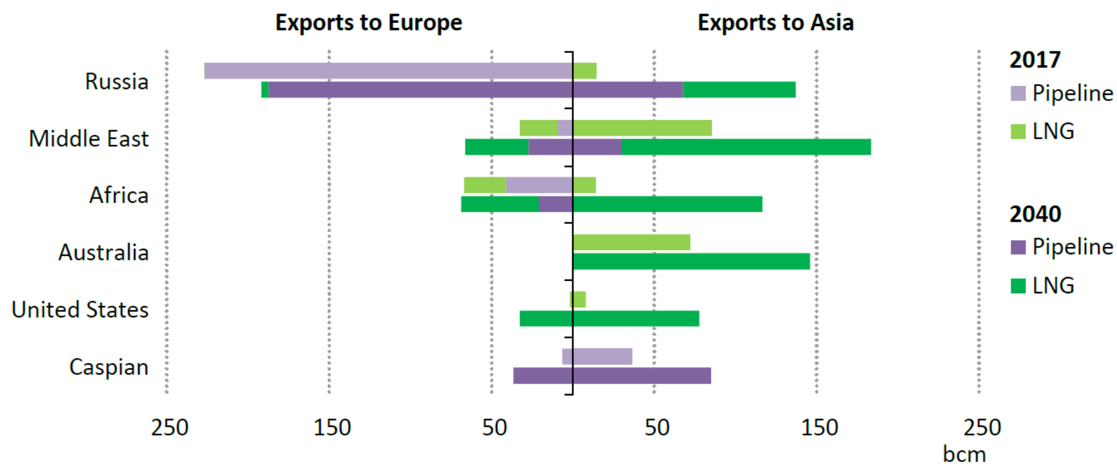

Figure 1.5: Selected LNG and Pipeline Gas Exports to Europe and Asia [33]

Geographical significance will prove to be a key factor for countries, such as the United States, looking to profit from their shale gas resources and will become a vital component when determining the validity of investment decisions with regard to increasing LNG infrastructure. LNG export companies will need the capability to accurately forecast future developments in order to better secure long term contracts for risk management in a ever increasingly competitive industry [33].

1.2 Focus & Outline of this Research

The goal of the research in this thesis is to develop a model that is ready, relevant, and capable to determine the market behavior of the global natural gas market to include the production, consumption, wholesale prices, storage capacities and international trade flows. An updated World Gas Model (WGM) derived from the 2014 WGM [44][12], utilizing the principles of mixed complementarity problems is presented in order to allow all players to make decisions simultaneously while working in regards to optimizing their individual objective function. The significance of this research is to utilize the developed model to analyze the potential market behavior that is likely to occur as a result of major development in the global natural gas market.

This thesis will utilize additional constraints, variables and costs, outlined in Chapter 2, to model the effects of an international dispute/event as well as a domestic workforce issue that can be solved through the appropriate modeling of the global market. The great flexibility of the model presented can be seen through the analysis in Chapter 3 where both the international and domestic issues are analyzed for better decision making from all players in the world gas model. Lastly in Chapter 4, the results and contributions made by this thesis as well as the potential for future research regarding mixed complementarity modeling and the World Gas Model is discussed.

1.3 Selected Literature Review

The purpose of this section is to provide a general overview of a selected group of alternatively developed models versus the 2020 World Gas Model in an effort to display the differences between the thesis' derived model and other models found in the field.

1.3.1 University of Maryland World Gas Model - 2014

The World Gas Model (WGM) is a multi-period numerical equilibrium model formulated as a mixed complementarity problem (MCP) developed at the University of Maryland with cooperation from The German Institute for Economic Research Berlin. The model was initially developed in 2010 based on other modeling efforts published in [19][20] that established the uniqueness for mixed complementarity gas models, exemplified by analysis of the North American gas market. The WGM deploys the use of endogenous decision-making for investments in pipeline, LNG trade, and storage capacities while considering the growth in demand and production expansions. The WGM also provides the capability to model an imperfectly competitive market through the use of Nash-Cournot market power. At the time of its initial model formulation in 2010, the WGM included more than 80 countries that represented over 98% of the global natural gas market production and consumption in 2005 [12] based on BP's Statistical Review of World Energy 2008 [53]. In accordance with game theory, the large-scale MCP model includes agents that display the economic behavior of the various players found in a gas market all of whom have objective functions that seek to maximize their net discounted profit. The greatest advantages of the WGM at the time of development was its level of detail for market agents, transportation options (pipeline & LNG), and regional coverage when compared to previous models at the time of publication [38][30][11]. In 2014, the WGM was updated and further developed for analysis of the Panama Canal expansion and its effects on the LNG industry [44]. In addition to updating the model's base year and reference data set, a canal operator player was developed and introduced to the WGM 2014 which included additional parameters and variables as well as KKT and market-clearing conditions [44]. This significantly increased the scope of the WGM from 2010 to 2014 and provided a modern and more accurate representation of the global gas market at that time.

1.3.2 U.S. Energy Information Agency International Natural Gas Model

The U.S. Energy Information Agency developed the International Natural Gas Model (INGM) in 2011 for the purpose of providing a reasonably detailed outlook for natural gas production, consumption, and international trade to include LNG and regional prices. Estimates for production included the production source (conventional or unconventional) and the estimates for consumption included data by demand sector. The INGM is a Linear Programming (LP) formulation that assumes a naturally competitive market with the objective function that minimizes the negative of the discounted net cash flows [65]. The model included 61 regions, 3 seasons, 7 demand sectors, 5 different natural gas supply types, demand & supply curves, as well as endogenous capacity expansion decisions. The supply and demand curves are linear and unit based transportation costs are used all of which allows for the model to remain linear. Contractual flows for both pipeline and LNG are not taken into account in the model under the premise that long term trends in the market will be subject to the conditions where gas will flow to the areas of high demand value [65].

1.3.3 The Baker Institute World Gas Trade Model

The Baker Institute World Gas Trade Model (BIWGTM) is a dynamic spatial equilibrium model and was developed by researchers at Rice University in Houston, Texas utilizing the licensed MarketBuilder software available from Deloitte [42] [27]. The BIWGTM and Deloitte's MarketBuilder software is an agent-based formulation which uses interacting autonomous agents to model individual economic behaviors [40]. Agent-based models (ABM) use microeconomics to model the autonomous agents desire to maximize profits subject to constraints [45]. This allows for each agent to behave in their own self-interest without regard for the natural gas market as a whole. This is similar to the MCP approach as individual players, like agents, are seeking to maximize their profit and minimize their total cost. The model calculates a dynamic spatial equilibrium that is not necessarily economically efficient but ensures that the supply and demand is balanced for each region for every time period. This eliminates all possibility of arbitrage. The model seeks to maximize the net present value of new supply and transportation investments while taking present and future prices into account. The model solves for the regional natural gas prices, gas transportation capacity flows and investments, growth in gas reserves, and regional production and demand [28][27]. The BIWGTM uses the United States Geological Survey (USGS) assessments for estimating supply-demand curves for the over 140 global regions that are included in the model. The model has more than 140 supply regions, each with different supply hubs in a sub-region. One of the limitations of the model is its use of USGS assessments in North America as a basis for the representation for other global markets which introduces a higher level of uncertainty, given that in reality no region behaves exactly in the same way with regards to energy production and demand [28].

1.3.4 University of Cologne (EWI) Global Gas Market Model

The COLUMBUS global gas market model was developed by The Institute for Energy Economics at the University of Cologne (EWI) in Germany as a MCP model. The model seeks to optimize the future development of production, transportation, and storage capacities while also optimizing the global gas pipeline and LNG flows around the world. COLUMBUS uses a vertex/edge approach by representing the vertices as the production and demand regions in the form of sources and sinks respectively. The edges are represented as the transportation arcs that come in the form of pipelines and LNG transportation routes. The model seeks out the optimization of future profit and development for the various players represented in the network. Players are identified as producers, traders, regasifiers, liquefiers, transmission system operators, and storage operators. In an effort to reduce model complexity, the researchers at EWI, did not model the LNG transportation network with a point-to-point but with a hub-and-spoke approach which created a network of virtual LNG hubs that reduced the number of variables by 60% [29]. The representation of the production and consumption of natural gas was done through the use of an inelastic demand and piece-wise-linear supply function. A limitation on the model is its assumption for a perfectly competitive global market which inhibits a real-world representation of actual occurring market power [29] [68].

1.3.5 Summary of Literature Review

Natural Gas Model Review					
Model Name	WGM - 2014	INGM	BIWGTM	COLUMBUS	WGM - 2020
Developer	UMD	EIA	Rice U.	EWI, Cologne	UMD
Formulation	MCP	LP	Agent-based	MCP	MCP
Regions	>80	61	>140	>110	>160
Competition	Imperfect	Perfect	Imperfect	Perfect	Imperfect
Obj. Funct.	Disc. Profit Max.	-Disc. Profit Min.	Profit Max. and Cost Min.	Profit Max. or Cost Min.	Disc. Profit Max.

Table 1.1: Review of Selected Natural Gas Models

The 2020 WGM, as seen in Table 1.1, is one of the most inclusive and representative models of the global natural gas market. Through its use of eight different players each with its own objective function, a vast representation of all international pipelines, complete network of real-world LNG arcs, and the most current reference data points available, the WGM is able to represent 98% of the global gas market at the time of the model's base year, 2017, making it one of the most up-to-date and comprehensive global gas models compared to those previously discussed. Most notably, the 2020 WGM differentiates its-self from the rest of the field through the use of imperfect competition modeling within an MCP formulation, providing the capability for a more realistic representation of the gas market. The processes in which the 2020 WGM was developed, as outlined in Chapter 2, further demonstrate how thorough and extensive the 2020 WGM is in relation to other model formulations and previous iterations of the WGM.

Chapter 2: World Gas Model 2020 Development

This chapter details the processes in which the WGM 2020 was developed and how it was expanded upon the previous iterations of the WGM [44][12][19]. First, the principles of mixed complementarity problems and their relation to the WGM is presented. Subsequently, the development of WGM players and data collection is discussed.

2.1 Mixed Complementarity Problems

Market equilibrium models using the mixed complementarity problem (MCP)[18] have been useful for both perfect and imperfect competition or mixtures thereof. For energy market models, typically consist of the Karush-Kuhn-Tucker (KKT) conditions to convex player optimization models combined with market-clearing conditions [3][12].

Given a function $F : \mathbb{R}^n \rightarrow \mathbb{R}^n$ pure complementarity problem is to find an $x \in \mathbb{R}^n$ such that for all i:

1. $F_i(x) \geq 0$

2. $x_i \geq 0$

3. $x_i \cdot F_i(x) = 0$

The fundamental mixed form of a complementarity problem (MCP) is similar to the pure complementarity problem; however, it permits equations $F_i(x) = 0$ with corresponding free variables and inequalities with non-negative variables. This correspondence is seen in the case of the WGM through valid KKT conditions. Thus, having a function F: $\mathbb{R}^n \to \mathbb{R}^n$, an MCP is to find vectors $x \in \mathbb{R}^{n_1}$, $y \in \mathbb{R}^{n_1}$ such that for all i:

1. $F_i(x, y) \geq 0, x_i \geq 0, x_i \cdot F_i(x) = 0, i = 1, ..., n_1$

2. $F_{j+n_1}(x, y) = 0, y_j free, j = 1, ..., n_2$

A mixed complementarity program can also be represented in terms of upper and lower bounds such that for every x_i and it's upper (u_i) and lower (l_i) bounds satisfy the following conditions:

1. $l_i = x_i \implies F_i(x) \geq 0$

2. $l_i < x_i < u_i \implies F_i(x) = 0$

3. $x_i = u_i \implies F_i \leq 0$

   where $l_i \leq u_i \forall i$ and $l_i \in \mathbb{R} \cup \{-\infty\}, u_i \in \mathbb{R} \cup \{+\infty\}$

The upper and lower bounds help in the case of modeling energy markets as they can represent the characteristics of trade flows such as capacities and contracts [18][12].

The World Gas Model is based on the economic behavior of players acting in accordance with Nash-Cournot game theory. The assumption is that all players of all types in the model are acting towards the goal of maximizing profit under certain constraints with distinct revenue and associated costs [12]. It should be noted that WGM is entirely deterministic and there are no elements of uncertainty being taken into effect in the model. This is due to the nature of equilibrium modeling and models of large time horizons being utilized primarily as a predictor of trends and patterns for macro-level decision making.

2.2 Players

In this section, a description of the various players developed for use in the World Gas Model by previous works [12][11][44] are presented as well as their associated objective function and operational constraints.

2.2.1 Producer

Natural gas production encompasses a wide array of natural gas operations and products. We are only focused on marketed natural gas production, i.e., natural gas that is available for the market. For each node within the model, there is only one producer agent that delivers gas to either the node's trading arm (trader) or, if applicable, a domestic liquefier. The producer performs based on the objective function of maximizing of discounted profits. The maximization of discounted profits with respect to the producer is found in Eq. 2.1:

$$\max_{SALES^P_{pdm}} \sum_{m\epsilon M} \gamma_m \left\{ \sum_{d\epsilon D} days_d \left[\pi^P_{n(p)dm} SALES^P_{pdm} - C^P_{pm} \left(SALES^P_{pdm} \right) \right] - b^P_{pm} \triangle^P_{pm} \right\} \tag{2.1}$$

The production rate $SALES^P_{pdm}$ is restricted by a production capacity CAP^{PR}_{pm} and the capacity investment expansion in all previous years $\sum_{m\epsilon M} \triangle^P_{pm}$:

$$s.t. \quad SALES^P_{pdm} \leq CAP^{PR}_{pm} + \sum_{m\epsilon M} \triangle^P_{pm} \quad \forall d, m \quad \left(\alpha^P_{pdm} \right) \tag{2.2}$$

Total sales are constrained by the domestic proved reserves over the time horizon:

$$s.t. \quad \sum_{m\epsilon M} \sum_{d\epsilon D} days_d SALES^P_{pdm} \leq RES^P_p \quad \forall m \left(\beta^P_{pdm} \right) \tag{2.3}$$

The daily sales rate and investment capacity expansion must be non-negative:

$$s.t. \quad SALES^P_{pdm} \geq 0 \quad \forall d, m \tag{2.4}$$

$$s.t. \quad \triangle^P_{pm} \geq 0 \quad \forall m \tag{2.5}$$

A nonlinear, logarithmic, Golombeck marginal production cost function Eq. 2.6 [24] is used to describe the production cost of fossil fuels. The function is used due to the increasing and convex form that allows for KKT conditions to be valid. We also implement the investment capacity investments from previous years [31].

$$C_{pm}^{P}\left(SALES_{pdm}^{P}\right) = \left(\alpha_{pm}^{cost} + \gamma_{pm}^{cost}\right) SALES_{pdm}^{P} + \beta_{pm}^{cost}\left(SALES_{pdm}^{P}\right)^{2}$$
$$+ \gamma_{pm}^{cost}\left(CAP_{pm}^{PR} + \sum_{m\epsilon M} \triangle_{pm}^{P} - SALES_{pdm}^{P}\right) \ln\left[1 - \left(\frac{SALES_{pdm}^{P}}{CAP_{pm}^{PR} + \sum_{m\epsilon M} \triangle_{pm}^{P}}\right)\right] \tag{2.6}$$

2.2.2 Trader

The trader agent in the WGM represents the trading arm for a producer in different markets around the world. The trading arms may or may not be a state-owned entity or an individual private company with access to different international markets. An example of the two different trading arms is Gazprom Export LLC, the state-owned trading arm under Russia's Gazprom, and Shell International Trading and Shipping Company Limited, a global business organization that manages trading arms around the world on behalf of Royal Dutch Shell (United Kingdom). The WGM takes into account of the different real-world trading operations through a binary map of all domestic players' access to different international markets. An example is the mapping of Gazprom Export's access to the multiple consumption nodes found in the European Union via a vast network of pipelines.

Traders maximize their discounted profits that result from selling gas at a daily rate to marketers for end-use consumption, $SALES_{tndm}^{T\rightarrow M}$, coupled with a market power coefficient, $\delta_{tn}^{C}\epsilon[0,1]$, and a weighted average of market prices, $\left(\delta_{tn}^{C}\Pi_{ndm}^{W}\left(1-\delta_{nn_i}^{C}\right)\pi_{ndm}^{W}\right)$, resulting from the inverse demand function, Π_{ndm}^{W}, and a perfect competition market clearing wholesale price, π^{W}_{ndm}. Traders operate the flows from the storage operators, for both the injection $INJ^{T\to S}_{tndm}$ and extraction $XTR^{T\to S}_{tndm}$ flows coupled with a cost to inject (τ^{SI}_{ndm}) and extract (τ^{SX}_{ndm}). The purchase and transportation costs from producers $\pi^{P}_{n(p(t))dm}PURCH^{P\leftarrow T}_{tndm}$ and regasifiers $\pi^{R}_{n(r(t))dm}PURCH^{R\leftarrow T}_{tndm}$ (if applicable) are also accounted for by the trader. Lastly, pipeline transportation costs include a regulated fee $\tau^{Reg}_{nn_idm}$ plus a congestion fee $\tau^{A}_{nn_idm}$ based on pipeline usage $FLOW^{T}_{nn_idm}$ from the trading source n and final destination n_i, represented as (n, n_i).

$$\max_{\substack{SALES^{T\to M}_{tndm}\\ INJ^{T\to S}_{tndm}\\ XTR^{T\leftarrow S}_{tndm}\\ PURCH^{P\to T}_{tndm}\\ PURCH^{R\to T}_{tndm}\\ FLOW^{T}_{nn_idm}}} \sum_{m\epsilon M} \gamma_m \sum_{d\epsilon D} days_d \left\{ \begin{array}{c} \sum\limits_{n\epsilon N(t)} \left[\begin{array}{c} \left(\left(\delta^{C}_{tn}\Pi^{W}_{ndm}\left(1-\delta^{C}_{nn_i}\right)\pi^{W}_{ndm}\right)\right)SALES^{T\to M}_{tndm} \\ -\pi^{P}_{n(p(t))dm}PURCH^{P\leftarrow T}_{tndm} \\ -\pi^{R}_{n(r(t))dm}PURCH^{P\leftarrow R}_{tndm} \\ -\sum\limits_{s\epsilon S(t)} \left(\begin{array}{c} \left(\tau^{SI}_{sndm}+\tau^{SI,reg}_{sndm}\right)INJ^{T\to S}_{tndm} \\ +\tau^{SX}_{sndm}XTR^{T\leftarrow S}_{tndm} \end{array} \right) \\ -CC^{ton}_{tm}SALES^{T}_{tndm}CE^{T}_{T} \end{array} \right] \\ -\sum\limits_{(n,n_i)\epsilon A(t)} \left[\left(\tau^{Reg}_{nn_idm}+\tau^{A}_{nn_idm}\right)FLOW^{T}_{nn_idm}\right] \end{array} \right\} \tag{2.7}$$

The mass balance between the total sales, purchases, flows as well as storage injection and extraction are accounted for in the following constraint:

$$\begin{aligned} s.t.\quad & XTR^{T\leftarrow S}_{tndm} + PURCH^{P\to T}_{tndm} + PURCH^{R\to T}_{tndm} + \sum_{n,n_i\epsilon A(t)} (1 - Loss_a) FLOW^{T}_{nn_idm} \\ & -SALES^{T}_{tndm} - INJ^{T\to S}_{tndm} - \sum_{n,n_i\epsilon A(t)} FLOW^{T}_{nn_idm} = 0 \quad \forall n, d, m \quad (\phi^{T}_{tndm}) \end{aligned} \tag{2.8}$$

Each year the total storage extraction must equal the loss-corrected injection net volume.

$$s.t. \quad \sum_{d \epsilon D} days_d \left(XTR^{T\leftarrow S}_{tndm} - (1 - Loss_s) INJ^{T\rightarrow S}_{tndm} \right) = 0 \quad \forall n, s\epsilon S(n(t)), d, m \quad (\phi^T_{tndm}) \tag{2.9}$$

All variables are non-negative:

$$s.t. \quad SALES^{T\rightarrow M}_{tndm} \geq 0 \quad \forall n, d, m \tag{2.10}$$

$$s.t. \quad INJ^{T\rightarrow S}_{tndm} \geq 0 \quad \forall n, d, m \tag{2.11}$$

$$s.t. \quad XTR^{T\leftarrow S}_{tndm} \geq 0 \quad \forall n, d, m \tag{2.12}$$

$$s.t. \quad PURCH^{P\rightarrow T}_{tndm} \geq 0 \quad \forall n, d, m \tag{2.13}$$

$$s.t. \quad PURCH^{R\rightarrow T}_{tndm} \geq 0 \quad \forall n, d, m \tag{2.14}$$

$$s.t. \quad FLOW^{T}_{nn_i dm} \geq 0 \quad \forall n, d, m \tag{2.15}$$

2.2.3 Liquefier

LNG liquefaction terminals are represented in the WGM as "liquefiers" that are able to buy gas from a domestic producer from their dedicated trader via pipeline, liquefy the gas, and ultimately sell the gas to LNG transportation companies. Each element of the process is modeled to include associated costs and losses. The liquefier maximizes the discounted profit $\pi^L_{n(l)dm} SALES^L_{ldm}$ minus the production costs $\pi^P_{n(l)dm} PURCH^{L\leftarrow P}_{ldm}$, liquefaction process costs $C^L_{ldm} SALES^L_{ldm}$, and capacity investment costs$b^L_{lm}\triangle^L_{lm}$.

$$\max_{\substack{SALES^L_{ldm}\\ PURCH^{L\leftarrow P}_{ldm}\\ \triangle^L_{lm}}} \sum_{m\epsilon M}\gamma_m \sum_{d\epsilon D} days_d \left\{ \begin{bmatrix} \pi^L_{n(l)dm} SALES^L_{ldm} \\ -\pi^P_{n(l)dm} PURCH^{L\leftarrow P}_{ldm} \\ -C^L_{ldm} SALES^L_{ldm} \end{bmatrix} - b^L_{lm}\triangle^L_{lm} \right\} \tag{2.16}$$

Total sales are constrained by the total capacity, which includes the initial capacity CAP^L_l plus total investment expansion $\sum\limits_{m'<m} \triangle^L_{lm'}$ from all previous time periods.

$$s.t. \quad CAP^L_l + \sum_{m'<m} \triangle^L_{lm'} - SALES^L_{ldm} \geq 0 \quad \forall d, m(\alpha^L_{ldm}) \tag{2.17}$$

The daily sales rate is restricted by the total production purchase rate accounted for losses from transportation and liquefaction.

$$s.t. \quad (1 - loss_l) PURCH^{L\leftarrow P}_{ldm} - SALES^L_{ldm} \geq 0 \quad \forall d, m(\phi^L_{ldm}) \tag{2.18}$$

All variables are non-negative:

$$s.t. \quad SALES^L_{ldm} \geq 0 \quad \forall d, m \tag{2.19}$$

$$s.t. \quad PURCH^{L\leftarrow P}_{ldm} \geq 0 \quad \forall d, m \tag{2.20}$$

$$s.t. \quad \triangle^L_{lm} \geq 0 \quad \forall d, m \tag{2.21}$$

2.2.4 Regasifier

LNG Regasification terminals are represented by the "regasifier" agent who buys LNG from various LNG transportation companies, gasifies the LNG, and sells the gas to the domestic trader or marketer. The regasifiers maximize their discounted profit from selling to traders $SALES^{R\to T}_{rdm}$ and marketers $SALES^{R\to M}_{rdm}$ minus the cost of purchasing LNG $\sum_{rlj} \pi^{L}_{n(l)dm} LNGFLOW^{B}_{rljdm}$, transporting LNG $\sum_{rlj} \tau^{B}_{n(l)dm} LNGFLOW^{B}_{rljdm}$, cost of gasifying LNG $C^{R}_{rm}\left(SALES^{R\to T} + SALES^{R\to M}_{rdm}\right)$ and any investment capacity expansion costs $b^{R}_{rm}\triangle^{R}_{rm}$.

$$\max_{\substack{SALES^{R\to T}_{rdm}\\ SALES^{R\to M}_{rdm}\\ LNGFLOW^{B}_{rljdm}\\ \triangle^{R}_{rm}}} \sum_{m\epsilon M}\gamma_m \sum_{d\epsilon D} days_d \left\{ \begin{bmatrix} \pi^{R}_{rdm} SALES^{R\to T}_{rdm} \\ +\pi^{R}_{rdm} SALES^{R\to M}_{rdm} \\ -\sum_{rlj} \pi^{L}_{n(l)dm} LNGFLOW^{B}_{rljdm} \\ -\sum_{rlj} \tau^{B}_{n(l)dm} LNGFLOW^{B}_{rljdm} \\ -C^{R}_{rm}\left(SALES^{R\to T} + SALES^{R\to M}_{rdm}\right) \end{bmatrix} - b^{R}_{rm}\triangle^{R}_{rm} \right\} \quad (2.22)$$

The daily sales rates to both the trader and marketer are constrained by the initial base year capacity and subsequent investment capacity expansions.

$$s.t. \quad CAP^{R}_{r} + \sum_{m'<m} \triangle^{R}_{rm} - SALES^{R\to T}_{rdm} - SALES^{R\to M}_{rdm} \geq 0 \quad \forall d,m \quad (\alpha^{R}_{rdm}) \quad (2.23)$$

The total amount of gas available for trading and marketing are constrained by the losses from the transportation of LNG, boil-off, and regasification process.

$$s.t. \quad \sum_{lrj} (1-loss_{lrj})(1-loss_r) LNGFLOW^{B}_{rljdm} - \begin{bmatrix} SALES^{R\to T}_{rdm} \\ +SALES^{R\to M}_{rdm} \end{bmatrix} \geq 0 \quad \forall d,m \quad (\alpha^{R}_{rdm}) \quad (2.24)$$

Long-term LNG contracts are taken into account and utilized as a lower bound for the total flow from node (l) to node (r), ensuring all contracts are met for all time periods.

$$s.t. \quad \sum_j LNGFLOW^{B}_{rljdm} - LNGDEST^{R}_{rldm} \geq 0 \quad \forall r, l, d, m (\varepsilon^{R}_{rldm}) \tag{2.25}$$

All variables are non-negative:

$$s.t. \quad SALES^{R \to T}_{rdm} \geq 0 \quad \forall d, m \tag{2.26}$$

$$s.t. \quad SALES^{R \to M}_{rdm} \geq 0 \quad \forall d, m \tag{2.27}$$

$$s.t. \quad LNGFLOW^{B}_{rljdm} \geq 0 \quad \forall d, m \tag{2.28}$$

$$s.t. \quad \triangle^{R}_{rm} \geq 0 \quad \forall m \tag{2.29}$$

2.2.5 LNG Shipping Operator

LNG transportation companies are represented by "LNG shipping operators" who are responsible for buying LNG from liquefiers (l) and selling the maritime transported LNG to regasifiers (r) located at different ports around the world. LNG vessels operate at a wide range of LNG load capacities; however, the WGM distinguishes three different load capacities of size $(c \epsilon C)$, detailed load capacities and costs can be found in Sec. 2.3.2.6. The modeled capacity of each transport vessel size is the total fleet capacity of active vessels within that size class. The

LNG shipping operator maximizes the discounted profit $\sum_{rlj} \tau^B_{rljdm} LNGFLOW^B_{crljdm}$ minus the shipping cost $C^B_{cjm} LNGFLOW^B_{crljdm}$, canal costs (if applicable) for both the Suez Canal $\tau^{S_toll}_{dm}$ and Panama Canal $\tau^{P_toll}_{dm}$, as well as respective canal congestion fees $\tau^{S_con}_{dm}$ and $\tau^{P_con}_{dm}$ for LNG flows on route $j \epsilon \{Panama, Suez\}$. An endogenous fleet capacity investment $b^B_{cm} \triangle^B_{cm}$ is also considered in future time periods.

$$\max_{\substack{LNGFLOW^B_{crljdm} \\ \triangle^B_{cm}}} \sum_{m \epsilon M} \gamma_m \sum_{d \epsilon D} days_d \left\{ \begin{bmatrix} \sum_{rlj} tau^B_{rljdm} LNGFLOW^B_{crljdm} \\ -C^B_{cjm} LNGFLOW^B_{crljdm} \\ -\sum rl, j \epsilon Pcanal \left(\tau^{P_toll}_{dm} + \tau^{P_con}_{dm} \right) LNGFLOW^B_{crljdm} \\ -\sum rl, j \epsilon Scanal \left(\tau^{S_toll}_{dm} + \tau^{S_con}_{dm} \right) LNGFLOW^B_{crljdm} \end{bmatrix} - b^B_{cm} \triangle^B_{cm} \right\} \tag{2.30}$$

The daily LNG flow via LNG vessel $(c \epsilon C)$ across route $(j \epsilon J)$ with a distance of $Dist_{rlj}$ is constrained by the daily maximum distance able to be traveled $MaxDist_c$ based on the respective average vessel speed. The total LNG flow capacity across route (j) with vessel (c) is the initial total fleet capacity for vessel (c) plus the fleet expansion investment $\sum_{m' < n} \triangle^B_{cm'}$ from all previous time periods. It is assumed LNG vessels will travel the same route back and forth, once laden and then subsequently unladen for the return voyage.

$$s.t. \quad MaxDist_c \left(CAP^B_c + \sum_{m' < n} \triangle^B_{cm'} \right) - \sum_{rl} 2 \left(LNGFLOW^B_{crljdm} Dist_{rlj} \right) \geq 0 \qquad \forall dm (\alpha^B_{cdm}) \tag{2.31}$$

LNG flow for the largest capacity vessels, also known as "Q-Max", are not permitted for travel via Panama and Suez Canal routes.

$$s.t. \quad LNGFLOW^{B}_{c\epsilon\{large\},rl,j\epsilon\{Scanal\},dm} = 0 \quad \forall r,l,d,m \left(\beta^{B}_{c\epsilon\{large\},rljdm}\right) \tag{2.32}$$

$$s.t. \quad LNGFLOW^{B}_{c\epsilon\{large\},rl,j\epsilon\{Pcanal\},dm} = 0 \quad \forall r,l,d,m \left(\beta^{B}_{c\epsilon\{large\},rljdm}\right) \tag{2.33}$$

All variables are non-negative:

$$s.t. \quad LNGFLOW^{B}_{crljdm} \geq 0 \quad \forall d,m \tag{2.34}$$

$$s.t. \quad \triangle^{B}_{cm} \geq 0 \quad \forall m \tag{2.35}$$

2.2.6 Canal Operator

The Panama and Suez Canal provide shorter route distances for LNG transportation companies for additional costs and fees based on congestion and vessel load. A canal operator player is defined as the agent who provides the canal service while maximizing the discounted profit from canal tolls $\tau^{P_toll}_{dm}, \tau^{S_toll}_{dm}$ and congestion fees $\tau^{P_con}_{dm}, \tau^{S_con}_{dm}$ based on vessel traffic minus the canal operating costs $C^{Pcanal}_{dm} LNGFLOW^{Pcanal}_{dm}$, $C^{Scanal}_{dm} LNGFLOW^{Scanal}_{dm}$.

$$\max_{\substack{LNGFLOW^{Pcanal}_{dm}\\ LNGFLOW^{Scanal}_{dm}}} \sum_{m\epsilon M} \gamma_m \sum_{d\epsilon D} days_d \left\{ \begin{bmatrix} \left(\tau^{P_toll}_{dm} + \tau^{P_con}_{dm}\right) LNGFLOW^{Pcanal}_{dm} \\ + \left(\tau^{S_toll}_{dm} + \tau^{S_con}_{dm}\right) LNGFLOW^{Scanal}_{dm} \\ - C^{Pcanal}_{dm} LNGFLOW^{Pcanal}_{dm} \\ - C^{Scanal}_{dm} LNGFLOW^{Scanal}_{dm} \end{bmatrix} \right\} \tag{2.36}$$

LNG Flows through the Panama and Suez Canals are constrained by a daily maximum capacity.

$$s.t. \quad CAP^{Scanal} - LNGFLOW_{dm}^{Scanal} \geq 0 \quad \forall d, m (\alpha_{dm}^{Scanal}) \tag{2.37}$$

$$s.t. \quad CAP^{Pcanal} - LNGFLOW_{dm}^{Pcanal} \geq 0 \quad \forall d, m (\alpha_{dm}^{Pcanal}) \tag{2.38}$$

All variables are non-negative:

$$s.t. \quad LNGFLOW_{dm}^{Scanal} \geq 0 \quad \forall d, m \tag{2.39}$$

$$s.t. \quad LNGFLOW_{dm}^{Pcanal} \geq 0 \quad \forall d, m \tag{2.40}$$

2.2.7 Transmission System Operator

Transmission system operators (TSO) are responsible for the efficient allocation of gas flow between pipelines, defined independently as arc (a), with access to various markets. The TSO maximizes the discounted profit from providing gas flow to traders $\tau_{adm}^{A} SALES_{adm}^{A}$ via arc (a) minus the investment capacity expansion costs $b_{am}^{A} \triangle_{am}^{A}$.

$$\max_{\substack{SALES_{adm}^{A} \\ \triangle_{am}^{A}}} \sum_{m \epsilon M} \gamma_m \sum_{d \epsilon D} days_d \left\{ \left[\sum_{a} \tau_{adm}^{A} SALES_{adm}^{A} \right] - \sum_{a} b_{am}^{A} \triangle_{am}^{A} \right\} \tag{2.41}$$

Arc capacity $SALES_{adm}^{A}$ is restricted by the maximum initial available pipeline capacity CAP_{am}^{A} for the same arc and the sum of all previous time period expansions

$\triangle^{A}_{am}$ for that same arc.

$$s.t. \quad CAP^{A}_{am} + \sum_{m'<m} \triangle^{A}_{am'} - SALES^{A}_{adm} \geq 0 \quad \forall a, d, m(\alpha^{A}_{adm}) \tag{2.42}$$

All variables are non-negative:

$$s.t. \quad SALES^{A}_{adm} \geq 0 \quad \forall d, m \tag{2.43}$$

$$s.t. \quad \triangle^{A}_{am} \geq 0 \quad \forall m \tag{2.44}$$

2.2.8 Storage Operator

Storage operators work in conjunction with traders, providing storage capacity during lower consumption periods. The operation of storage facilities is governed by the injection $SALES^{SI}_{sdm}$ and extraction $SALES^{SX}_{sdm}$ flows. The storage operator maximizes the discounted profit generated from injection and extraction flows $\tau^{SI}_{sdm} SALES^{SI}_{sdm} + \tau^{SX}_{sdm} SALES^{SX}_{sdm}$ minus a total storage capacity investment expansion cost which includes an injection $b^{SI}_{sm} \triangle^{SI}_{sm}$, extraction $b^{SX}_{sm} \triangle^{SX}_{sm}$, and a working gas expansion $b^{SW}_{sm} \triangle^{SW}_{sm}$. Carbon emission costs are also accounted for $CC^{ton}_{sm} \left(SALES^{SI}_{sdm} + SALES^{SX}_{sdm} \right) CE^{S}_{s}$

$$\max_{\substack{SALES^{SI}_{sdm} \\ SALES^{SX}_{sdm} \\ \triangle^{SI}_{sm}, \triangle^{SX}_{sm}, \triangle^{SW}_{sm}}} \sum_{m \epsilon M} \gamma_m \sum_{d \epsilon D} days_d \left\{ \begin{array}{c} \tau^{SI}_{sdm} SALES^{SI}_{sdm} + \tau^{SX}_{sdm} SALES^{SX}_{sdm} \\ -\left(b^{SI}_{sm} \triangle^{SI}_{sm} + b^{SX}_{sm} \triangle^{SX}_{sm} + b^{SW}_{sm} \triangle^{SW}_{sm} \right) \\ -CC^{ton}_{sm} \left(SALES^{SI}_{sdm} + SALES^{SX}_{sdm} \right) CE^{S}_{s} \end{array} \right\} \tag{2.45}$$

The injection rate $SALES_{sdm}^{SI}$ is constrained by the total injection capacity resulting from an initial capacity CAP_{sm}^{SI} and the aggregate yearly expansions $\sum_{m'<m} \triangle_{sm'}^{SI}$. The same constraint logic is held with regards to the extraction rate $SALES_{sdm}^{SX}$, initial capacity CAP_{sm}^{SX}, and aggregate yearly expansions $\sum_{m'<m} \triangle_{sm'}^{SX}$. In order to maintain storage facility performance, the total amount of gas extracted in a season is constrained by the amount of working gas volume WG_{sm}^{S} and the sum of yearly extraction capacity expansions $\sum_{m'<m} \triangle_{sm'}^{SX}$.

$$s.t. \quad CAP_{sm}^{SI} + \sum_{m'<m} \triangle_{sm'}^{SI} - SALES_{sdm}^{SI} \geq 0 \quad \forall d, m(\alpha_{sdm}^{SI}) \tag{2.46}$$

$$s.t. \quad CAP_{sm}^{SX} + \sum_{m'<m} \triangle_{sm'}^{SX} - SALES_{sdm}^{SX} \geq 0 \quad \forall d, m(\alpha_{sdm}^{SX}) \tag{2.47}$$

$$s.t. \quad WG_{sm}^{S} + \sum_{m'<m} \triangle_{sm'}^{SX} - \sum_{d \epsilon D} Days(SALES_{sdm}^{SX}) \geq 0 \quad \forall m(\alpha_{sdm}^{SW}) \tag{2.48}$$

Allowable capacity expansions are upper-bounded.

$$s.t. \quad \triangle_{sm}^{SI} \leq \overline{\triangle}_{sm}^{SI} \quad \forall m(\rho_m^{SI}) \tag{2.49}$$

$$s.t. \quad \triangle_{sm}^{SX} \leq \overline{\triangle}_{sm}^{SX} \quad \forall m(\rho_m^{SX}) \tag{2.50}$$

$$s.t. \quad \triangle_{sm}^{SW} \leq \overline{\triangle}_{sm}^{SW} \quad \forall m(\rho_m^{SW}) \tag{2.51}$$

All variables are non-negative:

$$s.t. \quad SALES_{sdm}^{SI} \geq 0 \quad \forall d, m \tag{2.52}$$

$$s.t. \quad SALES^{SX}_{sdm} \geq 0 \quad \forall d, m \tag{2.53}$$

$$s.t. \quad \triangle^{SI}_{sm} \geq 0 \quad \forall m \tag{2.54}$$

$$s.t. \quad \triangle^{SX}_{sm} \geq 0 \quad \forall m \tag{2.55}$$

$$s.t. \quad \triangle^{SW}_{sm} \geq 0 \quad \forall m \tag{2.56}$$

2.2.9 Market-Clearing Conditions

First, the total sales from an individual producer must equal the sum of all sales to both traders and liquefiers.

$$SALES^{P}_{pdm} = \sum_{l \epsilon L(p)} PURCH^{L \leftarrow P}_{ldm} + \sum_{t(p)} PURCH^{T}_{t(p)dm} \quad \forall p, d, m \quad (\pi^{P}_{pdm}) \tag{2.57}$$

The total injection volume over a time period for an individual storage operator is equal to the total amount of injection performed by a trader during that same period for the same individual storage facility.

$$SALES^{SI}_{sdm} = \sum_{t \epsilon T(s)} INJ^{T}_{tsdm} \quad \forall s, d, m \quad (\tau^{SI}_{sdm}) \tag{2.58}$$

The same constraint logic applies for the extraction capacity during a time period for an individual storage operator.

$$SALES^{SX}_{sdm} = \sum_{t \epsilon T(s)} XTR^{T}_{tsdm} \quad \forall s, d, m \quad (\tau^{SX}_{sdm}) \tag{2.59}$$

The pipeline capacity for a pipeline of arc (a) equals the total volume-metric flow by all traders with access to that arc/pipeline.

$$SALES^{A}_{adm} = \sum_{t} FLOW^{T}_{tadm} \quad \forall a, d, m \quad (\tau^{A}_{adm}) \tag{2.60}$$

The total sales from an individual liquefier to LNG shipping operators equals the total of all LNG flows across all routes (j) from the same liquefier to all available regasifiers.

$$\sum_{l \epsilon L} SALES^{L}_{ldm} = \sum_{j \epsilon J} \sum_{r \epsilon R} LNGFLOW^{R \leftarrow L}_{rljdm} \quad \forall l, d, m \quad (\pi^{L}_{l} dm) \tag{2.61}$$

The total of all LNG flows across all routes (j) from all liquefiers to all available regasifiers is equal to the total LNG shipping operator capacity.

$$\sum_{c} SALES^{B}_{crljdm} = LNGFLOW^{B}_{rljdm} \quad \forall r, l, j, d, m \quad (\tau^{B}_{r} ljdm) \tag{2.62}$$

Both the Panama and Suez Canal's capacities are equal to the total amount of LNG flow through the canals for all shipping operators (B) on associated routes $(j \epsilon \{Pcanal\}), (j \epsilon \{Pcanal\})$.

$$SALES^{Pcanal}_{dm} = \sum_{crl} SALES^{B}_{crljdm} \quad \forall j \epsilon \{Pcanal\}, d, m \quad (\tau^{Pcanaltoll}_{dm}) \tag{2.63}$$

$$SALES^{Scanal}_{dm} = \sum_{crl} SALES^{B}_{crljdm} \quad \forall j \epsilon \{Scanal\}, d, m \quad (\tau^{Scanaltoll}_{dm}) \tag{2.64}$$

The final demand market-clearing condition determines the wholesale price of gas for an individual market (n) based on the linear inverse demand curve equation, where INT^W_{ndm} represents the intercept, and the slope of the inverse demand curve is represented by SLP^W_{ndm} which is multiplied by the total sales to the market by accessible traders $\sum_t SALES^T_{tndm}$.

$$\pi^W_{ndm} = INT^W_{ndm} + SLP^W_{ndm} \sum_t SALES^T_{tndm} \quad \forall n, d, m \quad (\pi^W_{ndm}) \tag{2.65}$$

The resulting network that was developed through the shared use of parameters and variables found in the market-clearing conditions, shown visually in Fig. 2.1, demonstrates the inter-connectivity of all players within the WGM. This underlying network of market-clearing conditions, in conjunction with KKT conditions, provides the WGM with the ability to reach market equilibrium for all players and countries within the model.

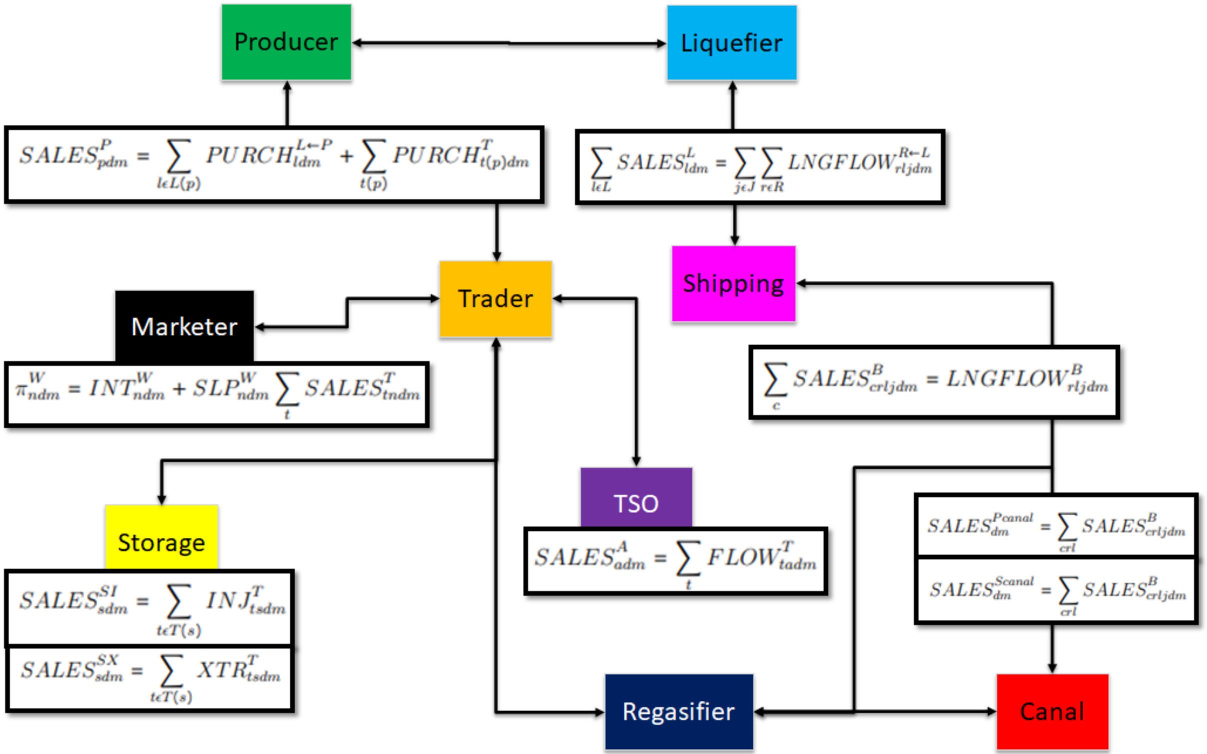

Figure 2.1: WGM Network of Market-Clearing Conditions [1]

[1] Arrows represent data flow between market-clearing conditions and players.

2.3 Data Collection

2.3.1 Sources

The model utilizes open source data found primarily from BP's 2019 Statistical Review of World Energy [48], International Gas Union's 2019 World LNG Report [35], and the United States Energy Information Agency's (EIA) 2019 Annual Energy Outlook [33]. The base model year data was taken from the year 2017 in order to provide a complete set of data for all players in the same calendar year, this was due to the availability of data from each agency's report.

2.3.2 Player Data

2.3.2.1 Consumer/Marketer

The consumption reference data was taken from BP's 2019 Statistical Review of World Energy from the 2017 base year and utilized each individual country's growth over a 5-year period to forecast future values for that country's demand as well as the global growth rate over the same time period. For example, Australia's natural gas consumption growth rate per annum from 2012 to 2017 was 3.1%. This growth rate was then used in conjunction with the global gas demand growth rate from 2012 to 2017 (2.0%) and a estimated growth rate per annum for each future time period to forecast Australia's future natural gas demands for the subsequent model years. The growth rates were used together in the following equation that solves for individual country demand over a 5-year period:

$$D_{y_i} = D_{y_{i-1}} \times (1 + (dr \times \Delta gr))^5 \quad (2.66)$$

y =Year

D=Domestic Natural Gas Demand

dr=Domestic Natural Gas Demand Growth Rate per Annum

Δgr= Change in global Natural Gas Demand Growth Rate per Annum from $y_{i-1} to y_i$

Eq. 2.66 takes advantage of each individual country's growth rate over the same time period as the model as well as the overall global growth rate change. Through implementing an overall global growth rate change in the forecasting of reference demand values, the globalization of the natural gas market can be accounted for. This implementation allows the user of the WGM to determine global market behavior due to global growth rates of their determination. For the base model, the global growth rate increases to 2.2% per annum by 2022 and then linearly decreases to 1.0% by 2037. This was done based on the International Energy Agency's (IEA) Sustainable Development Scenario in which "natural gas consumption increases over the next decade at an annual average rate of 0.9% before reaching a high point by the end of the 2020s. After this, accelerated deployment of renewables and energy efficiency measures, together with a pickup in production of biomethane and later of hydrogen, begins to reduce consumption" [33]. The calculated sum of each individual country's demand in the model versus the forecasted global growth based on growth rate per annum can be seen in Fig. 2.2.

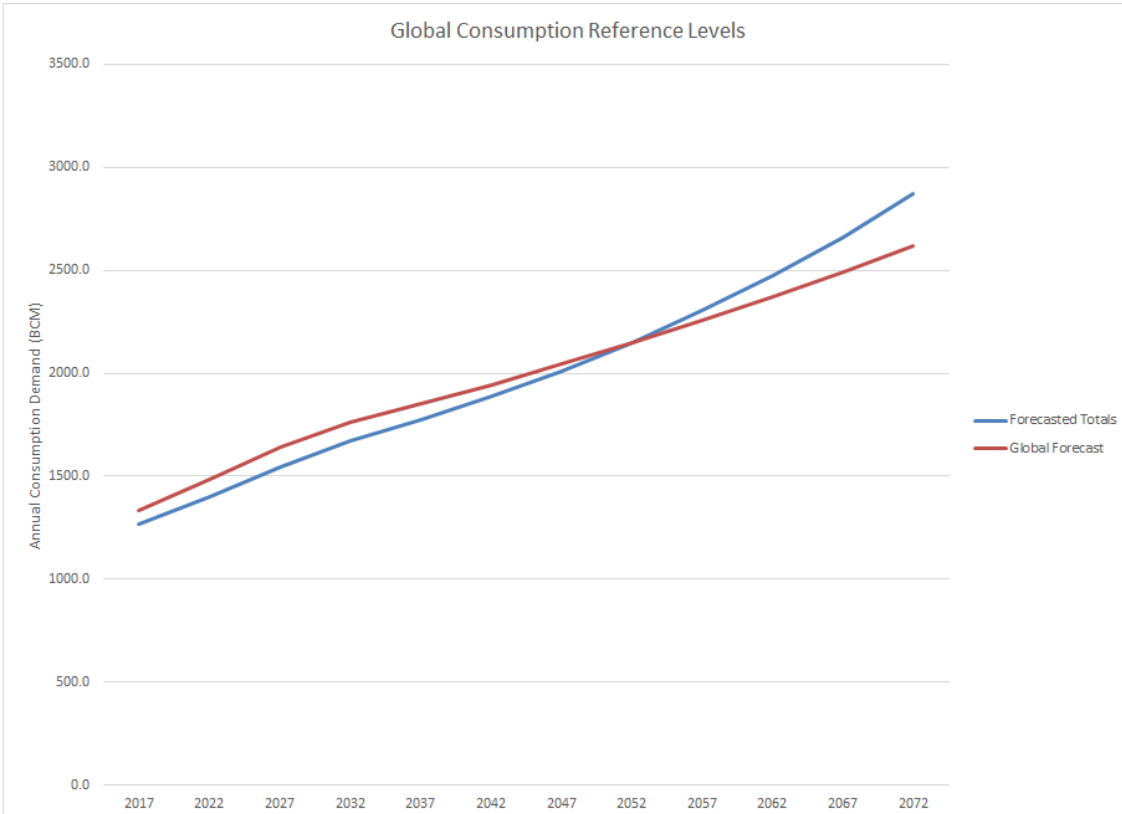

Figure 2.2: Total Sum of WGM Demand vs. Forecasted Global Demand (BP Statistical Review 2019) [48]

2.3.2.2 Producer

The production reference data was similarly taken primarily from BP's 2019 Statistical Review of World Energy from the 2017 base year and utilized each individual country's growth over a 5-year period to forecast future values for that country's production as well as the global growth rate over the same time period. For example, Colombia's natural gas production growth rate per annum from 2012 to 2017 was 1.3%. This growth rate was then used in conjunction with the global gas production growth rate from 2012 to 2017 (2.0%) and a estimated growth rate per annum for each future time period to forecast Colombia's future natural gas production for the subsequent model years. The growth rates were used together in the following Eq. 2.67:

$$P_{y_i} = P_{y_{i-1}} \times (1 + (pr \times \Delta gr))^5 \tag{2.67}$$

y =Year

P=Domestic Natural Gas Production

pr=Domestic Natural Gas Production Growth Rate per Annum

Δgr=Change in global Natural Gas Production Growth Rate per Annum from $y_{i-1} to y_i$

Eq. 2.67 takes advantage of each individual country's growth rate over the same time period as the model as well as the overall global growth rate change. Through implementing overall global growth rate change in the forecasting of reference production values, the globalization of the natural gas market can be accounted for. This implementation allows the user to determine global market behavior due to global growth rates of their determination. For the base model, the global growth rate increases to 2.3% per annum by 2022 and then linearly decreases to 1.1% by 2037. This was performed based on the International Energy Agency's (IEA) Sustainable Development Scenario in which "natural gas consumption increases over the next decade at an annual average rate of 0.9% before reaching a high point by the end of the 2020s. After this, accelerated deployment of renewables and energy efficiency measures, together with a pickup in production of biomethane and later of hydrogen, begins to reduce consumption" [33]. The calculated sum of each individual country's production in the model versus the forecasted global growth based on growth rate per annum can be seen visually in Fig. 2.3.

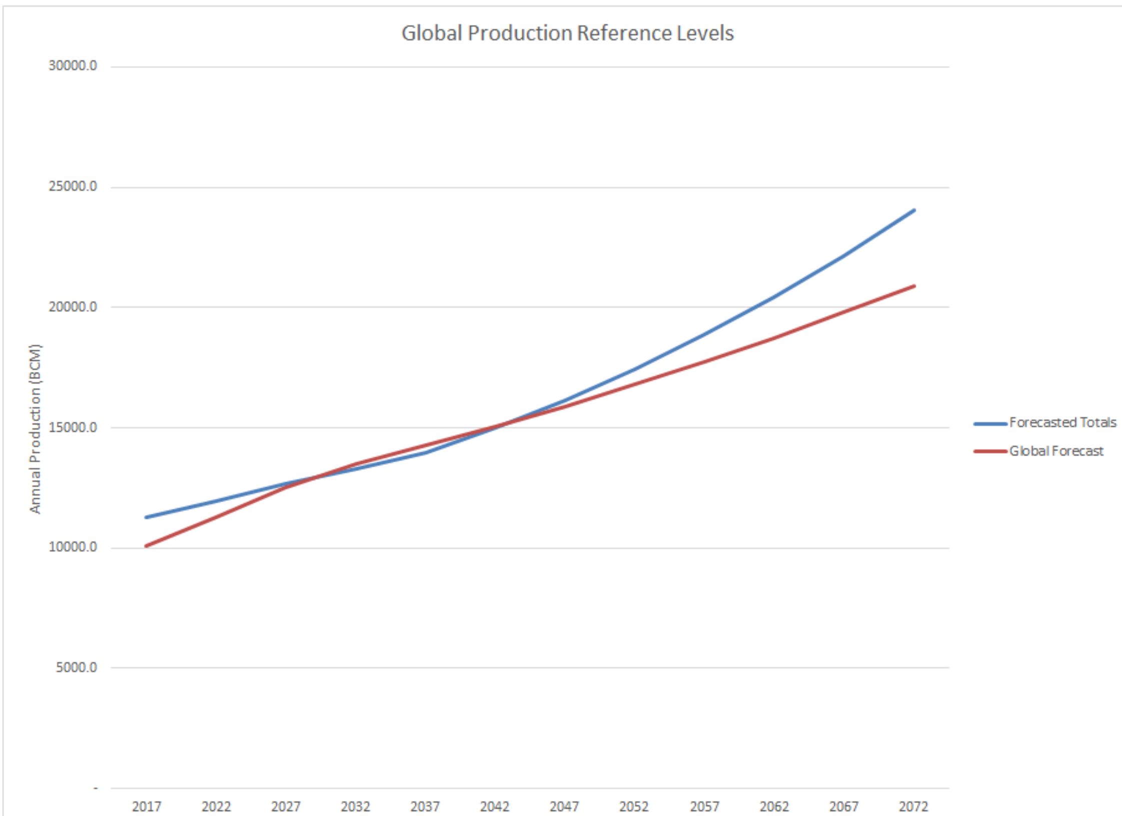

Figure 2.3: Total Sum of WGM Production vs. Forecasted Global Production [33]

2.3.2.3 Transmission System Operator

The transmission system operator(TSO) or pipeline operator data was primarily taken from BP's 2019 Statistical Review of World Energy [48] as well as the Global Gas & Oil Network's Global Fossil Infrastructure Tracker [22]. BP's Statistical Review provides information on many of the major international pipeline lines that are considered in the model. The Global Fossil Infrastructure Tracker was used to provide additional information to supplement BP's Statistical Review in regards to 2017 natural gas movement such as smaller scale developments. In addition to these sources, future pipeline developments and considerations were found through various online news sources that highlighted any international pipeline projects that are in construction, approved, or in consideration. An example of an anticipated pipeline that was used in the model would be the Altai Gas Pipeline. The Altai Gas Pipeline is reported to come online within the next decade (2027) and will provide 30 BCM per year of natural gas from Russia to China [41]. The major pipelines that were added to the model and not found in BP's Statistical Review of World Energy includes but is not limited to:

1. Alliance Pipeline System + Foothills (Canada to U.S.) – Runs from Western Canadian Sedimentary Basin through North Dakota ending in Chicago, started in 2000 expands in 2021 [49].

2. Altai Gas Pipeline (Russia to China) – Runs from Western-Siberia into China's Xinjiang province, expected to be online in late 2020s [41].

3. Arab Gas Pipeline (Israel to Jordan) – Runs from Israel to Jordan completed in 2019 and online in early 2020 [58].

4. Gasoducto del Noreste Argentino Gas Pipeline (Bolivia to Argentina) – Runs from Bolivia to Argentina, online in September 2019 [4].

5. Iraq-Kuwait Pipeline (Iraq to Kuwait) – Runs from Iraq to Kuwait however our model does not include Iraq, so the pipeline is connected to the nearby country of Iran. Online in 2019 [21].

6. Trans-Anatolian Gas Pipeline (Azerbaijan to Turkey + Other Europe) – Runs from Azerbaijan to Europe. Construction was started in 2015 and inaugurated in 2018 [57].

7. Mier Monterrey Gas Pipeline (U.S. to Mexico) – Runs from Starr County in Texas to Monterrey, Neuvo Leon in Mexico. The 85-mile pipeline started construction in the year 2003 and has been online since 2017 [56].

8. Gas Atacama Pipeline (Argentina to Chile) – Runs from Salta Argentina to Mejilones in Chile. The 585-mile pipeline began construction in 1997 and finished in 1999 [15].

9. Trans-Saharan Gas Pipeline (Nigeria to Algeria) – Currently still in the prospect phase and our model plans for this to be online in the 2020s [5].

10. GASBOL (Bolivia to Brazil) – Runs from Bolivia's gas fields to south-east regions in Brazil. Operational in 1999. Expansions completed in March 2000 [52].

11. East-West Gas Pipeline (Turkmenistan to Russia) – Finished in 2015 [51].

12. Dolphin Gas Project (Oman to United Arab Emirates) – Runs from Qatar's North Field into Oman and into United Arab Emirates. Operational in the year 2003. An expansion also occurred in 2006 [50].

13. Antonio Ricaurte Pipeline (Columbia to Venezuela) – Runs from Columbia to Venezuela and came online in 2008 [47].

2.3.2.4 Liquefier

Liquefier data was taken primarily from the International Gas Union's 2019 World LNG Report [35] and the Global Fossil Infrastructure Tracker (GFIT) [22]. The data collection process began with analysis of the leading liquefaction countries throughout the world and determining which would be placed in the model. Using a selection criteria, countries that contributed at least 0.5% to global market share of LNG exports were placed into the WGM. Table 2.1 outlines the countries their respective total liquefaction capacities as of 2017. Note, the United States of America and Russia were separated by region for increased analysis detail. Total liquefaction capacity was taken from IGU's World LNG Report and supplemented by the GFIT. Consideration was taken for all operating LNG liquefaction plants within a country's borders to be included in the initial capacity, as listed in Table 2.1. LNG liquefaction plants that are currently under construction or are awaiting a final investment decision are included in the WGM as allowable capacity expansions for a predetermined time period [35][22]. LNG Liquefaction plant costs and losses

World Gas Model - Natural Gas Liquefaction Nodes		
Country Name	Global Market Share	Liquefaction Capacity (mcm/d)[2]
Algeria	4.2%	142.2
Angola	1.3%	21
Equatorial Guinea	1.2%	14.8
Nigeria	7.3%	88.5
Australia	19.2%	254.7
Brunei	2.4%	27.2
Indonesia	5.5%	125.8
Malaysia	9.0%	95.6
Papua New Guinea	2.6%	32.3
Norway	1.4%	18.9
Qatar	27.6%	293.1
Oman	2.9%	40.8
United Arab Emirates	1.8%	28.9
Russia - East	1.5%	45.3
Russia - West	2.3%	70.0
United States - Gulf	4.5%	198.5
United States - Alaska	0.0%	0.1
Peru	1.4%	17.0
Trinidad & Tobago	3.7%	57.8
Total	99.8%	1572.5

Table 2.1: Liquefier Nodes [35][22]

per million cubic meter (mcm) were taken as a fixed linear value for all countries as \$125,000/mcm of natural gas [55].

2.3.2.5 Regasifier

Regasifier data was taken primarily from the International Gas Union's 2019 World LNG Report [35] and the Global Fossil Infrastructure Tracker (GFIT) [22]. The data collection process began with analysis of the leading regasification countries throughout the world and determining which would be placed in the model. Using a selection criteria, countries that contributed at least 0.25% to global market share of LNG imports were placed into the WGM. Table 2.2 outlines the countries their respective total liquefaction capacities as of 2017. Note, the United States of America and Mexico were separated by region for increased analysis detail.

Total regasification capacity was taken from IGU's World LNG Report and supplemented by the GFIT. Consideration was taken for all operating LNG regasification plants within a country's borders to be included in the initial capacity, as listed in Table 2.2. LNG regasification plants that are currently under construction or are awaiting a final investment decision are included in the WGM as allowable capacity expansions for a predetermined time period [35][22]. LNG regasification plant costs and losses per million cubic meter (mcm) were taken as a fixed linear value for all countries as $30,000/mcm of natural gas [39].

World Gas Model - Natural Gas Regasification Nodes		
Country Name	Global Market Share	Regasification Capacity (mcm per day)[3]
Egypt	2.1%	35.6
China	13.5%	525.0
India	7.1%	93.7
Indonesia	0.5%	24.7
Japan	28.8%	755.1
Malaysia	0.5%	27.4
Pakistan	1.7%	36.4
South Korea	13.2%	448.8
Taiwan	5.7%	57.5
Thailand	1.3%	40.0
Singapore	0.8%	66.3
France	2.6%	94.0
Italy	2.1%	120.5
Portugal	0.9%	21.6
Spain	4.2%	188.8
Turkey	2.7%	47.1
United Kingdom	1.7%	111.0
Jordan	1.2%	14.2
Israel	0.5%	11.3
Kuwait	1.5%	21.6
United Arab Emirates	0.8%	36.7
Mexico - Atlantic	0.70%	21.4
Mexico - Pacific	1.00%	42.5
U.S.A. - Everett, MA	0.2%	81.4
U.S.A. - Cove Point, MD	0.2%	77.5
U.S.A. - Gulf	0.40%	330.4
Argentina	1.1%	30.7
Brazil	0.5%	43.3
Chile	1.1%	20.5
Total	98.6%	3425

Table 2.2: Regasifier Nodes [35][22]

2.3.2.6 LNG Shipping Operator

Data for the LNG shipping operator came primarily from IGU's World LNG Report. The most critical information when modeling the LNG shipping player were the characteristics of the LNG fleet. The global LNG fleet was comprised of

478 vessels at the end of 2017 and 525 at the end of 2018, a 10% growth in fleet capacity in 1 year. Modeling the fleet was first broken down by vessel size into three categories (small, medium, large). The average LNG vessel capacity is around 175,000 cubic meters(cm) of LNG [35]. This was chosen as the capacity know in the WGM as a "medium" LNG vessel, which is assumed to travel around 19 knots. Following IGU's report, it is found that in 2017 there was 167 vessels of this size (+/-25,000 cm) which gives a total fleet capacity for "medium" vessels of 29.225 mcm. "Small" LNG vessels were modeled as the next most represented vessel size in industry. Vessels smaller than the "medium" vessel are most commonly around 125,000 cm (+/-25,000 cm) of capacity and can travel up to 21 knots. In 2017, there were 175 vessels that fell into this size range, providing an average "small" vessel fleet capacity of 21.875 mcm. "Large" vessels were modeled as those vessels that are too large for the Panama Canal a well-known industry example is that of the Q-max ships most owned by Qatar. These "large" vessels were modeled to have average capacities of 240,000 cm and be able to operate at 19 knots. In the WGM, based on IGU data, it was determined that there are 45 vessels of this size (+/-25,000 cm) for a total "large" vessel fleet capacity of 10.8 mcm [35].

An integral component to the performance of the LNG shipping operator is the proper modeling of the various routes that vessels can take to reach their final destination. The model holds every route possible from each liquefier to every regasifier. From each liquefier (l) to regasifier (r) there are three routes: through the Panama Canal, through the Suez Canal, and by avoiding the canals. This produced $\{(l) \times (r) \times 3\}$ routes for a total of 1,653 possible routes that the WGM considers while the LNG shipping operator determines its most profitable LNG routes. Each route has a unique nautical distance [54] which was used to calculate the cost from liquefier (l) to regasifier (r) in \$USD/mcm(NG). The shipping cost was calculated through Eq. 2.68 by taking an average spot charter rate in 2017 of \$44,500 USD [35] and the respective average vessel speed $VesselSpeed_c$ and total fleet capacity $Tot.FleetCap_c$ for vessels of size (c).

$$C^{B}_{crljdm}\left(\frac{\$USD}{mcm}\right) = \frac{SpotCharterRate \times Dist_{rlj}}{VesselSpeed_c \times 24} \times \frac{1}{Tot.FleetCap_c} \tag{2.68}$$

The LNG fleet capacity expansion and laid-up capacity[4] were taken into account in order to allow the WGM to adjust fleet capacity based on demand and real-world conditions. By calculating the \$(USD)/mcm cost of building a new vessel of size "small", "medium", and "large" the WGM is able to make an endogenous investment capacity decision, bounded by an upper capacity expansion limit. A laid-up capacity was taken as the number of vessels in year 2017 that were retired or taken out of commission in order to reflect the aging of the LNG fleet and the need for increased investment.

2.3.2.7 Canal Operator

The canal operator data was taken directly from both the Panama and Suez Canal authorities [59][60]. In order to accurately model the cost of using the Panama

[4] laid-up capacity: idle/unavailable LNG fleet capacity due the withholding of vessels from commercial operations for a period of time.

Canal for an LNG vessel, the toll tariffs that were in place for 2017 were used in the base year of the WGM. The toll tariffs are based on the LNG gas carrier specific tolls found in Table 2.3 [5][6][7] from the Panama Canal Authority (PCA) [59]. The maximum Panama Canal LNG capacity was taken from the daily total number of LNG vessels allowed to transit the canal. The restrictions in place by the PCA allow for a maximum of four LNG vessels per day as of 2020 [46]; however, in the WGM base year of 2017 a maximum of two LNG vessels traveled the Panama Canal in a day. The growth of the Panama Canal, in regards to LNG vessel transits, is modeled as a gradual linear increase over time with the assumption that canal efficiency and overall capacity will increase with demand [17].

Table 2.3: Panama Canal Authority LNG Vessel Tolls [59]

Tolls - LNG Vessels			
Bands in cm	**Laden**	**Ballast**	**Ballast (Roundtrip)**
First 60,000	$2.50	$2.23	$2.00
Next 30,000	$2.15	$1.88	$2.00

Continued on next page

[5]laden: holding LNG cargo
[6]ballast: without LNG cargo
[7]ballast(roundtrip): without cargo for both canal transits

Table 2.3 – continued from previous page

Bands in cm	Laden	Ballast	Ballast (Roundtrip)
Next 30,000	$2.07	$1.80	$2.00
Rest	$1.96	$1.71	$1.50

In order to accurately model the cost of using the Suez Canal for an LNG vessel, the toll tariffs that are in place since 2015 were used in the base year of the WGM (2017). The toll tariffs are based on the LNG gas carrier specific tolls found in Fig. 2.4 from the Suez Canal Authority [60]. The maximum Suez Canal LNG capacity was taken from the largest daily total of LNG vessels in history that have transited the canal, this equates to around 113 mcm/day [6].

Vessel Type	SC Net Tonnage SDR / SCNT													
	First 5000		Next 5000		Next 10000		Next 20000		Next 30000		Next 50000		Rest	
	Laden	Ballast	Laden	Ballast	Laden	Ballast	Laden	Ballast	Laden	Ballast	Laden	Ballast	Laden	Ballast
LNG Carriers	7.88	6.7	6.13	5.21	5.3	4.51	4.1	3.49	3.8	3.23	3.63	3.09	3.53	3

Figure 2.4: Suez Canal Authority LNG Vessel Tolls [60]

2.3.2.8 Storage Operator

Data for the storage operator primarily came from the EIA and includes the working and reserve storage capacity for every country. Future storage capacities beyond the base year are determined endogenously by the model through capacity expansion investment decisions. The data for the capacity expansion costs came from the Federal Energy Regulatory Commission (FERC). The development costs per mcm is around $353,000 USD for a standard 6-12 cycle salt cavern in the Gulf Coast of the United States [13].

2.4 Calibration

The model was calibrated according to past performance history as well as economic outlooks from widely used and available sources. These sources include IGU's World LNG Report [35], EIA's Annual Energy Outlook [64], and the IEA's World Energy Outlook [33]. All sources reflected the state and projections of the natural gas market in 2017 in order to ensure full data coverage for the base year. Past performance data was used to project future short term performance based on BP's Statistical Review of World Energy. Past performance, such as the average growths experienced in the last 5-10 years, provide a baseline for the next 5-10 years when used in conjunction with global future outlooks from other sources. By looking at data from both the past and projections to the future, a reference data set was developed to calibrate the production and demand for each individual node. For the purpose of calibration, geographical regions were designed in order to calibrate objectively based on model output by region. Calibration was complete when the model determined the production and consumption for every region within 5% of the reference data set. Results of the base year calibration are seen below in Fig. 2.5 for consumption by region and Fig. 2.6 for production by region, note all regions within model are to within 5% of reference levels for both production and consumption.

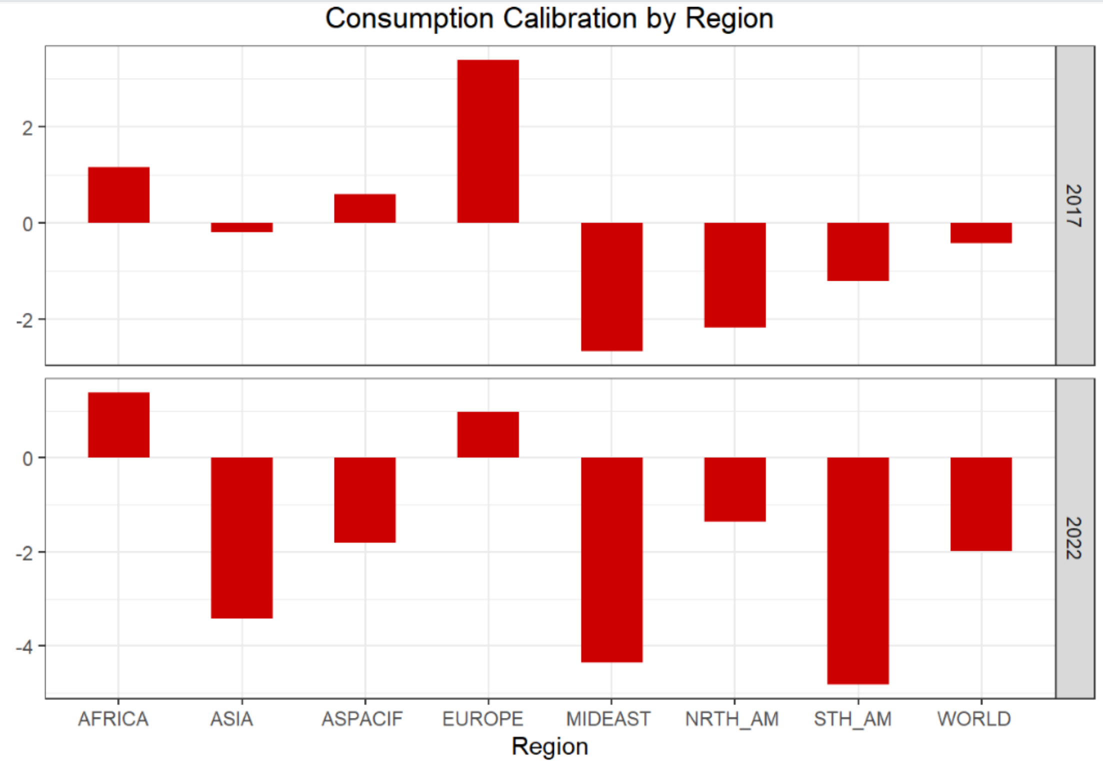

Figure 2.5: Consumption Calibration by Region[8]

[8]Consumption calibration levels shown are the calculated percentage of the WGM output to the reference consumption levels

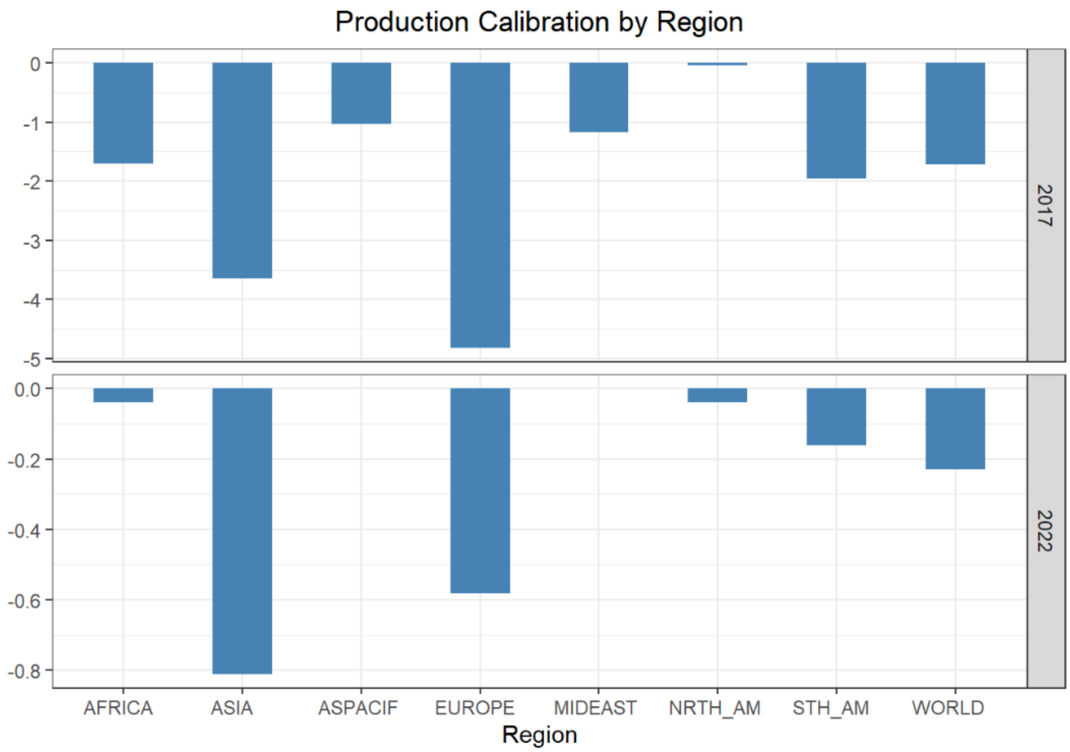

Figure 2.6: Production Calibration by Region [9]

[9]Production calibration levels shown are the calculated percentage of the WGM output to the reference production levels

Chapter 3: Model Analysis

3.1 U.S. and China Trade War

3.1.1 Background

The trade war between the United States and China that has evolved since mid 2017 has been of great concern for the natural gas industry as both the largest international economies battle. The natural gas industry realized the effects of the trade war beginning in September 2018 when a 10% punitive tariff was levied on U.S. LNG exports in response to U.S. levied tariffs on Chinese imports. Later in June of 2019, in response to an increase in U.S. levied tariffs, the Chinese government imposed a 25% tariff on U.S. LNG imports. The realized effects were shown by China's decrease of U.S. LNG imports by 88.0% from 2.92 BCM in 2018 to 0.35 BCM in 2019. Fig. 3.1 displays the sharp decline in U.S. exports to China despite U.S. LNG exports continuing to grow through 2019. Fig. 3.1 also displays the tariff's effects as the decline in U.S. exports to China start in late 2018 and continues until eventually reaching zero shipments through 2019, assisted by the tariff increase in the June 2019.

Figure 3.1: U.S. LNG Exports to China [25]

China's total LNG imports for 2018 were 73.0 BCM which makes U.S. LNG imports only 4% of the total amount imported in 2018 prior to the trade war effects. By contrast in 2019, China's U.S. LNG imports represented only 0.4% of total Chinese LNG imports, shown graphically in Fig. 3.2. It is seen that, most notably, Australia, Malaysia and Russia have increased LNG exports to China due, not only, to the rise in demand but the sharp decline of U.S. LNG imports as a result of the tariffs and on-going trade war.

Figure 3.2: Chinese LNG Imports by Country (tons LNG[1])[39]

3.1.2 Objective

The purpose of this chapter is to analyze the potential long-term and short-term effects of the on-going trade war between the United States and China with specific regard to the consequences following the imposed tariffs, China's domestic natural gas production and resulting decline in U.S. LNG exports to China. A Base Case is presented in which zero tariffs are imposed and forecasts for U.S. and Chinese demand and production levels are held consistent with the methodology found in Sec. 2.2. Starting with the Base Case as the initial solution for computational purposes, all subsequent cases are outlined in Table 3.1 and are solved using the results from the Base Case.

[1] 10 million metric tons LNG = 22.1 million cubic meters

WGM U.S. & China Trade War - Case Studies		
Case Study	Chinese Import Tariff	Chinese Domestic Production (% of forecasted total)
1 -25T/100P	25%	100%
2 -25T/150P	25%	150%
3 -10T/100P	10%	100%
4 -10T/150P	10%	150%
5 -5T/100P	5%	100%
6 -5T/150P	5%	150%
7 -0T/150P	0%	150%
Base - 0T/100P	0%	100%

Table 3.1: Trade War Case Studies

3.1.3 Analysis & Results

The U.S. & China trade war analysis was run on a 5-year interval from a base year of 2017 to 2037. This time frame provided solutions for years 2017,2022, 2027, 2032, & 2037. First, the Base Case, outlined in Table 3.1, was solved for prior to any other cases. The solutions from the base case provided an initial solution for the remaining cases for the solver to determine a final solution from. This ensured that the same local equilibrium was first initially used, indicating that differences in solutions were due to all things being equal, the differing case scenarios as opposed to the potential for the solver to determine a different solution simply from a different initial starting point.

The results from the Base Case were used as a benchmark in comparison to all other results from the different scenarios. In order to determine the accuracy of the Base Case, the reference production, consumption and LNG exports for the years 2017 and 2022 are considered as previously discussed in Sec. 2.4.

3.1.3.1 Tariff Effects on LNG Trade

One of the major foreseen effects that the U.S. & Chinese tariffs have is the reorganization of the global LNG trade flows. However, the extent and future implications that a long-term tariff has on the global LNG market cannot be fully understood without sufficient modeling and analysis. Cases 1,3, &5 present different scenarios in which the tariffs are adjusted based on recently used metrics and compared against the base case for analysis. One obvious and previously mentioned result for an increase in tariffs is the reduction in total LNG flow from the U.S. to China. As seen in Fig. 3.3, the rise in tariffs is correlated with a decrease in LNG flow.

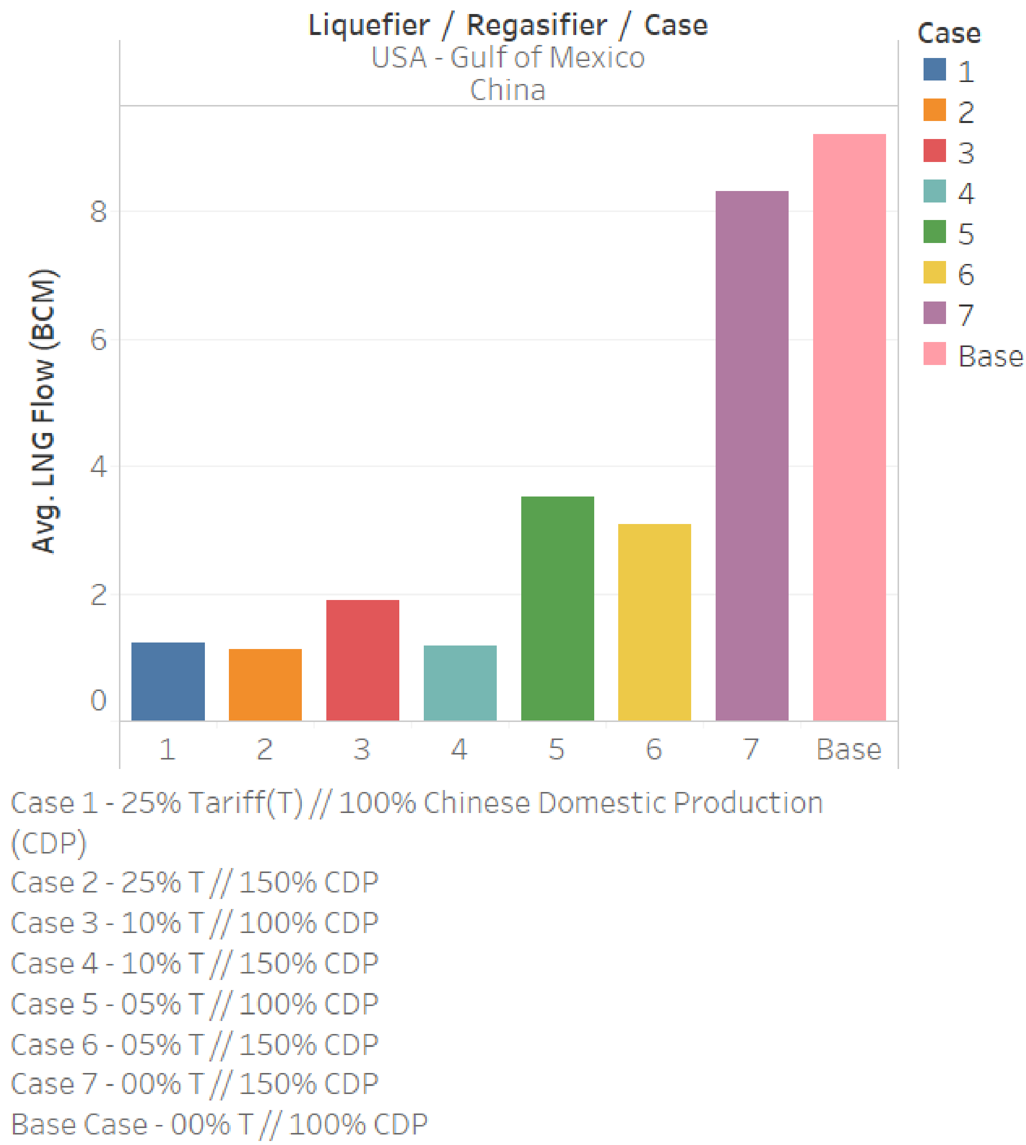

Figure 3.3: Chinese LNG Imports from USA - Gulf of Mexico by Case

It is not until Chinese domestic demand becomes large enough in year 2037 that for the highest tariff case scenario of 25% for cases 1&2 that we seen a resumption in U.S. Chinese LNG trade. There is marginal improvement for increased trade flow when the tariff is ≤ 5% (Case 5); however, this figure is still significantly lower than when there is no tariff imposed. These results concur with recent real-world actions and common understanding regarding LNG trade between the U.S. and China. *For as long as the tariff on U.S. LNG exports to China remains at a level greater than 5% we can assume that there will be little to no LNG trade between the two nations.*

Due to the globalized nature of the LNG market, it is predicted that the effects of the LNG tariffs between the U.S. and China will be far reaching beyond just the flow between the two nations. First, an understanding of China's LNG sources comes into consideration for the Base Case. In Fig. 3.4, a visual representation of the global LNG trade flows to China is displayed where the darker and thicker the arc the greater the amount of LNG flow. It is seen that a majority of the LNG exports to China are from the relatively local regions such as Australia, countries in the Middle East, and the remainder of the exporting Asia pacific countries.

Figure 3.4: Chinese LNG Imports Map

Taking the regional sourcing of China's LNG into consideration, it is anticipated that the tariff-imposed reduction in U.S. LNG flow to China has an altering effect on China's local LNG sources. This effect can be seen in Fig. 3.5 where it is noted that while U.S. - Gulf of Mexico trade flow to China decreases with the increase in tariffs to 25%,10%, &5%, cases 1,3,&5 respectively, the average yearly trade to China from Australia is increased. This concurs with recent observations as since September of 2018 to September of 2019, Australian LNG exports to China have risen 33% [10]. It can be expected that for as long as the tariffs remain and Chinese natural gas demand increases over time, as forecasted, Australia and other local Pacific nations are well poised to gain from a prolonged trade war.

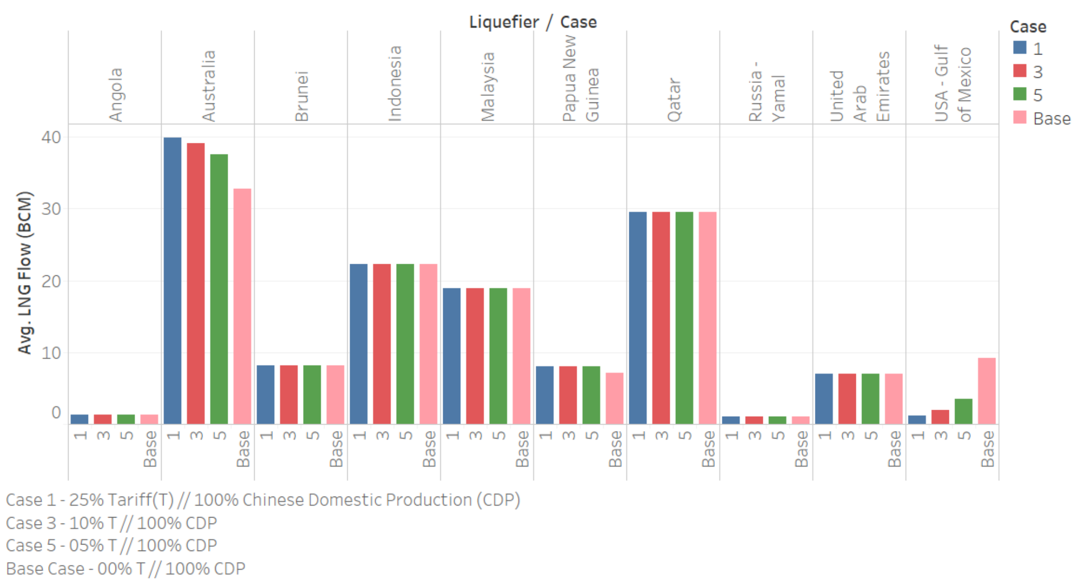

Figure 3.5: Chinese LNG Imports

While much focus has been on U.S. LNG trade with China, implications on the pipeline transmission systems supplying a majority of Chinese natural gas demand should also be evaluated. According to BP Statistical Review, 70% of all Chinese natural gas pipeline imports come from Turkmenistan at around 33 BCM/yr [48]. In regards to the effects of import tariffs on U.S. LNG, no effect can be found on the pipeline trade flow between central Asia and China. Fig. 3.6 represents this visually as the difference in natural gas flow remains unchanged with varying U.S. LNG tariffs.

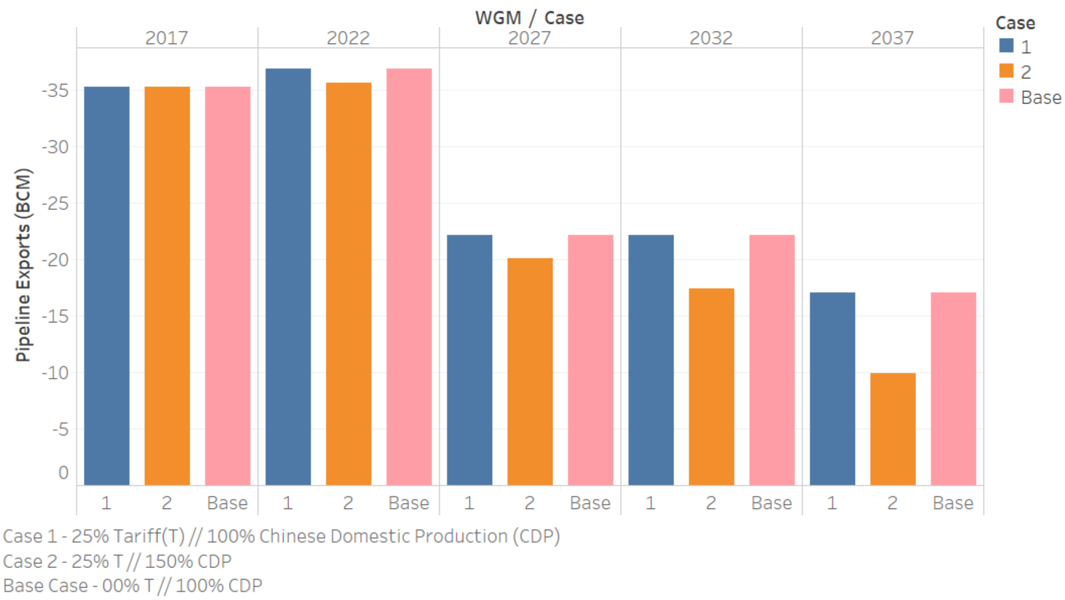

Figure 3.6: Turkmenistan Natural Gas Exports to China by Case & Year

The tariffs imposed on U.S. trade to China has altered the distribution of LNG exports around the globe. Further insight into the final destination and opportunities for U.S. LNG exports must be examined. A quick analysis of U.S. LNG exports and their final destination market is seen in Fig. 3.7. It can be seen that in the Base Case, a majority of the U.S. LNG exports are directed toward the Pacific Asian markets, most notably China, Japan & South Korea.

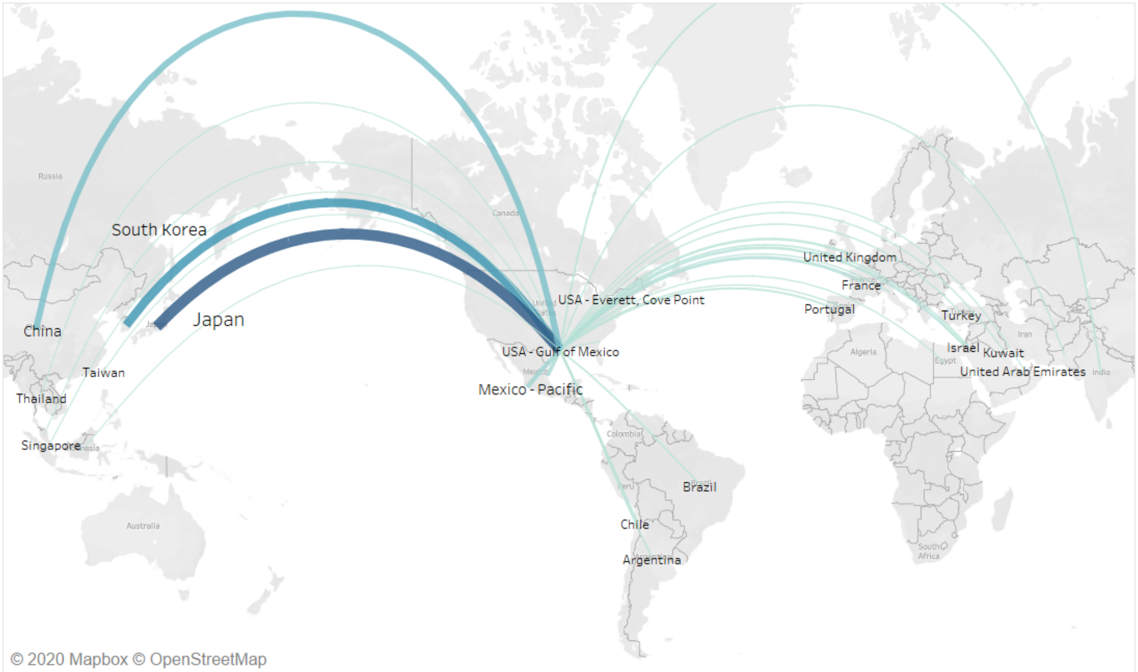

Figure 3.7: U.S. Global LNG Exports - Base Case

Taking this into account, the effect that Chinese tariffs have on these trade patterns is found to be of significance for Japan and South Korea as countries in high demand and higher global wholesale prices are ideal for U.S. exports. These effects are seen visually in the results of Fig. 3.8 where U.S. LNG exports, as a result of increased tariffs, compete for increased market share of the Japanese markets.

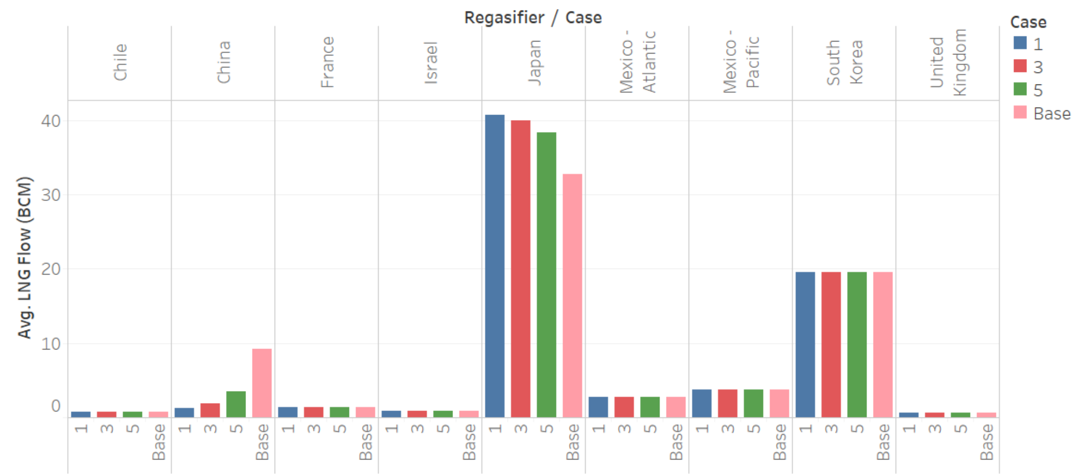

Figure 3.8: U.S. Global LNG Exports & Year

It is seen that with the decrease in Chinese LNG imports from the U.S., as a result of increased tariffs, U.S. LNG exports to Japan increase. The question arises as to why the United States increases its Japanese LNG market share when the shipping cost is one of the largest in the world. Further analysis into the WGM results reveals that with China's investment into alternative regional sources of LNG, most notably Australia, has drawn competitive supply from other local importing countries. In Fig. 3.9, it can seen that for each year in the case study, U.S. LNG market share for the Japanese import market increases with the increase in tariffs. This comes as a result of Australia's potential increased market share of gas imports in China due to the absence of the U.S. LNG imports there. From the results of the WGM, the United States would continue LNG exports to Asia-Pacific countries, such as Japan or South Korea, in response to the tariffs, capturing LNG markets with remaining demand as other localized suppliers gain share of Chinese LNG import demand.

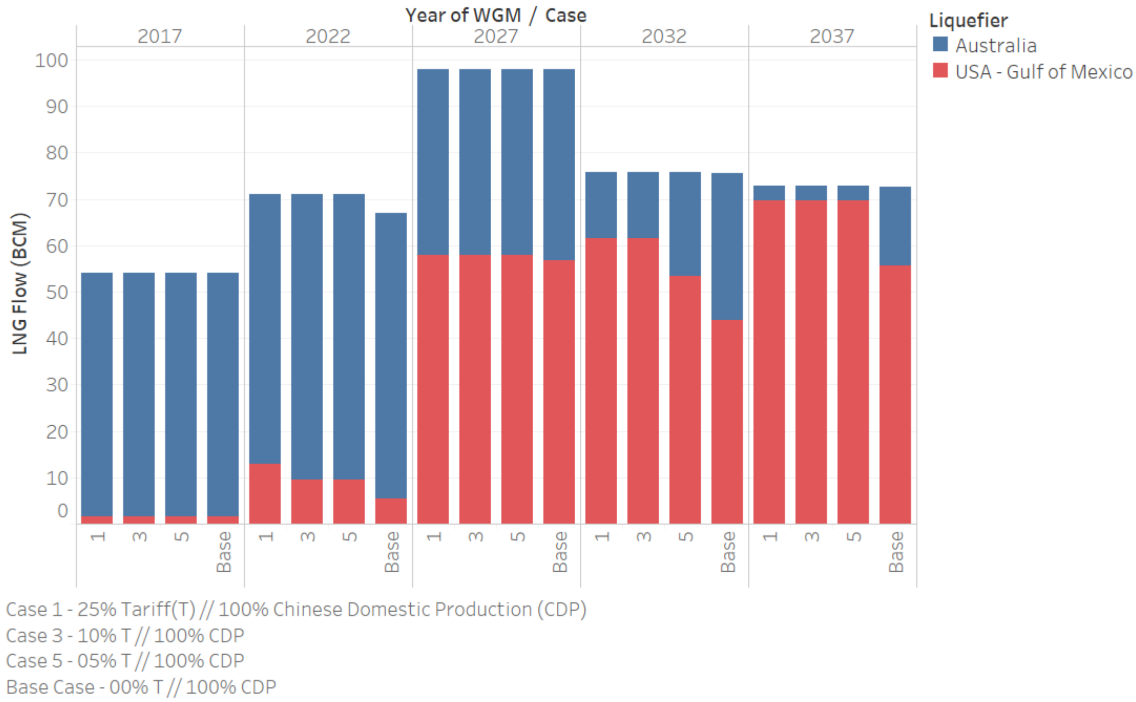

Figure 3.9: U.S. vs Australia LNG Exports to Japan

3.1.3.2 Increased Tariffs & Chinese Natural Gas Production

Cases 1,3, & 5 all assume that Chinese domestic production remains as forecasted previously. However, China holds one of the greatest shale gas reserves [8], and plans to increase domestic production, therefore, reducing reliance on imports. With the potential for bolstered motivation in boosting domestic production due to the trade war, Cases 2,4,6, &7 address the scenarios in which China increases its domestic production capacity to levels stated by the Chinese State Council, defined as 200 BCM/yr by 2020 [8]. The WGM achieves this increased level of domestic production by elevating the reference production of China by 150% ultimately providing an average domestic production level of 243 BCM/yr by 2022, shown visually in Fig. 3.10.

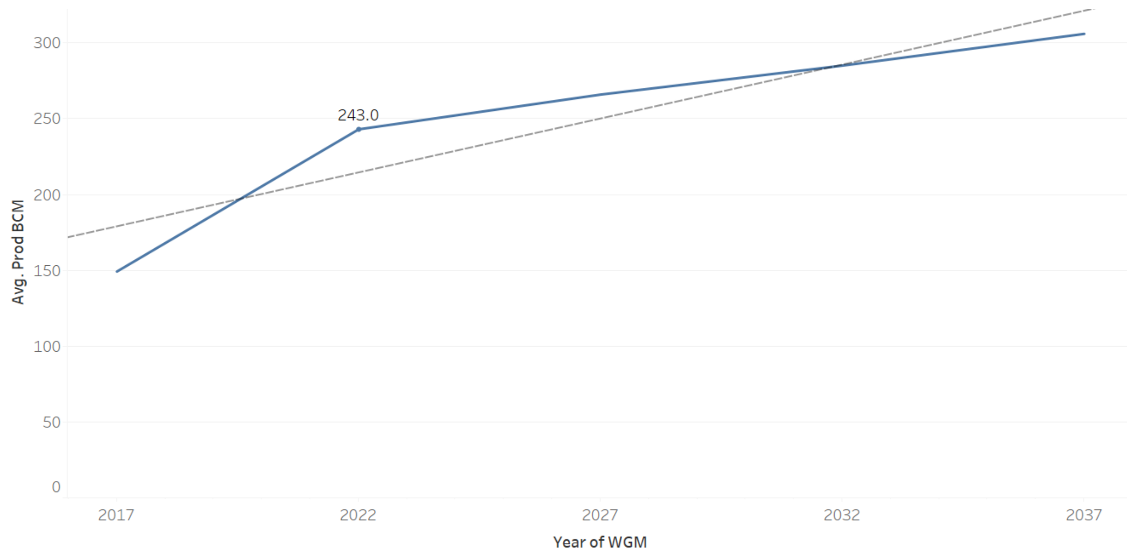

Figure 3.10: 150% Chinese WGM Domestic Natural Gas Production by Year

It is suspected that all natural gas imports, both pipeline and LNG, will be impacted directly by increased Chinese domestic production. An analysis was performed to determine those countries that are most affected from increased Chinese production coupled with a pro-longed trade war. First, the LNG exports by region were analyzed for each case with special regard towards the difference between Cases 1,3,5, Base & 2,4,6,7. It is noticed in Fig. 3.11, that the LNG exports for Africa, Asia Pacific, Middle East, & South America are most affected by the increase in Chinese domestic production. It is significant that U.S. LNG exports remain unchanged regardless of Chinese domestic production levels and import tariffs. These results highlight the dependency that some LNG markets have on China.

Figure 3.11: Average Yearly LNG Exports by Region & Case

The same results were found while analyzing the potential effects that increased Chinese production would have on global pipeline trade. As central Asia is China's largest supplier of pipeline gas imports, results indicated that the region with the greatest impact from increased Chinese production was in fact Central Asia and focus was given specifically on that region. Each country in the central Asian region, Turkmenistan, Kazakhstan, Uzbekistan and Russia was analyzed in terms of pipeline exports against all cases. Fig. 3.12 highlights the regional dependency that Central Asian states have on Chinese domestic demand and their susceptibility to increased Chinese domestic production.

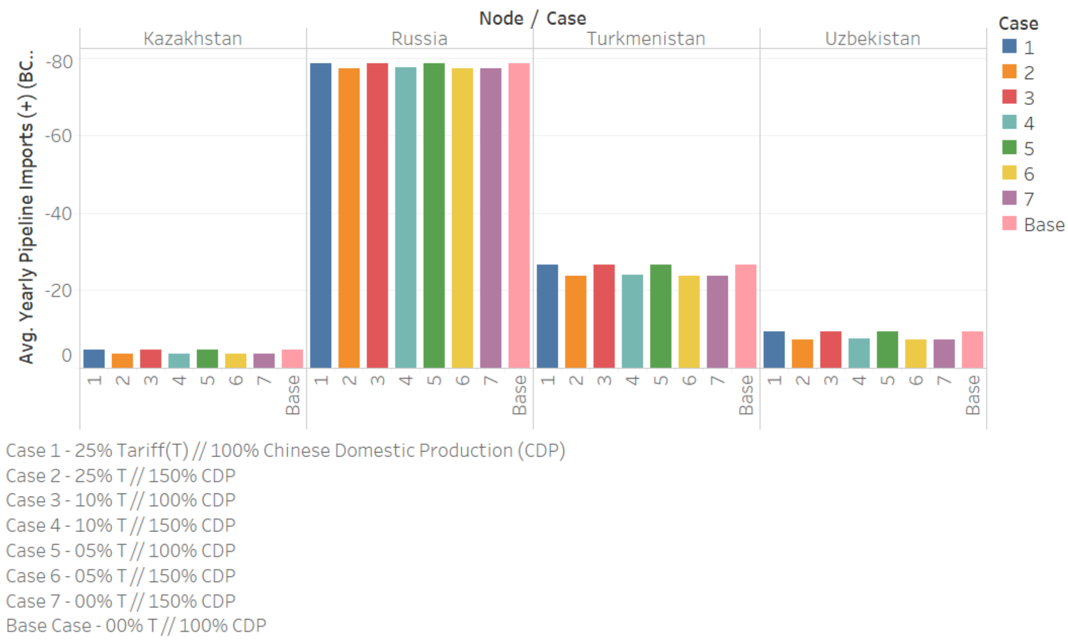

Figure 3.12: Average Yearly Net Pipeline by Region & Case

The significance of increased Chinese domestic production can be seen primarily in the relationship between Turkmenistan natural gas production and pipeline exports. Referring to Fig. 3.13, it can be seen that a large portion of Turkmenistan's natural gas exports are sent to China as Turkmenistan supplied China with 33.3 BCM of natural gas in 2017 [48]. This is significant as the majority of Turkmenistan's natural gas production is devoted to exports only to China followed by the domestic demand of Turkmenistan. This indicates that there is a direct inverse relationship between the levels of Chinese domestic production and the domestic production of Turkmenistan.

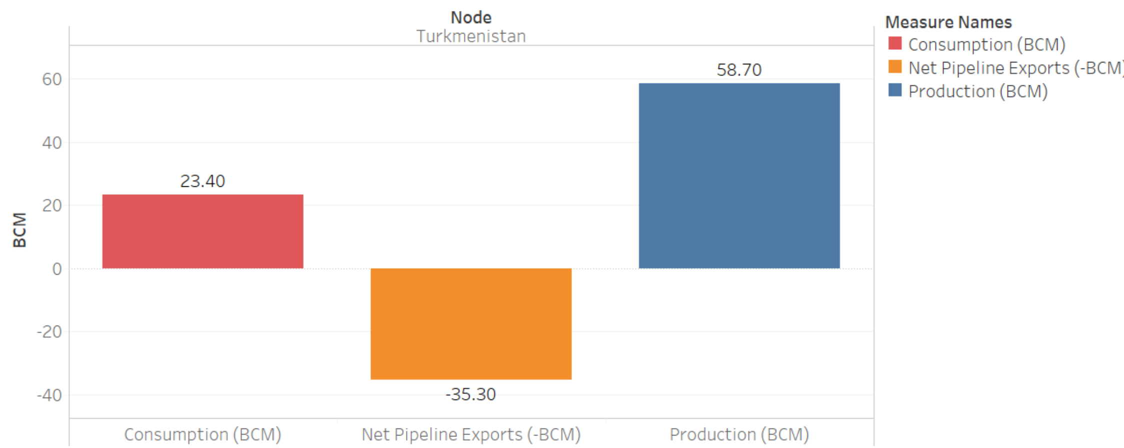

Figure 3.13: Turkmenistan Natural Gas Consumption, Imports, and Production in Year 2017

3.1.3.3 Consumer Surplus

Due to the endogenous and linear nature of the inverse demand curve, determining consumer surplus was the preferred method for analyzing the economic well-being of a society at node n from the WGM results. Consumer surplus is computed for each country and year included in the model via Eq. 3.1. Visually represented in Fig. 3.14, consumer surplus is the area under the inverse demand curve up to equilibrium (e), identified as the area in red, which is determined via the difference between the inverse demand intercept, $\sum_{d\epsilon Days} INT^{W}_{ndm}$, and wholesale price, $\sum_{d\epsilon Days} \pi^{W}_{ndm}$, for a node, n, over all seasons, d, in a year, m, multiplied by $\left(\frac{1}{2}\right)$ and the total demand at equilibrium, $\sum_{d\epsilon Days} Days_d \left(\begin{smallmatrix} \sum_{t\epsilon T} SALES^{T\rightarrow M}_{tndm} \\ + \sum_{r\epsilon R} SALES^{R\rightarrow M}_{rndm} \end{smallmatrix} \right)$.

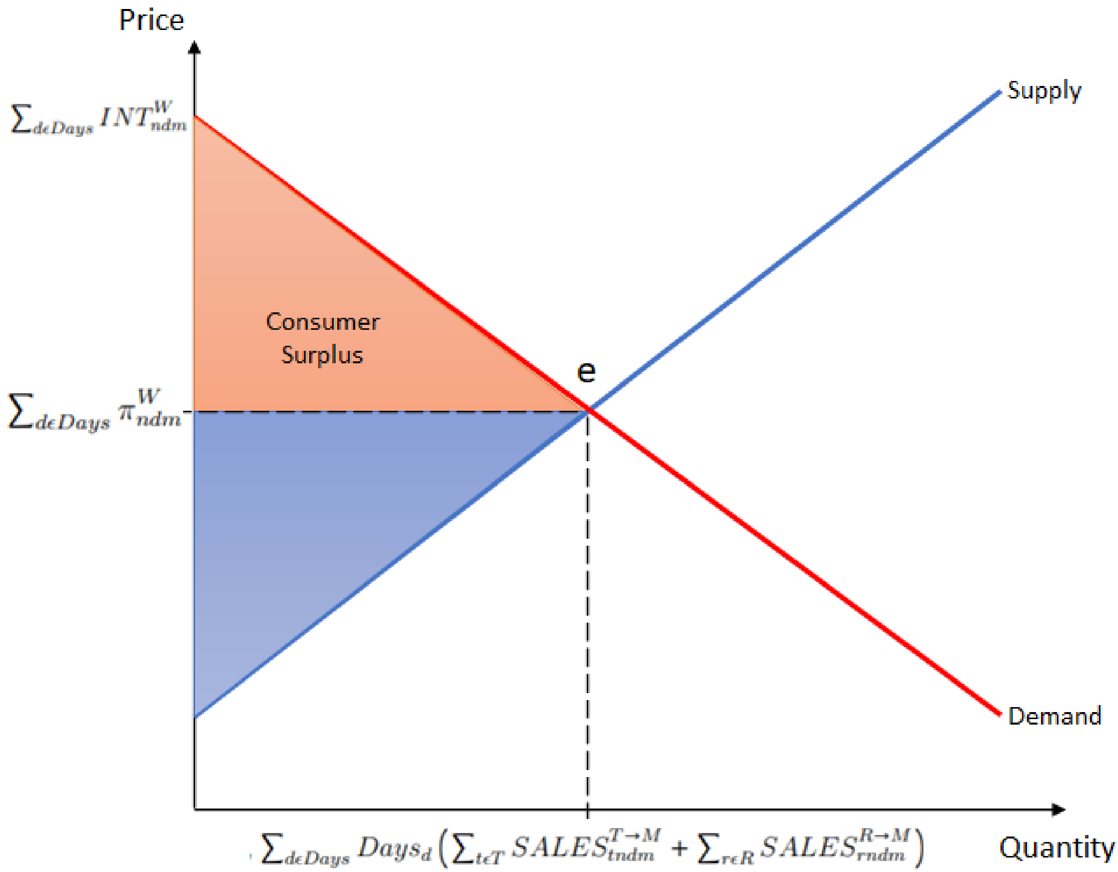

Figure 3.14: Consumer Surplus at Market Equilibrium (e) for Node (n) in Year (m)

$$ConSur_{nm} = \left(\frac{1}{2}\right) \sum_{d\epsilon Days} Days_d \left[\left(INT^{W}_{ndm} - \pi^{W}_{ndm}\right) \times \left(\begin{array}{c}\sum_{t\epsilon T} SALES^{T\rightarrow M}_{tndm} \\ + \sum_{r\epsilon R} SALES^{R\rightarrow M}_{rndm}\end{array}\right)\right] \quad (3.1)$$

This overall well-being can be examined globally, regionally, and on a national scale via the WGM. The effects of the trade war and potential increase in Chinese domestic production of natural gas are first analyzed on a regional basis. In Fig. 3.15, the impact of the increased tariffs alone are negligible according to WGM results. The greater impact on the global natural gas market is the increase in domestic Chinese production. With the United States only providing 2% of Chinese LNG imports in 2017, the consumer surplus impact due to an absence of U.S. & China natural gas trade has minimal impact and easily absorbed by other relatively local countries with already larger market share and the capacity to meet Chinese demand.

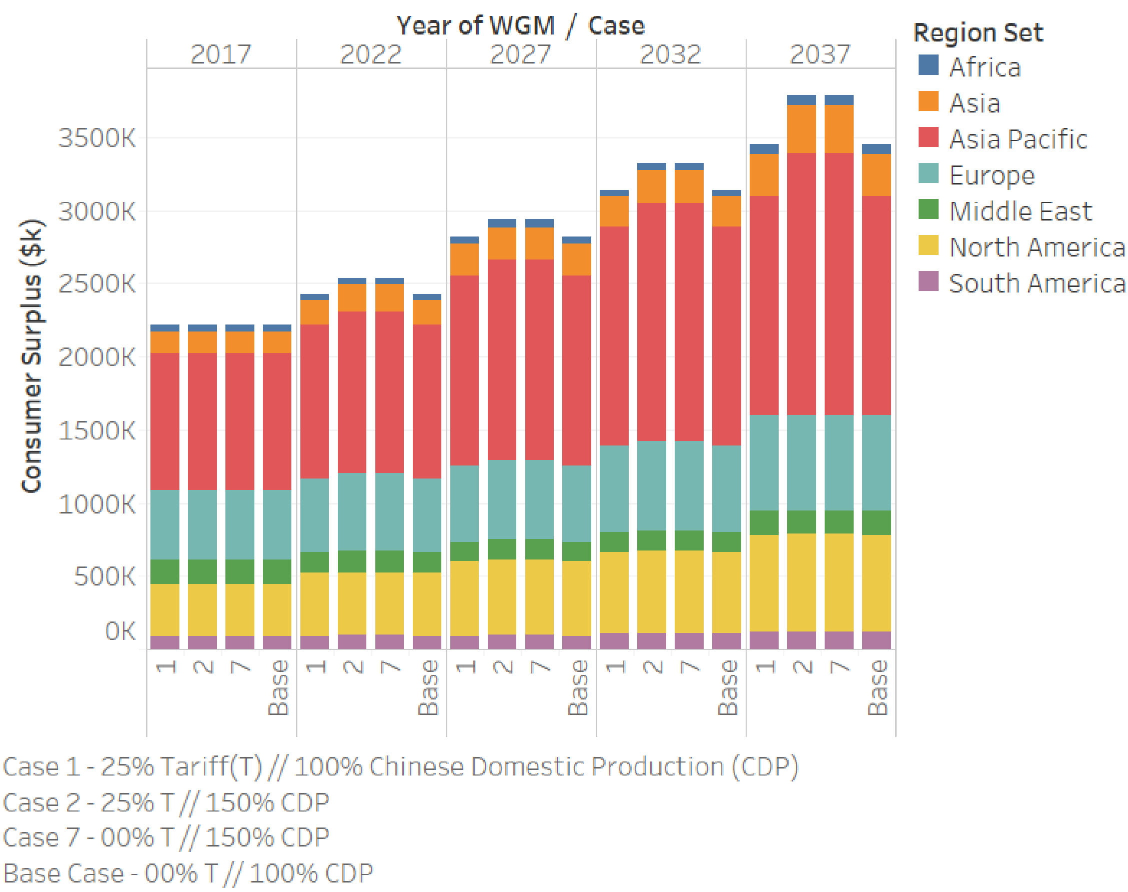

Figure 3.15: WGM Consumer Surplus by Region - U.S. China Trade War

The greatest global consumer surplus impact stems from a significant rise in domestic Chinese production irregardless of the trade war. China has motivation to boost natural gas production in an effort to decrease reliance on imports and when posed with an issue of a trade war with the world's biggest economy, the motivation increases. The results from the WGM demonstrate this as the consumer surplus for China greatly increases with a rise in domestic production levels to the level expressed earlier by the Chinese State Council (200 BCM/yr by 2020). The impact can be seen visually in Fig. 3.16, where the increase in consumer surplus can be directly attributed to the rise in production versus the rise in tariffs over the base case.

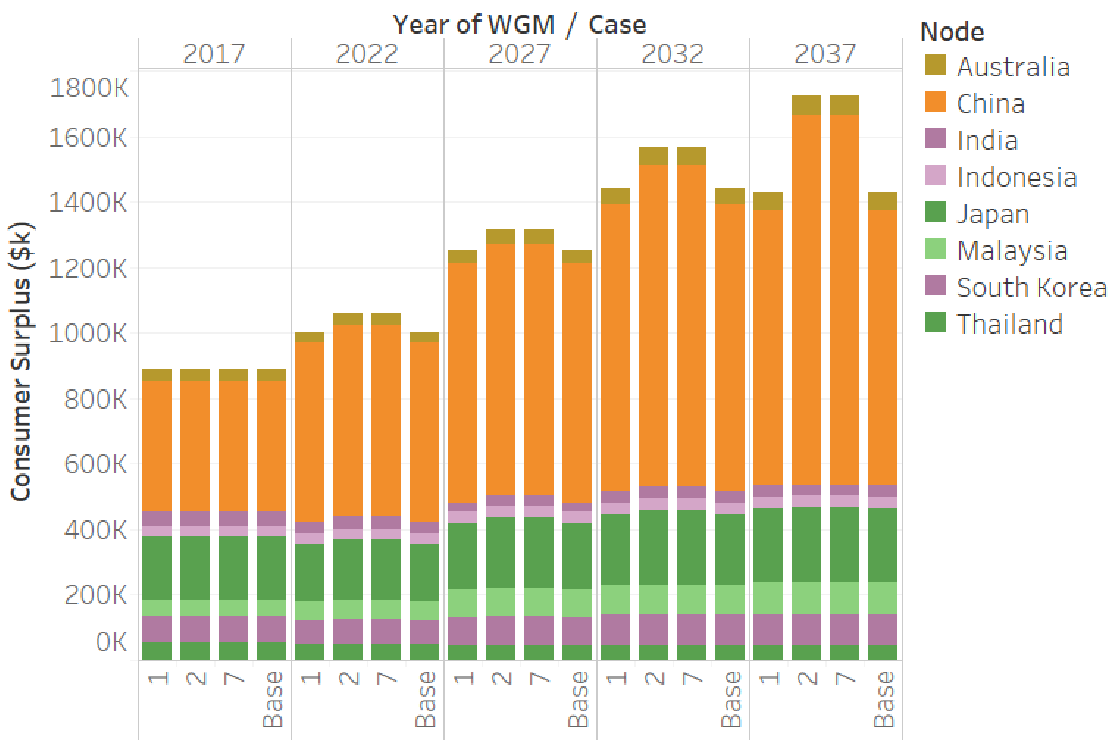

Case 1 - 25% Tariff(T) // 100% Chinese Domestic Production (CDP)
Case 2 - 25% T // 150% CDP
Case 7 - 00% T // 150% CDP
Base Case - 00% T // 100% CDP

Figure 3.16: WGM Consumer Surplus - China

The effects of Chinese production are seen globally, specifically in regions of high demand and low production such as Europe and the remainder of the Asia-Pacific. In Fig. 3.17 and Fig. 3.16, it can be seen that the improvement of the overall consumer surplus is felt strongly in these two regions correlating to an increase in Chinese production. The same level of impact is lessened in other regions of the world where production and net exports are greater. These results can be found visually in Appendix B.

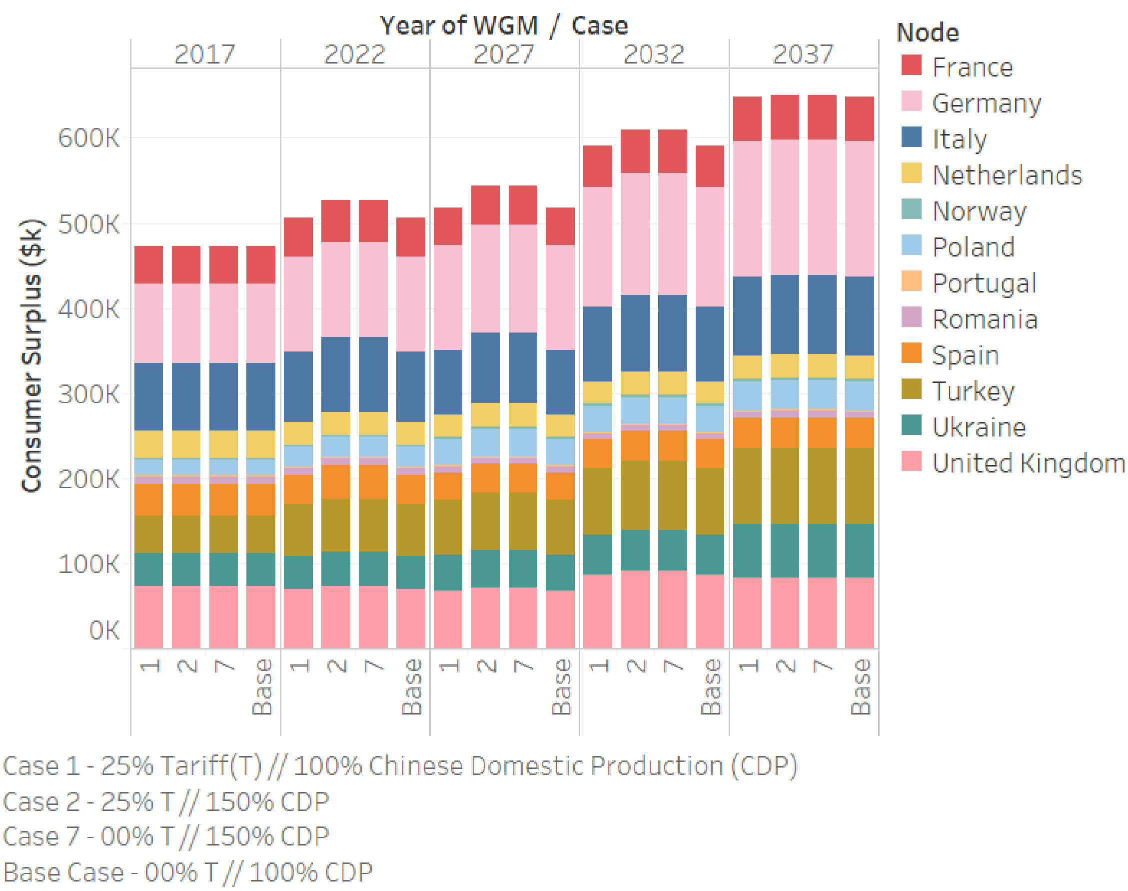

Figure 3.17: WGM Consumer Surplus - Europe

In conclusion, the rise in tariffs due to a prolonged trade war show minimal effect of the overall well-being of the natural gas economy. The significant aspect of the trade war is China's potential response to reduce reliance on exporting countries to avoid future trade conflicts. If China were to increase production levels as stated, it would be a net benefit to the world by measure of consumer surplus. The elevated Chinese production levels would also be negligible for the U.S. natural gas market as exporters would shift focus towards more local consumers with increased prices and demand.

3.2 U.S. Coast Guard LNG Inspection Workforce

3.2.1 Background

The United States Coast Guard (USCG) is the United States' oldest continuous sea-going service and represents one of the nation's five armed services. Comprised of 40,992 active duty military members and 8,577 civilian employees, as of 2018, and under the Department of Homeland Security, the USCG is charged with missions such as maritime security, law enforcement, search and rescue, and marine environmental protection. The Coast Guard has both an international and domestic presence divided into nine districts, Fig. 3.18, each deals with the duty of upholding the USCG's missions in their respective area of responsibility.

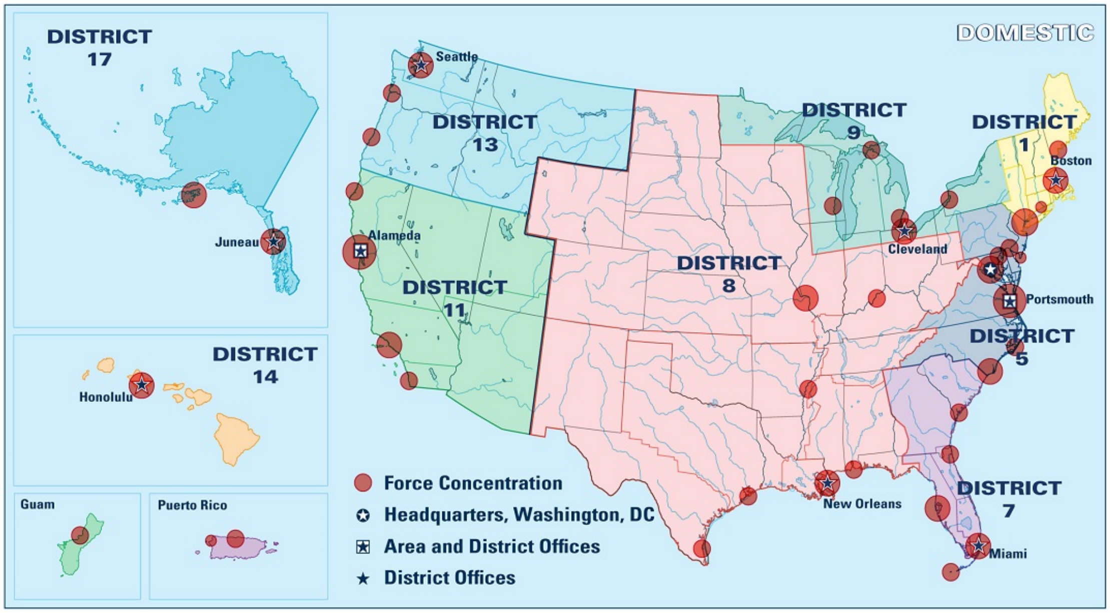

Figure 3.18: United States Coast Guard Domestic Force Lay-down[9]

An integral component to the nation's economy and national security is the regulation of commercial vessels in U.S. waters and ports. The regulation of commercial vessels falls under the responsibility of the Coast Guard throughout the nation's maritime domain. The Coast Guard boards and inspects, on average, 122 vessels per day and monitors the transit of 2,557 commercials ships throughout U.S. ports. This level of regulation requires an experienced and competent workforce in order to effectively ensure the safety and security of the commercial shipping industry, including transportation of LNG. As of 2019, "the Coast Guard's marine inspection staff consists of 533 military and 138 civilian personnel", 71 of whom are qualified and certified to conduct LNG vessel inspections, roughly 10.6% of the total marine inspection workforce [16]. Under the United States Code of Federal

Regulations (CFR) 46 CFR § 153, Every LNG vessel operating in U.S. national waters and ports is required to obtain an endorsed Certificate of Inspection and/or Compliance issued by the USCG. As of 2019, the Coast Guard's LNG inspection workforce was able to meet the demand of LNG inspections for all LNG vessels entering and leaving U.S. ports. However, the need for forecasting future workforce levels is critical in maintaining the degree of regulation required to keep the LNG industry safe and secure. As a government agency, understanding future budgetary needs is vital for the Coast Guard as the Coast Guard's budget is finite and has been in a "declining resource environment" [2]. With an average salary of $80,000USD, a qualified marine inspector requires significant amount of time and money on behalf of the Coast Guard to qualify and certify an efficient workforce. This comes at a critical time for the service as the LNG industry is growing at a fast rate as the number of commissioned vessels are increasing at a yearly rate and the size of the vessels are increasing as infrastructure and demand for natural gas increases around the world.

3.2.2 Objective

The objective of this case study is to analyze the future demand for Coast Guard LNG inspectors through utilization of the World Gas Model. With the World Gas Model, the cost for both the LNG industry and the Coast Guard will be determined. The relationship between the LNG industry and the Coast Guard's regulation therein will be analyzed through the use of additional complementarity conditions and variables specific to this case study. WGM results will be compared against current forecasting developed by the USCG Liquefied Gas Carrier National Center of Expertise (LGCNCOE).

3.2.3 Analysis & Results

In order to perform the analysis forecasting USCG workforce requirements, a new complementarity condition and variables were developed. First, the USCG's value of LNG vessel inspections was developed using the variable $USCG^B_{lm}$ which represents the yearly number of LNG vessel inspections completed ($\frac{\#vesselinspections}{year}$). This variable is computed for each time period based on a user-specified growth rate and on the Coast Guard's current inspection rate of $8\frac{inspections/yr}{\#ofinspectors}$. The Coast Guard LNG inspection rate was found through data provided by the LGCNCOE and computed from the total number of LNG inspections completed in 2017 and the number of active qualified LNG inspectors. Next, this rate is multiplied by the current number of certified LNG inspectors for the base year value. Future $USCG^B_{lm}$ values are determined via a growth rate formula based on a user-supplied growth rate.

The additional complementarity condition was placed into the WGM in order to model the relationship between the Coast Guard's inspection availability to the number of LNG inspections required by industry. The developed complementarity condition found in Eq. 3.2 represents an upper-bound to the amount of inspections required by industry subject to the availability of the number of USCG inspections for each time period in the model. The number of required inspections is found by taking the amount LNG to be transported by the LNG shipping operator $LNGFLOW^{B}_{crljdm}$ divided by vessel capacity $ShipCap^{C}_{c}$ which provides a unit of $(\frac{\#vesselinspections}{year})$ for computation of the complementarity condition, Eq. 3.2. The dual variable λ^{B}_{m} represents the congestion fee $\frac{\$USD}{vessel/yr}$ imposed on the LNG shipping operator implemented in Eq. 3.3. The units for this dual variable were determined by taking the units for the LNG shipping operator's objective function $discounted\$USD$ over the units of the complementarity condition $(\frac{\#vesselinspections}{year})$. Eq. 3.3 replaces the previously used LNG shipping operator's complementarity condition found in Appendix A, Eq. B1S for further computation in the WGM regarding the case study.

$$0 \leq USCG^{B}_{m} - \sum_{c,j,r,d,USA\epsilon L} \left(\frac{LNGFLOW^{B}_{crljdm}}{ShipCAP^{C}_{c}} \right) \perp \lambda^{B}_{m} \geq 0 \quad \forall m \tag{3.2}$$

$$0 \leq days_{d}\gamma_{m} \left\{ -\tau^{B}_{rljdm} + \left[\begin{matrix} \tau^{Ptoll}_{jdm} j\epsilon\{P_{canal}\} \\ \tau^{Stoll}_{jdm} j\epsilon\{S_{canal}\} \end{matrix} \right] \right\} + \left\{ \begin{matrix} C^{B}_{crljm} \\ +(2 \times Dist_{rlj} \times \alpha^{B}_{cdm}) \\ +(\lambda^{B}_{m} \times ShipCAP^{C}_{c}) \end{matrix} \right\} \perp SALES^{B}_{crljdm} \geq 0 \quad \forall c,d,m \tag{3.3}$$

Several cases were designed in order to properly analyze the full extent of the Coast Guard's future LNG inspection workforce forecast. In Fig. 3.19, the various cases designed are represented in terms of their defining factor, LNG inspection workforce growth rate per annum. Case studies were selected around the USCG

LGCNCOE's current use of 7.5% growth rate per annum used to forecast future LNG inspection workforce needs [63].

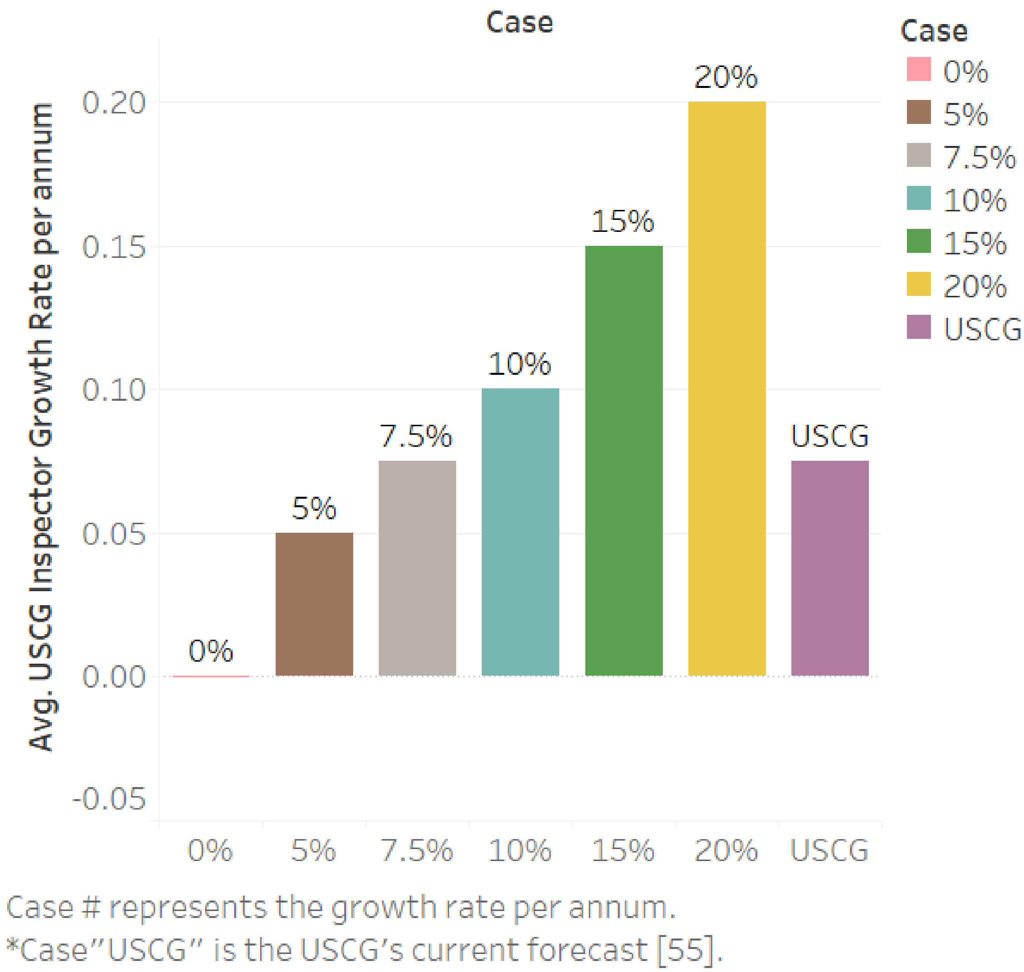

Figure 3.19: USCG Case Study Breakdown

First, the number of inspections per year determined as a result from the WGM was analyzed in order to further understand the workforce demand imposed on the Coast Guard by the LNG industry.[2] In Fig. 3.20, the number of inspections increase per year by case in relation to the rise in the growth rate of the USCG

[2]The USCG number of inspections are based on a provided forecast from the USCG LGCNCOE up to 2022, future number of inspections were extrapolated out to 2032.

inspection workforce. This implies that with an increasing rate of growth by the USCG inspection workforce, industry will be able to grow at a greater rate in relation and provides a connection between the USCG workforce and the LNG industry.

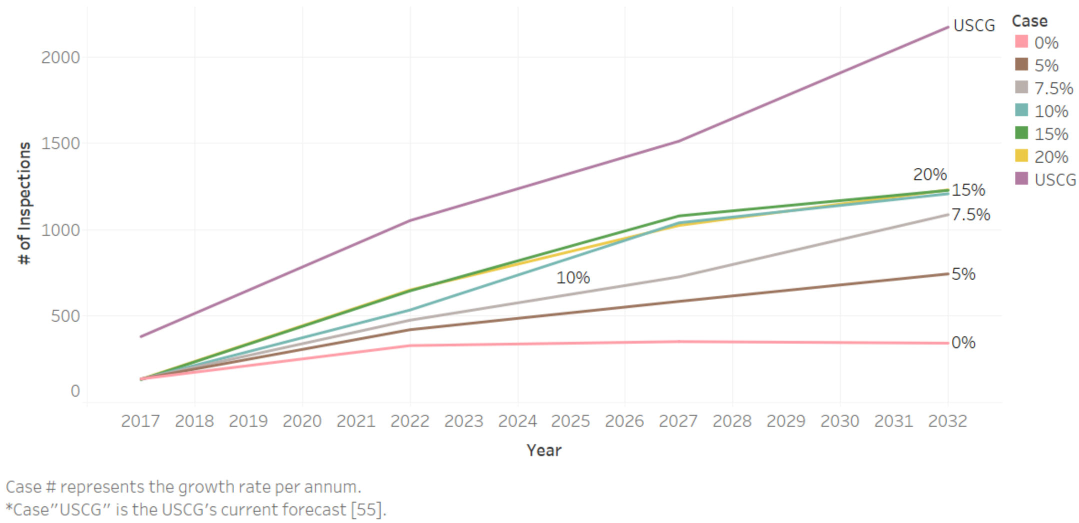

Figure 3.20: Number of USCG Inspections by Year & Case

Moving forward in the analysis, the determined number of inspectors as a result of the WGM was analyzed in order to further understand the implications of the Coast Guard's current forecasting against the results from the WGM. In Fig. 3.21, the number of required inspectors for the "USCG" case represents the number forecasted by the LGCNCOE. Comparative to the "USCG" case, cases 20, 15 and 10 demonstrate similar results found in Fig. 3.20. The results indicate that as the USCG workforce grows at a faster rate, industry's demand on the USCG, in the form of the number of LNG inspections required, also increases at at more accelerated rate. A conclusion made from Fig. 3.21 is that the USCG's workforce forecasting, with a growth rate of 7.5% per annum, is on par with the WGM results from case

"7.5" demonstrating validity of results found by the WGM.

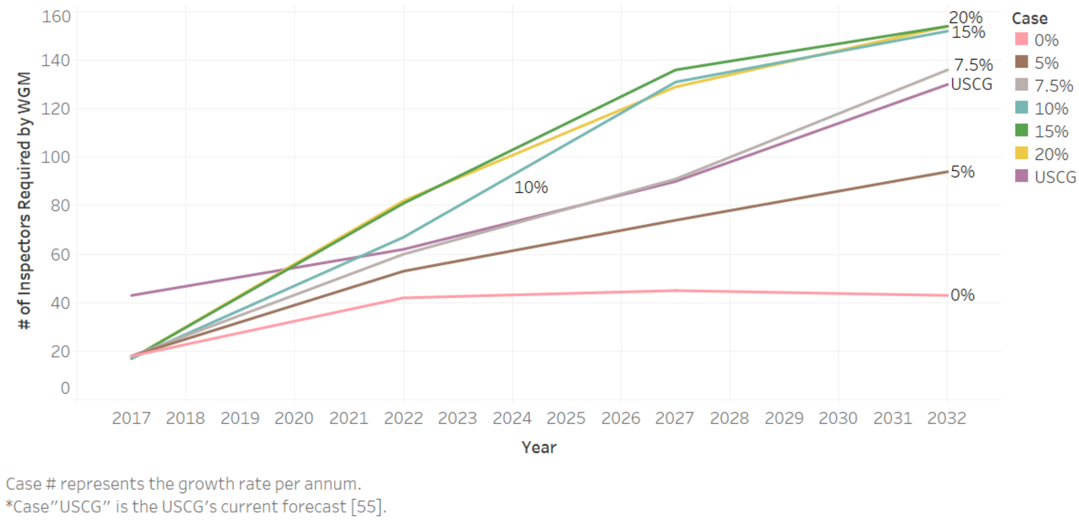

Figure 3.21: Number of Required USCG Inspectors by Year & Case

In order to properly understand the relationship between the USCG LNG inspection workforce and the effect of it's growth on the LNG industry, an analysis on the dual variable, λ_m^B representing the congestion fee $\frac{\$USD}{vessel/yr}$ imposed on LNG shipping operators, must be made.

In Fig. 3.22, it is shown that as the USCG's LNG inspection workforce grows at a rate ≥ 15% per annum, the dual variable remains at zero. With $\lambda_m^B = 0$, the effects of the additional KKT condition and constraint, Eqs. 3.2 and 3.3, are negligible as the nature of complementarity constraints dictate that if the constraint is not active, the dual variable goes to zero, meaning that the gas market is unaffected by the additional constraint imposed by the USCG conditions in the WGM. This is significant when compared to the dual variable's values for growth rates ≤ 10% per annum, where the imposed cost on the LNG shipping operator spans from \$6k

USD to $20k USD. What this means for both industry and the USCG is that in order for the USCG to enable the LNG industry to grow unrestricted with the requirement of LNG vessel inspections, the USCG LNG inspection workforce must grow somewhere between 33% and 100% greater than that of which it currently forecasts. If the USCG, according to WGM results, were to continue to expand it's LNG inspection workforce at the current forecasted rate of 7.5%, case 7.5%, it would impose a cost, in the form of time and/or money, on industry and inhibit a degree of growth desired by industry.

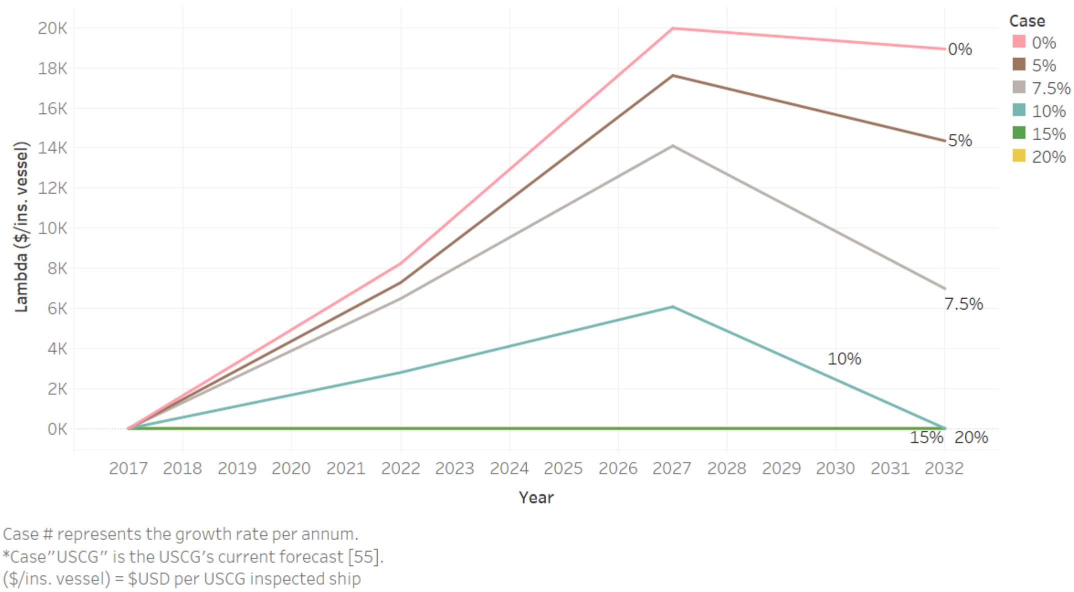

Figure 3.22: USCG Inspection Congestion Fee by USCG Case Study & Year

The major takeaway from this case study is that if the Coast Guard seeks to meet industry's demand with enough inspectors so that industry is not constrained by the availability of inspections, the Coast Guard LNG inspection workforce must grow at a rate between 10% and 15% anywhere from 33% - 100% greater than what *is currently being forecasted by the USCG*. This can be seen visually through Fig. 3.23, where the median[3] number of inspectors available represents the availability of inspectors by the USCG when the workforce is grown at the respective case growth rate versus the median number of required inspectors as a result from industry's demand determined by the WGM. Only considering the increase in payroll expenses, the disparity between the Coast Guard's planned workforce growth rate and minimal required growth rate determined via results from WGM is equivalent to an increase in over $1.4 Million USD to the USCG's annual operating budget[4]. This number increases significantly when factoring in the additional costs of training, health care, and operational expenses that come with an increase in workforce size.

[3]Median taken instead of average in an effort to avoid skewness due to the limited number of data points

[4]The FY 2020 President's Budget requests $11.34 billion for the Coast Guard, including $9.32 billion in discretionary funding [62].

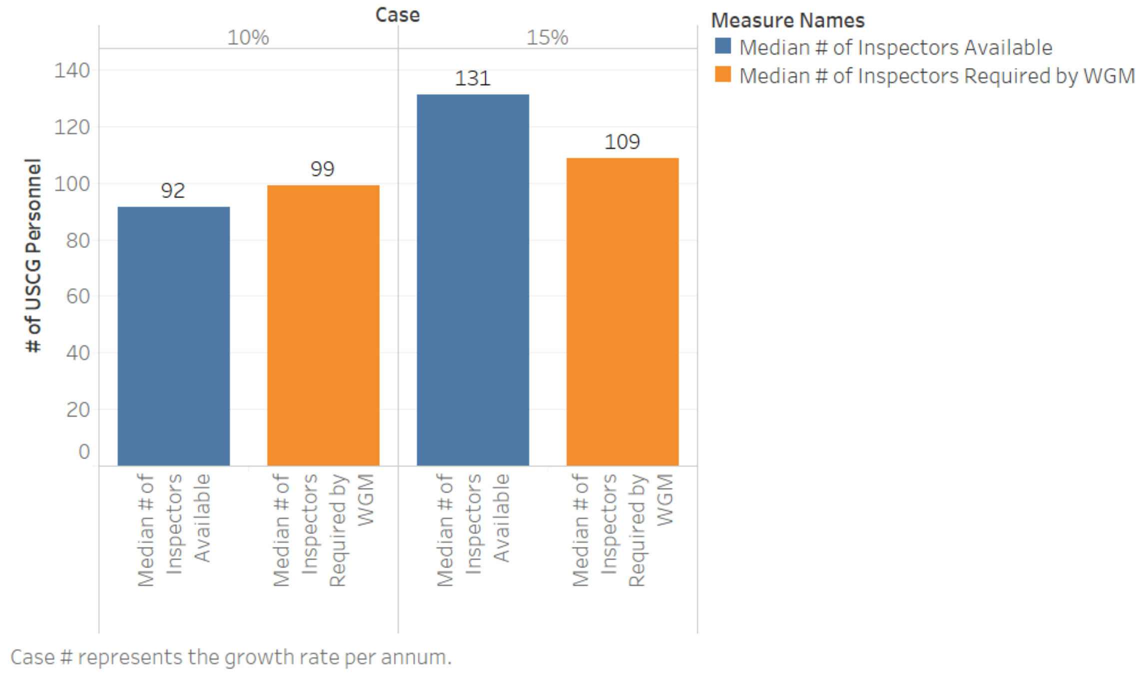

Figure 3.23: Required vs. Available Number of Inspectors

3.2.3.1 USCG & U.S.-China Trade War

Highlighting the flexibility and capability of the WGM, the two case studies discussed in the thesis are briefly analyzed in regards to the effect of the U.S.-China trade war on the Coast Guard's LNG inspection workforce. In Fig. 3.24, it can be seen that while subject to the most restrictive conditions found in the U.S. - China trade war case study,[5] the USCG's forecasted LNG inspection workforce's effect on the LNG industry remains unchanged as demonstrated by the determined values of the WGM's dual variable, λ_m^B.

[5] Case 2: 25% tariff on U.S. imports to China w/ 150% of reference Chinese domestic production

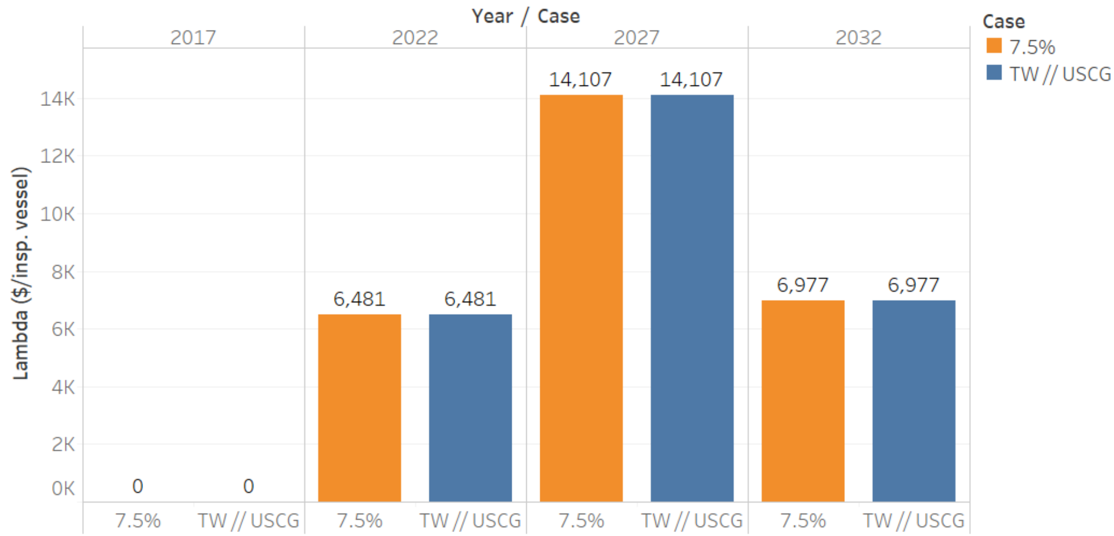

Case 7.5 = 7.5% growth rate per annum of USCG LNG Inspection Workforce

TW // USCG = 7.5% growth rate per annum for LNG workforce under the conditions of Case 2 in U.S. - China Trade War case study (25% Tariff // 150% Chinese Domestic Production)

($/insp. vessel) = $USD per inspected LNG vessel

Figure 3.24: USCG Case Study Results under Case 2 of Trade War

Chapter 4: Summary

4.1 Summary of Results

This thesis explored the uses of mixed complementary modeling specifically through deployment of the WGM. Exploring the dynamics of the U.S.-China Trade War in 2019, the WGM determined the short and long term effects of a prolonged trade war under several different scenarios. The overall results of this case study illustrated the tariff imposed by China on U.S. LNG exports does not hold any significance directly to the U.S. or China regardless of the tariff amount. The only visible effect that can be seen as a direct result of the tariffs would be an increase in alternative LNG sourcing by China, most notably Australia and the United States' refocus of LNG exports towards other markets of high profitability such as Japan. The most significant result that came from the case study was the global effect of an increase in Chinese domestic natural gas production. It was shown that a production increase to levels prescribed by the Chinese State Council would result in a rise in consumer surplus around the world, most significantly for countries with high levels of natural gas imports. In conclusion, the major result that can be drawn from the successful WGM analysis into the U.S. and China trade war is that while the tariffs do restrict the amount of LNG flow from the U.S. to China, the tariffs hold no adverse effect on either country; however, the geopolitical consequences that could arise and elevate China's motivation to increase domestic gas production are of greater significance for the entire global market.

The use of the WGM to analyze future workforce demands demonstrated the flexibility and capability of the WGM to be used in a variety of applications beyond previous conventional use. Through the case study, the WGM determined the significance of the U.S. Coast Guard's growth of it's LNG inspection workforce. This was shown through comparison of current USCG forecasting statistics and the output of the WGM. Made successful through the use of additional KKT conditions and variables never previously implemented into the WGM. The significance of the results come at a time when the Coast Guard is subject to a declining resource environment [2] and is regularly competing for additional funding from congress while amidst a growing LNG industry [16]. In conclusion, the USCG LNG inspection workforce should grow at a rate or otherwise increase the efficiency of inspections at a greater rate than currently performed and forecasted in order to avoid an adverse effect on the LNG industry through vessel inspection availability.

4.2 Contributions

The principal contributions that this thesis provides are of benefit for individuals in both the energy industry and academia. One of the major contributions is the modernization and further development of the WGM, which is one of the few MCP models that is able to accurately employ imperfect competition in modeling of the global natural gas market. The use of a mixed complementarity problem model to forecast the short-term and long-term effects of a prolonged trade war between the United States and China demonstrates the applicability of the WGM to address some of the major issues facing the natural gas industry as they arise, benefiting those seeking to understand the future implications of real-time events and decisions. This research has also demonstrated the flexibility of the WGM and broadened the range of stakeholders surrounding the modeling of the gas market through the analysis performed for the USCG LNG inspection workforce. This analysis has provided a new lens and way of thinking surrounding use of the WGM for decision making and forecasting.

4.3 Future Work

Implementing USCG or a fellow government player representing a regulatory stakeholder within the natural gas market is the source of continue WGM expansion and development. The case study regarding USCG workforce forecasting uncovered potential for development of an additional player that interacts with other players in the market through regulatory fees. This player could hold weight in all facets of the natural gas supply chain placing taxes on industry in the form of "green" initiatives and other political agendas as well as regulatory fees as seen in the USCG case study.

Expanding the endogenous market access decisions are a continued source for further development. This area of research could focus on developing country decisions to expand or contract the variety of players within their domestic market as well as their level of market access. Endogenous decision making expansion could include pipeline creation, player additions & subtraction, and new market access points. The benefit from further research into endogenous decision making could potentially help identify potential areas for global gas market development, therefore benefiting the entire gas ecosystem.

As a result of the thesis research process and further understanding of the WGM an opportunity to further increase the WGM's depiction of the real-world gas market would be to integrate source diversity variables for importing and exporting countries. The diversity variables could act similar to the WGM's unique market power variables. These diversity variables could help model some of the non-optimal decisions made by players in regards to natural gas trade. For example, the implementation would help analyze the effects of Japanese LNG import source diversity as a function of increasing resiliency and lowering the lack of dependency on one individual LNG source.

Recent events in 2020 have unfolded the inter-dependency of the global supply chain and underlying volatility of the natural gas markets. Future research in relation to the WGM and mixed complementary modeling could revolve around better forecasting of short and long-term economic effects surrounding pandemics and global financial crises.

Appendix A: Karush-Kuhn-Tucker & Market-Clearing Conditions

A.1 KKT - Producer

$$0 \leq days_d \left\{ \gamma_m \left[-\pi_{n(p)dm} + C^P_{pm} \right] + \beta^P_{pm} \right\} + \alpha_{pdm} \perp SALES^P_{pdm} \geq 0 \quad \forall d, m \tag{P1}$$

$$0 \leq CAP^{PR}_{pm} - days_d \left\{ SALES^P_{pdm} \right\} \perp \alpha_{pdm} \geq 0 \quad \forall d, m \tag{P2}$$

$$0 \leq CAP^{PH}_{pm} - days_d \left\{ SALES^P_{pdm} \right\} \perp \beta^P_{pdm} \geq 0 \quad \forall d, m \tag{P3}$$

A.1.1 Market Clearing - Producer

$$0 = days_d \left\{ SALES^P_{pdm} - PURCH^{P \to T}_{tndm} - PURCH^{P \to L}_{lndm} \right\} \perp \pi^P_{n(p)dm} \geq 0 \quad \forall d, m \tag{MCC P}$$

A.2 KKT - Trader

$$0 \leq days_d \left\{ \gamma_m \left[\begin{smallmatrix} \delta^C_{tn} SLP^M_{ndm} SALES^T_{tndm} \\ -\left(\delta^C_{tn} \Pi^{W(t)}_{ndm} + (1-\delta^C_{tn}) \pi^W_{ndm}) \right) \end{smallmatrix} \right] \right\} + \phi^T_{tndm} \perp SALES^T_{tndm} \geq 0 \quad \forall n, d, m \tag{T Sales}$$

$$0 \leq days_d \left\{ \gamma_m \left[\pi_{n(p)dm} \right] \right\} - \phi^T_{tndm} \perp PURCH^{P \rightarrow T}_{pdm} \geq 0 \quad \forall d, m \tag{P→ T Purch}$$

$$0 \leq days_d \left\{ \gamma_m \left[\pi_{n(r)dm} \right] \right\} - \phi^T_{tndm} \perp PURCH^{R \rightarrow T}_{rdm} \geq 0 \quad \forall d, m \tag{R→ T Purch}$$

$$0 \leq days_d \left\{ \gamma_m \left[\tau^{SI}_{ndm} \right] \right\} + \phi^T_{tndm} - (1 - loss_n) days_d \phi^S_{tnm} \perp INJ^T_{tndm} \geq 0 \quad \forall d, m \tag{T → S Inj}$$

$$0 \leq days_d \left\{ \gamma_m \left[\tau^{SX}_{ndm} \right] \right\} + \phi^T_{tndm} + days_d \phi^S_{tnm} \perp XTR^T_{tndm} \geq 0 \quad \forall d, m \tag{S → T Xtr}$$

$$0 \leq days_d \left\{ \gamma_m \left[\tau^{A}_{adm} \right] \right\} + \phi^T_{tndm} - (1 - loss_a) days_d \phi^T_{tnm} \perp FLOW^T_{tndm} \geq 0 \quad \forall d, m \tag{Trade Flow}$$

$$\left[\begin{smallmatrix} PURCH^{P \rightarrow T}_{tndm} \\ +PURCH^{R \rightarrow T}_{tndm} \\ -INJ^T_{tndm} \\ +XTR^T_{tndm} \\ -SALES^T_{tndm} \end{smallmatrix} \right] + \sum_{a \epsilon a^+(n)} (1 - loss_a) FLOW^T_{tndm} - \sum_{a \epsilon a^-(n)} FLOW^T_{tndm} \perp \phi^T_{tndm} \geq 0 \quad \forall n, d, m \tag{Mass Balance}$$

$$(1 - loss_a) \sum_{d \epsilon D} days_d INJ^T_{tndm} - \sum_{d \epsilon D} days_d XTR^T_{tndm} \perp \phi^S_{tndm} \geq 0 \quad \forall n, d, m \tag{Storage Cycle}$$

A.3 KKT - Liquefier

$$0 \leq days_d \left\{ \gamma_m \begin{bmatrix} -\pi^L_{nldm} \\ +C^L_l m \end{bmatrix} \right\} + \alpha^L_{ldm} + \phi^L_{ldm} \perp SALES^L_{ldm} \geq 0 \quad \forall d, m \tag{L1}$$

$$0 \leq days_d \left\{ \gamma_m \left[-\pi^P_{ndm} \right] \right\} - (1 - loss_l)\phi^L_{ldm} \perp PURCH^{L \leftarrow P}_{ldm} \geq 0 \quad \forall d, m \tag{L2}$$

$$0 \leq CAP^L_l - SALES^L_{ldm} + \sum_{m' < m} \triangle^L_{lm'} \perp \alpha^L_{ldm} \geq 0 \quad \forall d, m \tag{L3}$$

$$0 \leq (1 - loss_l) PURCH^{L \leftarrow P}_{ldm} - SALES^L_{ldm} \perp \phi^L_{ldm} \geq 0 \quad \forall d, m \tag{L4}$$

$$0 \leq \gamma_m b^L_l m - \sum_d \sum_{m' > m} \alpha^L_{ldm} + \rho^L_{lm} \perp \triangle^L_{lm} \geq 0 \quad \forall m \tag{L Investment}$$

$$0 \leq \overline{\triangle}^L_{lm} - \triangle^L_{lm} \perp \rho^L_{lm} \geq 0 \quad \forall m \tag{L Capacity}$$

A.3.1 Market Clearing - Liquefier

$$0 = days_d \left\{ \sum_{l \epsilon L} SALES^L_{ldm} - \sum_{r \epsilon R} \sum_{j \epsilon J} LNGFLOW^{R \leftarrow L}_{rljdm} \right\} \perp \pi^L_{ldm} \geq 0 \quad \forall l, d, m \tag{MCC L}$$

A.4 LNG Shipping Operator

$$0 \leq days_d \gamma_m \left\{ -\tau^B_{rljdm} + \left[\begin{matrix} \tau^{Ptoll}_{jdm} j\epsilon\{P_{canal}\} \\ \tau^{Stoll}_{jdm} j\epsilon\{S_{canal}\} \end{matrix} \right] \right\} + \left\{ \begin{matrix} C^B_{crljm} \\ +(2 * Dist_{rlj} * \alpha^B_{cdm}) \end{matrix} \right\} \perp SALES^B_{crljdm} \geq 0 \quad \forall c, d, m \tag{B1S}$$

$$0 \leq \left(CAP^B_c * MaxDist_c \right) - \sum_{r,l,j} \left(LNGFLOW^B_{crljdm} * Dist_{rlj} \right) \perp \alpha_{cdm} \geq 0 \quad \forall c, d, m \tag{Boat}$$

$$0 \leq \left(\gamma_m \beta^B_m \right) - \sum_{d,m' > m} \left(MaxDist_c * \alpha^B_c dm \right) + \rho^B_{cm} \perp \triangle_{crm} \geq 0 \quad \forall c, d, m \tag{Investment}$$

$$0 \leq \overline{\triangle}^B_{cm} - \triangle^B_{cm} \perp \rho^B_m \geq 0 \quad \forall m \tag{Capacity}$$

$$0 \leq USCG^B_{lm} - \sum_{c,j,r,d} \left(\frac{LNGFLOW^B_{crljdm}}{ShipCAP^C_c} \right) \perp \lambda^B_{lm} \geq 0 \quad \forall l, m \tag{USCG}$$

A.4.1 Market Clearing - LNG Shipping Operator

$$0 = \sum_{c\epsilon C} SALES^B_{crljdm} - LNGFLOW_{rljdm} \perp \tau^B_{dm} \geq 0 \quad \forall d, m \tag{MCC B}$$

A.5 Regasifier

$$0 \leq \gamma_m Days_d \left(C^R_{rm} - \pi^R_{rdm} \right) + \alpha^R_{rdm} + \phi^R_{rdm} \perp SALES^{R \to M}_{rndm} \geq 0 \quad \forall dm \tag{R1M}$$

$$0 \leq \gamma_m Days_d \left(C^R_{nm} - \pi^R S_{ndm} \right) + \alpha^R_{ndm} + \phi^R_{ndm} \perp SALES^{R \to T}_{rndm} \geq 0 \quad \forall d, m \quad \text{(R1T)}$$

$$0 \leq \gamma_m Days_d \left(\pi^L_{ldm} + \tau^B_{rljdm} \right) + \epsilon^R_{rldm} + \left([1 - Loss^R] * [1 - Loss^B] \right) \phi^R_{rdm} \quad \text{(R2)}$$
$$\perp LNGFLOW^R_{rljdm} \geq 0 \quad \forall d, m$$

$$0 \leq \gamma_m \triangle^R_{rm} - \alpha^R_{rdm} + \rho^R_{rm} \perp CAP^R_{rm} \geq 0 \quad \forall d, m \quad \text{(R Inv)}$$

$$0 \leq \overline{CAP}^R_{rm} - CAP^R_{rm} \perp \rho^R_{rm} \geq 0 \quad \forall m \quad \text{(R CAP)}$$

$$0 \leq CAP^R_{rm} + \sum_{m' > m} \triangle^R_{rm'} - SALES^{R \to T}_{rdm} - SALES^{R \to M}_{rdm} \perp \alpha^R_{rdm} \geq 0 \quad \forall d, m \quad \text{(R3)}$$

$$0 \leq \sum_{l,j} \left\{ \left([1 - Loss^R] * [1 - Loss^B] \right) LNGFLOW^R_{rljdm} \right\} \quad \text{(R4)}$$
$$- SALES^{R \to T}_{rdm} - SALES^{R \to M}_{rdm} \perp \phi^R_{rdm} \geq 0 \quad \forall d, m$$

$$0 \leq \sum_{r,l,j} LNGFLOW^R_{rljdm} - LNGDest^R_{lrm} \perp \epsilon^R_{rdm} \geq 0 \quad \forall d, m \quad \text{(R Contracts)}$$

A.5.1 Market Clearing - Regasifier

$$0 = \sum_r SALES^{R \to T}_{rdm} - \sum_t PURCH^{T \leftarrow R}_{tndm} \perp \pi^{RS}_{ndm} \geq 0 \quad \forall d, m \quad \text{(MCC R)}$$

A.6 Storage Operator

$$0 \leq -days_d \gamma_m \left(\tau^{SI}_{sdm} - C^{S}_{sm} \right) + \alpha^{SI}_{sdm} \perp SALES^{SI}_{sdm} \geq 0 \quad \forall d, m$$

(Sales Storage Injection)

$$0 \leq -days_d \gamma_m \left(\tau^{SX}_{sdm} - C^{S}_{sm} \right) + \alpha^{SX}_{sdm} + days_d \alpha^{SW}_{sdm} \perp SALES^{SX}_{sdm} \geq 0 \quad \forall d, m$$

(Sales Storage Extraction)

$$0 \leq \gamma_m \beta^{S} I_{sm} - \sum_{d \epsilon D, m' > m} \alpha^{SI}_{sdm} \perp \triangle^{SI}_{sm} \geq 0 \quad \forall m$$

(Injection Capacity Expansion Investment)

$$0 \leq \gamma_m \beta^{S} X_{sm} - \sum_{d \epsilon D, m' > m} \alpha^{SX}_{sdm} \perp \triangle^{SX}_{sm} \geq 0 \quad \forall m$$

(Extraction Capacity Expansion Investment)

$$0 \leq \gamma_m \beta^{S} W_{sm} - \sum_{d \epsilon D, m' > m} \alpha^{SW}_{sdm} + \rho^{SW}_{sm} \perp \triangle^{SW}_{sm} \geq 0 \quad \forall m$$

(Working Capacity Expansion Investment)

$$0 \leq \triangle^{SI}_{sm} + \sum_{m' > m} \overline{CAP}^{SI}_{sm} - SALES^{SI}_{sdm} \perp \alpha^{SI}_{sdm} \geq 0 \quad \forall d, m \quad \text{(Injection Capacity)}$$

$$0 \leq \triangle^{SX}_{sm} + \sum_{m' > m} \overline{CAP}^{SX}_{sm} - SALES^{SX}_{sdm} \perp \alpha^{SX}_{sdm} \geq 0 \quad \forall d, m \quad \text{(Extraction Capacity)}$$

$$0 \leq \triangle^{SW}_{sm} + \sum_{m' > m} \overline{CAP}^{SW}_{sm} - SALES^{SW}_{sdm} \perp \alpha^{SW}_{sdm} \geq 0 \quad \forall d, m \quad \text{(Working Capacity)}$$

$$0 \leq \overline{CAP}^{SW}_{sm} - CAP^{SW}_{sm} \perp \rho^{SW}_{sm} \geq 0 \quad \forall m \qquad \text{(Working Expansion)}$$

A.6.1 Market Clearing - Storage Operator

$$0 = \sum_{s \epsilon S} SALES^{SI}_{sdm} - \sum_{t \epsilon T} INJ^{T}_{tndm} \perp \tau^{SI}_{sdm} \geq 0 \quad \forall d, m \quad \text{(MCC Storage Injection)}$$

$$0 = \sum_{s \epsilon S} SALES^{SX}_{sdm} - \sum_{t \epsilon T} XTR^{T}_{tndm} \perp \tau^{SX}_{sdm} \geq 0 \quad \forall d, m \quad \text{(MCC Storage Extraction)}$$

A.7 Canal Operator

$$0 \leq days_d \gamma_m \left(-\tau^{Pcanal}_{pcanal,d,m} - C^{Pcanal}_{pcanal,d,m} \right) + \alpha^{Pcanal}_{pcanal,d,m} \perp SALES^{Pcanal}_{pcanal,d,m} \geq 0 \quad \forall d, m \tag{C1P}$$

$$0 \leq CAP^{Pcanal}_{pcanal,d,m} - SALES^{Pcanal}_{pcanal,d,m} \perp \alpha^{Pcanal}_{pcanal,d,m} \geq 0 \quad \forall d, m \tag{C2P}$$

$$0 \leq days_d \gamma_m \left(-\tau^{Scanal}_{scanal,d,m} - C^{Scanal}_{scanal,d,m} \right) + \alpha^{Scanal}_{scanal,d,m} \perp SALES^{Scanal}_{scanal,d,m} \geq 0 \quad \forall d, m \tag{C1S}$$

$$0 \leq CAP^{Scanal}_{scanal,d,m} - SALES^{Scanal}_{scanal,d,m} \perp \alpha^{Scanal}_{scanal,d,m} \geq 0 \quad \forall d, m \tag{C2S}$$

A.7.1 Market Clearing - Canal Operator

$$0 = SALES^{Pcanal}_{pcanal,d,m} - LNGShip^{B}_{large \notin C,r,l,pcanal,d,m} \perp \tau^{Pcanal}_{pcanal,d,m} \geq 0 \quad \forall d, m \quad \text{(MCC Panama Canal)}$$

$$0 = SALES^{Scanal}_{scanal,d,m} - LNGShip^{B}_{large \notin C,r,l,scanal,d,m} \perp \tau^{Scanal}_{scanal,d,m} \geq 0 \quad \forall d, m$$

(MCC Suez Canal)

A.8 Transmission System Operator

$$0 \leq days_d \gamma_m (-\tau^A_{adm}) + \alpha^A_{adm} \perp SALES^A_{adm} \geq 0 \quad \forall d, m \tag{A1}$$

$$0 \leq CAP^A_{am} + \triangle^A_{am} - SALES^A_a dm \perp \alpha^A_{adm} \geq 0 \quad \forall d, m \tag{A2}$$

$$0 \leq \overline{CAP}^A_{am} - CAP^A_{am} \perp \rho^A_{am} \geq 0 \quad \forall d, m \tag{A Capacity}$$

$$0 \leq \gamma_m \left[\sum_{d \epsilon D} (days_d \tau^A_{adm}) + \beta^A_{am} \right] + \rho^A_{am} \perp CAP^A_{am} \geq 0 \quad \forall d, m \tag{A Investment}$$

A.8.1 Market Clearing - Transmission System Operator

$$0 = SALES^A_{adm} - \sum_{t \epsilon T} FLOW^T_{tadm} \perp \tau^A_{adm} \geq 0 \quad \forall d, m$$

(MCC Transmission System Operator)

A.9 Market Clearing - Marketer

$$\pi^W_{ndm} = INT^W_{ndm} + SLP^W_{ndm} \left(\sum_{t \epsilon T} SALES^T_{tndm} + \sum_{r \epsilon R} SALES^{R \to M}_r ndm \right) \geq 0 \quad \forall d, m \quad (\pi^W_{ndm})$$

(MCC Marketer)

Appendix B: Figures

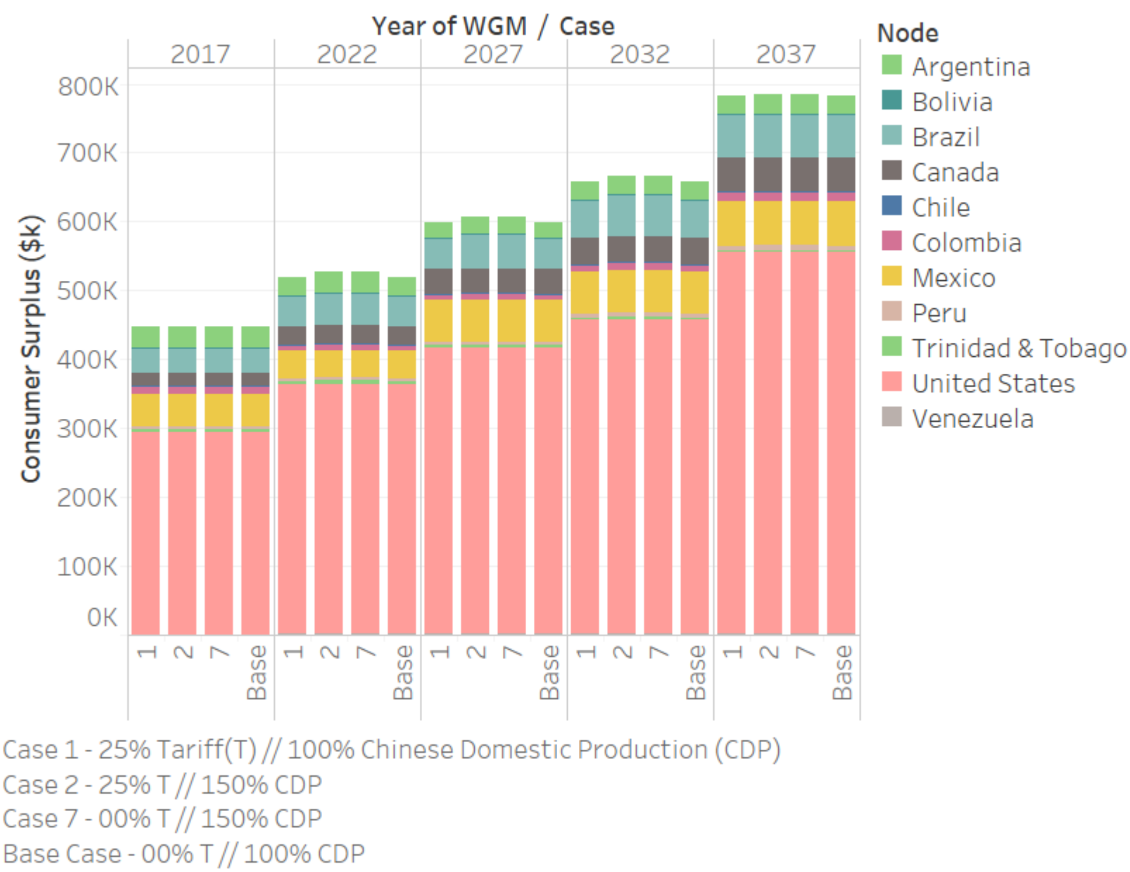

Figure B.1: WGM Consumer Surplus - Americas

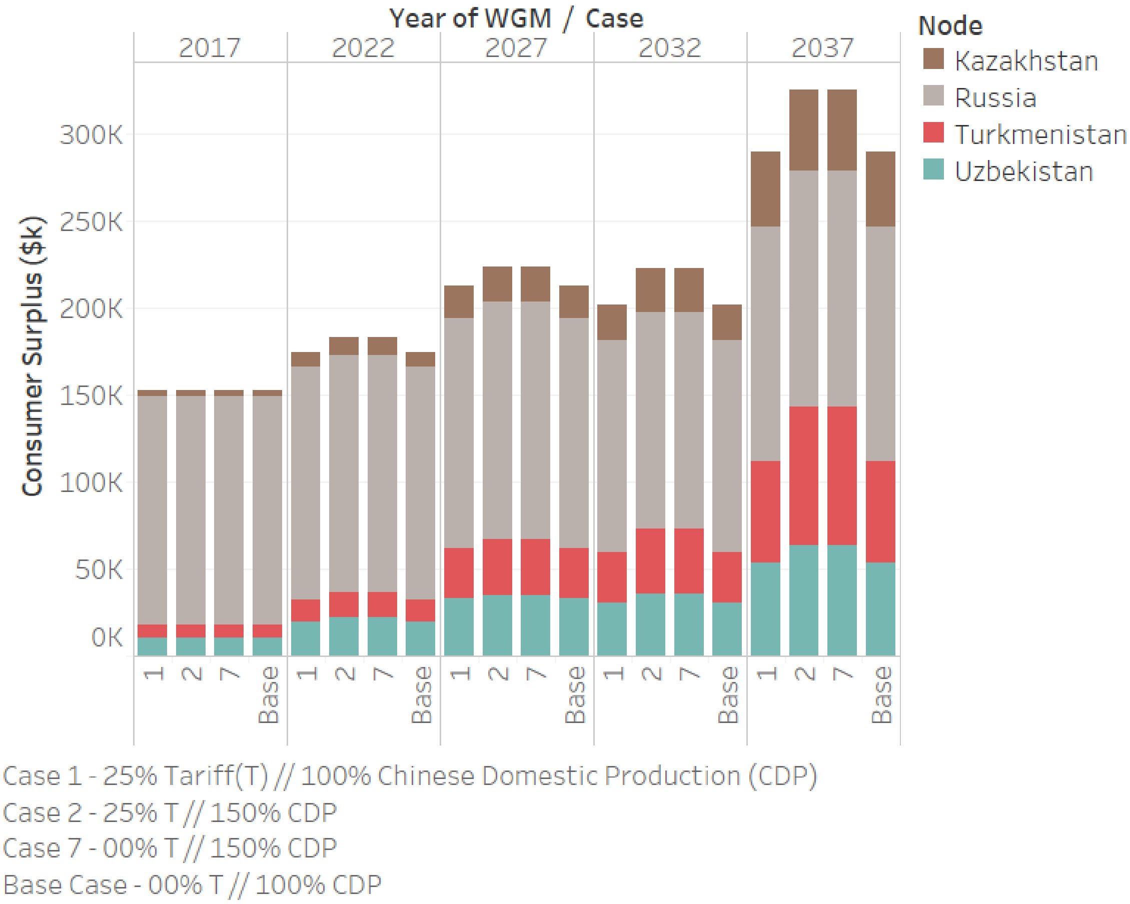

Figure B.2: WGM Consumer Surplus - Central Asia

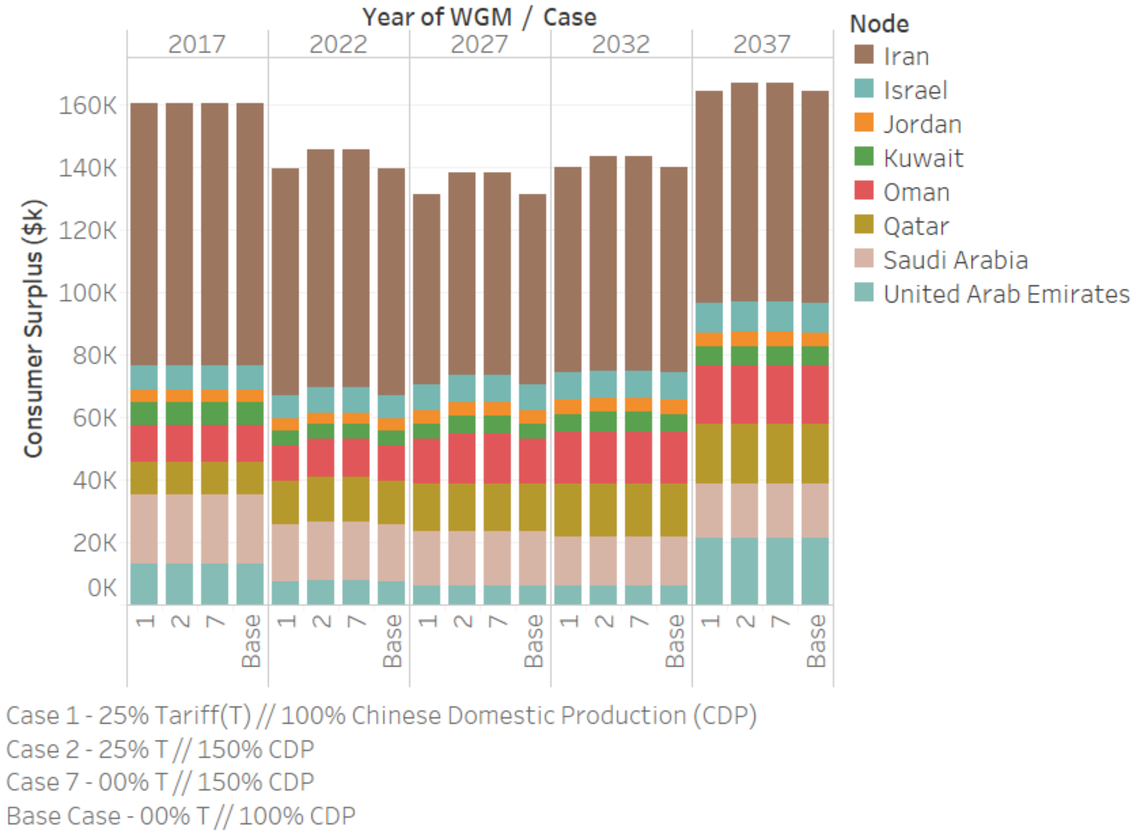

Figure B.3: WGM Consumer Surplus - Middle East

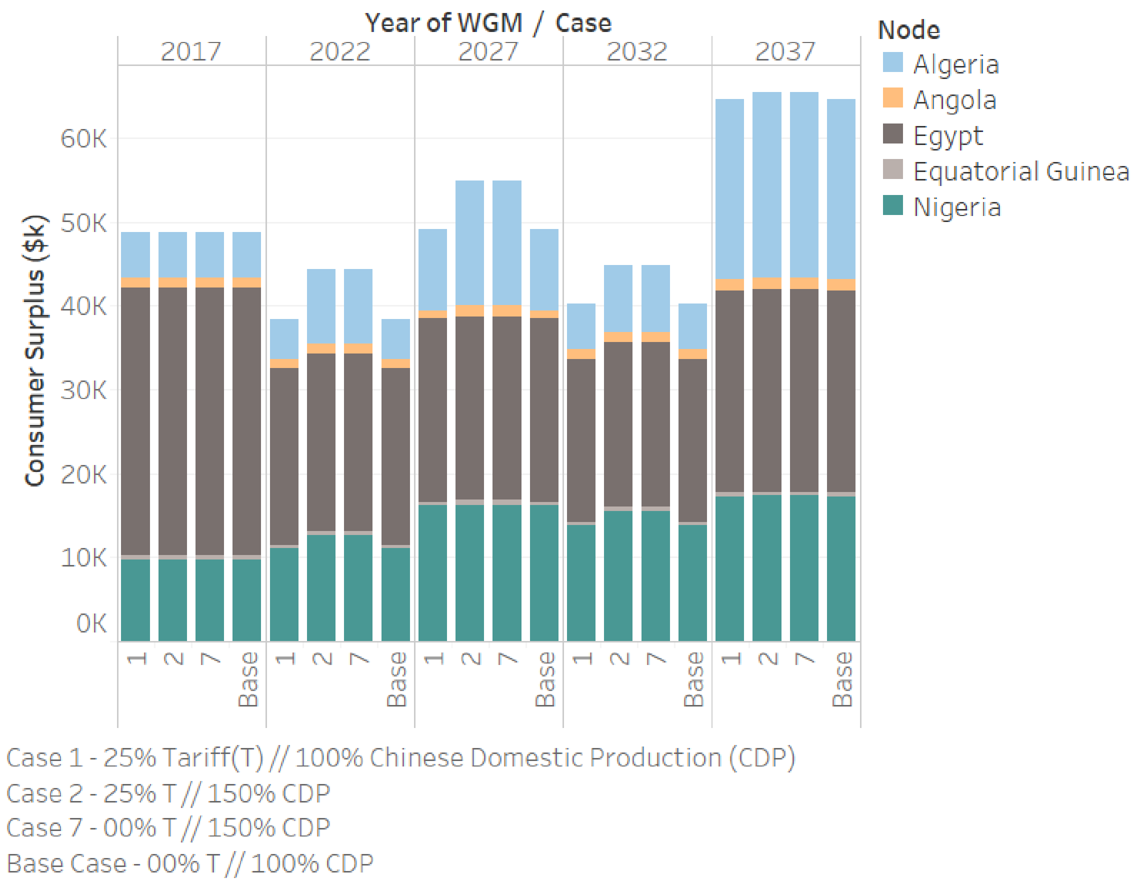

Figure B.4: WGM Consumer Surplus - Africa

Appendix C: Sets

Table C.1: WGM Variable Sets

Set	**Definition**
$\alpha \in A$	Pipeline Arcs i to j (e.g., capacity)
$c \in C$	LNG carrier shipping sizes (e.g., s_ship, m_ship, l_ship)
$d \in D$	demand seasons (e.g., low, high)
$j \in J$	LNG shipping route (e.g., Scanal,Pcanal,Nocanal)
$l \in L$	liquefier (liquefaction nodes)
$m \in M$	year
$n \in N$	model node
$p \in P$	producer
$r \in R$	regasifier (regasification nodes)
$s \in S$	storage facility (storage operators)
$t \in T$	traders

Appendix D: Variables

Table D.1: WGM Variables

Variable	Remark
CanalDist	distance from start to end of Panama Canal
$C^{B}_{cm}(\cdot)$	shipping (LNG) cost function
$C^{canal}_{dm}(\cdot)$	canal operating cost function
$C^{P\_canal}_{jdm}$	Panama Canal operating cost function
$C^{S\_canal}_{jdm}$	Suez Canal operating cost function
$C^{L}_{lm}(\cdot)$	liquefaction cost function
$C^{P}_{pm}(\cdot)$	production cost function
$C^{R}_{rm}(\cdot)$	regasification cost function
$\overline{CAP}^{A}_{am}$	arc (i.e., pipe) capacity (mcm/d)
$\overline{CAP}^{B}_{cm}$	LNG shipping capacity (mcm/d)
CAP^{B}_{c}	LNG shipping capacity (mcm/d)
$\overline{CAP}^{CJ}_{jm}$	canal capacity (mcm/d)
$\overline{CAP}^{L}_{lm}$	liquefaction capacity (mcm/d)

Continued on next page

Table D.1 – continued from previous page

Variable	Definition
CAP^{P_canal}	Panama Canal Capacity after converted to mcm/d
$ShipCAP_c^C$	Individual ship of size c capacity mcm LNG
$\overline{CAP}_{lm}^R$	Maximum regasification capacity (mcm/d)
CAP_r^R	Regasification Capacity
CAP^{S_canal}	Suez Canal Capacity after converted to mcm/d
$\overline{CAP}_{sm}^{SI}$ $\overline{CAP}_{sm}^{SX}$	Maximum storage injection capacity (mcm/d) Maximum storage extraction capacity (mcm/d)
$LNGDEST_{rldm}^R$	LNG shipment under contract from node l to node r (mcm/d)
$days_d$	number of days in a season
$Dist_{rlj}$	distance from r to l through route j in units of 1,000 nautical miles
$FLOW_{tadm}^T$	arc flow by a trader (mcm/d)
INJ_{tndm}^T	Storage injection flow by a trader (mcm/d)
INT_{ndm}^W	intercept of inverse demand curve (mcm/d)
$LNGFLOW_{crljdm}^B$	LNG transported from node l to node r through route j (mcm/d)
$loss_a$	loss rate of gas in the transport arc, $l_a \in [0, 1)$
$loss_l$	loss rate of liquefaction process $l_l \in [0, 1)$
	Continued on next page

Table D.1 – continued from previous page

Variable	Definition
$loss_s$	loss rate of gas storage injection, $l_s \in [0, 1)$
$loss_r$	loss rate of regasification process $l_r \in [0, 1)$
$loss_{lrj}$	loss rate of LNG transportation via LNGarc j from l to r
$\overline{PP^P_{pm}}$	Maximum daily production capacity (mcm/d)
$\overline{PH^P_p}$	Maxmimum total producible reserves in the time horizon (mcm)
$PURCH^{L\leftarrow P}_{ldm}$	Quantity bought from a producer by a liquefier (mcm/d)
$PURCH^{T\leftarrow P}_{tndm}$	quantity bought from a producer by a trader (mcm/d)
$PURCH^{T\leftarrow R}_{tdm}$	quantity bought from a regasifier by a trader (mcm/d)
$SALES^A_{adm}$	quantity transported via arc a (mcm/d)
$SALES^B_{crljdm}$	LNG transported from liquefier l to node r through route j by LNG shipper c (mcm/d)
$SALES^{canal\rightarrow B}_{dm}$	quantity of LNG transported through $\_canal$ by Canal Operators (mcm/d)
$SALES^{P\_canal\rightarrow B}_{dm}$	quantity of LNG transported through Panama Canal by LNG transporters (mcm/d)
$SALES^{S\_canal\rightarrow B}_{dm}$	Suez Canal capacity assigned for use by LNG transporters (mcm/d)

Continued on next page

Table D.1 – continued from previous page

Variable	Definition
$SALES^{L}_{ldm}$	quantity sold to regasifiers by a liquefier (mcm/d)
$SALES^{P}_{pdm}$	quantity sold by a producer to traders and liquefiers (mcm/d)
$SALES^{R\to M}_{rdm}$	quantity sold to Markets by regasifiers (mcm/d)
$SALES^{R\to T}_{rdm}$	quantity sold to traders by regasifiers (mcm/d)
$SALES^{SI}_{sdm}$	storage injection quantity performed by traders (mcm/d)
$SALES^{SX}_{sdm}$	storage extraction quantity performed by traders (mcm/d)
$SALES^{T}_{tndm}$	quantity sold to end-user markets by traders (mcm/d)
SLP^{W}_{ndm}	slope of the inverse demand curve (mcm/d/k$)
$\overline{WG}^{S}_{sm}$	Maximum storage working gas capacity (mcm/d)
XTR^{T}_{tndm}	quantity extracted from storage by a trader (mcm/d)
$\triangle^{A}_{am}$	arc capacity expansion (mcm/d)
$\triangle^{A}_{am'}$	future arc capacity expansion (mcm/d)
$\overline{\triangle}^{A}_{am}$	upper bound of arc capacity expansion (mcm/d)
$\triangle^{SI}_{snm}$	storage injection capacity expansion (mcm/d)
$\triangle^{SI}_{sm'}$	future storage injection capacity expansion (mcm/d)
$\overline{\triangle}^{SI}_{sm}$	upper bound of injection capacity expansion (mcm/d)

Continued on next page

Table D.1 – continued from previous page

Variable	Definition
$\triangle^{SX}_{snm}$	storage extraction capacity expansion (mcm/d)
$\triangle^{SX}_{sm'}$	future storage extraction capacity expansion (mcm/d)
$\overline{\triangle}^{SX}_{sm}$	upper bound of extraction capacity expansion (mcm/d)
$\triangle^{SW}_{snm}$	storage working gas capacity expansion (mcm/d)
$\triangle^{SW}_{sm'}$	future storage working gas capacity expansion (mcm/d)
$\overline{\triangle}^{SW}_{sm}$	upper bound of working gas capacity expansion (mcm/d)
$\triangle^{R}_{rm}$	regasification capacity expansion (mcm/d)
$\triangle^{R}_{rm'}$	future regasification capacity expansion (mcm/d)
$\overline{\triangle}^{R}_{rm}$	upper bound of regasification capacity expansion costs (mcm/d)
$\triangle^{L}_{lm}$	liquefaction capacity expansion (mcm/d)
$\triangle^{L}_{lm'}$	future liquefaction capacity expansion (mcm/d)
$\overline{\triangle}^{L}_{lm}$	upper bound of liquefaction capacity expansion costs (mcm/d)
$\triangle^{P}_{pm}$	production capacity expansion (mcm/d)
$\overline{\triangle}^{P}_{pm}$	upper bound of production capacity expansion (mcm)
$\triangle^{B}_{cm}$	LNG transportation capacity expansion (mcm/d)
$\triangle^{B}_{cm'}$	future LNG transportation capacity expansion (mcm/d)

Continued on next page

Table D.1 – continued from previous page

Variable	Definition
$\overline{\triangle}^{B}_{cm}$	upper bound of LNG shipping capacity expansion (mcm)
α^{A}_{adm}	dual variable of arc capacity constraints
$\alpha^{A}_{adm'}$	future dual variable of arc capacity constraints
α^{B}_{cdm}	dual variable of LNG shipping capacity restrictions
α^{canal}_{dm}	dual variable of canal capacity constraints
$\alpha^{P\_canal}_{jdm}$	dual variable of Panama Canal capacity constraints
$\alpha^{S\_canal}_{jdm}$	dual variable of Suez Canal capacity constraints
α^{cost}_{pm}	linear term in production cost function
α^{L}_{ldm}	dual variable of liquefaction capacity restrictions
α^{P}_{pm}	dual variable of production capacity restrictions
α^{R}_{rdm}	dual variable of regasification capacity restrictions
α^{SI}_{sdm}	dual variable of storage injection capacity constraints
$\alpha^{SX}_{sdm'}$	dual variable of storage extraction capacity constraints
α^{SX}_{sdm}	dual variable of storage extraction capacity constraints
α^{SW}_{sm}	dual variable of working gas capacity constraints
$\alpha^{SW}_{sdm'}$	dual variable of future working gas capacity constraints
$\alpha^{+}(n)$	gas transportation sent to node n
$\alpha^{-}(n)$	gas transportation sent from node n
	Continued on next page

Table D.1 – continued from previous page

Variable	Definition
b^{A}_{cm}	LNG shipping capacity expansion costs (k$/mcm)
b^{B}_{am}	arc capacity expansion costs (k$/mcm)
b^{L}_{lm}	LNG shipping capacity expansion costs (k$/mcm)
b^{P}_{pm}	production capacity expansion costs (k$/mcm)
b^{R}_{rm}	regasification capacity expansion costs (k$/mcm)
b^{SI}_{sm}	storage injection capacity expansion costs (k$/mcm)
b^{SX}_{sm}	storage extraction capacity expansion costs (k$/mcm)
b^{SW}_{sm}	storage working gas capacity expansion costs (k$/mcm)
$\beta^{B}_{c\in\{c_{large}\}rldm}$	dual variables of size limitation of large-size LNG tankers
β^{cost}_{pm}	quadratic cost term in production cost function
β^{PH}_{p}	dual variable of production capacity over time horizon
γ_m	discount rate for year$m$, $\gamma_m \in (0,1]$
δ^{C}_{tn}	level of market power exerted by a trader in a market, $\delta^{C}_{tn} \in [0,1]$
ε^{R}_{rldm}	dual variable for LNG contract constraints
$\pi^{L}_{n(l)dm}$	market-clearing price for LNG trade ($/kcm)
$\pi^{P}_{n(p)dm}$	market-clearing price between gas producers and traders

Continued on next page

Table D.1 – continued from previous page

Variable	Definition
$\pi^{R}_{n(r)dm}$	market-clearing price between regasification and traders ($/kcm)
π^{W}_{ndm}	wholesale prices ($/kcm)
φ^{S}_{tndm}	dual variable of storage balance constraints
φ^{T}_{tndm}	dual variable of mass balance constraints
ϕ^{L}_{ldm}	dual variable of LNG sale by liquefiers
ϕ^{R}_{rdm}	dueal variable of LNG sale by regasifiers -
ρ^{A}_{am}	dual variable of arc capacity expansion
ρ^{B}_{cm}	dual variable of LNG shipping capacity expansion
ρ^{L}_{lm}	dual variable of LNG liquefaction capacity expansion
ρ^{P}_{pm}	dual variable of production capacity expansion
ρ^{R}_{rm}	dual variable of regasification capacity expansion
ρ^{SI}_{m}	dual variable of storage injection capacity expansion
ρ^{SX}_{m}	dual variable of storage extraction capacity expansion
ρ^{SW}_{m}	dual variable of storage working gas capacity expansion
τ^{A}_{adm}	dual prices of transportation arc (k/kcm)
$\tau^{A,reg}_{adm}$	regulated fee for arc usage (k$/mcm)
τ^{B}_{rljdm}	dual variable of LNG transportation cost
$\tau^{Pcanal_{con}}_{dm}$	congestion fees for Panama Canal usage
	Continued on next page

Table D.1 – continued from previous page

Variable	Definition
$\tau_{jdm}^{P_{canal}toll}$	canal fees for Panama Canal usage
$\tau_{dm}^{Scanal_{con}}$	congestion fees for Suez Canal usage
$\tau_{jdm}^{S_{canal}toll}$	canal fees for Suez Canal usage
τ_{sndm}^{SI}	dual prices of storage injection ($/kcm)
τ_{sndm}^{SX}	dual prices of storage extraction ($/kcm)
$\tau_{sdm}^{SI,reg}$	regulated fee for storage injection (k$/mcm)

Bibliography

[1] T. Alexander, J. Baihly, C. Boyer, B. Clark, G. Waters, V. Jochen, J. Le Calvez, R. Lewis, C. K. Miller, J. Thaeler, *et al.*, "Shale gas revolution", *Oilfield review*, vol. 23, no. 3, pp. 40–55, 2011.

[2] F. L. Ames, "The drive to improve performance in the federal government: A longitudinal case study of managing for results", PhD thesis, George Mason University, 2015.

[3] M. S. Bazaraa, H. D. Sherali, and C. M. Shetty, *Nonlinear programming: theory and algorithms*. John Wiley & Sons, 2013.

[4] *Bolivia, argentina plan $2 billion pipeline, gas production project*, Mar 9th, 2004. [Online]. Available: `https://www.ogj.com/exploration-development/reserves/article/17290895/bolivia-argentina-plan-2-billion-pipeline-gas-production-project`.

[5] B. Bungane, *Nigeria: Trans-saharan gas pipeline project remains a dream*, Mar. 2018. [Online]. Available: `https://www.esi-africa.com/industry-sectors/business-and-markets/nigeria-trans-saharan-gas-pipeline-project-remains-a-dream/`.

[6] N. K. Candace Dunn, "The suez canal and sumed pipeline are critical chokepoints for oil and natural gas trade", *U.S. Energy Information Administration*,

[7] L. Capuano, "International energy outlook 2018 (ieo2018)", *US Energy Information Administration (EIA): Washington, DC, USA*, vol. 2018, p. 21, 2018.

[8] J. Chen, "Shale gas exploration and development progress in china and the way forward", in *IOP Conference Series: Earth and Environmental Science*, IOP Publishing, vol. 113, 2018.

[9] *Domestic force laydown*. [Online]. Available: `https://www.work.uscg.mil/Force_Laydown/`.

[10] E. DOWNS, "High anxiety: The trade war and china's oil and gas supply security", 2019.

[11] R. Egging, S. A. Gabriel, F. Holz, and J. Zhuang, "A complementarity model for the european natural gas market", *Energy policy*, vol. 36, no. 7, pp. 2385–2414, 2008.

[12] R. Egging, F. Holz, and S. A. Gabriel, "The world gas model: A multi-period mixed complementarity model for the global natural gas market", *Energy*, vol. 35, no. 10, pp. 4016–4029, 2010.

[13] FERC, “Current state of and issues concerning underground natural gas storage”, *Federal Energy Regulatory Commission Staff Report*, September 30, 2004.

[14] S. Flowers, “Challenges in a growing lng market”, *Wood Mackenzie*, Sep. 2019.

[15] Fluor, *Atacama natural gas pipeline*. [Online]. Available: https://www.fluor.com/projects/onshore-natural-gas-pipeline-epcm.

[16] J. Frittelli, “The coast guard’s need for experienced marine safety personnel”, Tech. Rep., 2019.

[17] I. Furtado, *Number of lng tankers passing through panama canal in 2018 up 77% on year: Canal authority*. [Online]. Available: https://www.spglobal.com/platts/en/market-insights/latest-news/natural-gas/050219-number-of-lng-tankers-passing-through-panama-canal-in-2018-up-77-on-year-canal-authority.

[18] S. A. Gabriel, A. J. Conejo, J. D. Fuller, B. F. Hobbs, and C. Ruiz, *Complementarity modeling in energy markets*. Springer Science & Business Media, 2012, vol. 180.

[19] S. A. Gabriel, S. Kiet, and J. Zhuang, “A mixed complementarity-based equilibrium model of natural gas markets”, *Operations Research*, vol. 53, no. 5, pp. 799–818, 2005.

[20] S. A. Gabriel, J. Zhuang, and S. Kiet, “A large-scale linear complementarity model of the north american natural gas market”, *Energy economics*, vol. 27, no. 4, pp. 639–665, 2005.

[21] R. E. Gamal, *Exclusive: Iraq looks to kuwait gas pipeline to pay off reparations*, Nov. 2017. [Online]. Available: %5Curl%7Bhttps://www.reuters.com/article/us-iraq-kuwait-gas-exclusive/exclusive-iraq-looks-to-kuwait-gas-pipeline-to-pay-off-reparations-idUSKBN1DM1LU%7D.

[22] *Global fossil infrastructure tracker*, Global Energy Monitor, 2020.

[23] “Global gas and lng market outlook to 2035”, McKinsey & Company, Tech. Rep., 2019. [Online]. Available: https://www.mckinsey.com/industries/oil-and-gas/our-insights/global-gas-and-lng-outlook-to-2035.

[24] R. Golombek, E. Gjelsvik, and K. E. Rosendahl, “Increased competition on the supply side of the western european natural gas market”, *The Energy Journal*, vol. 19, no. 3, 1998.

[25] R. Graphics, *U.s. lng shipments to china fall through trade war*. [Online]. Available: https://fingfx.thomsonreuters.com/gfx/editorcharts/USA-TRADE-CHINA-LNG/0H001PBVL68W/index.html.

[26] M. Hart, L. Bassett, and B. Johnson, “Do not fall for the hype on us–china natural gas trade”, *Center for American Progress, April*, vol. 18, 2018.

[27] P. Hartley, K. B. Medlock III, and J. Nesbitt, “Rice university world gas trade model”, 2004.

[28] P. Hartley and K. B. Medlock, “The baker institute world gas trade model”, 2005.

[29] H. Hecking and T. Panke, “Columbus-a global gas market model”, EWI Working Paper, Tech. Rep., 2012.

[30] F. Holz, C. Von Hirschhausen, and C. Kemfert, “A strategic model of european gas supply (gasmod)”, *Energy Economics*, vol. 30, no. 3, pp. 766–788, 2008.

[31] D. Huppmann, “Endogenous production capacity investment in natural gas market equilibrium models”, *European Journal of Operational Research*, vol. 231, no. 2, pp. 503–506, 2013.

[32] I.E.A., *Natural gas information*, Paris, 2020.

[33] ——, “World energy outlook 2019”, International Energy Agency, Paris, Tech. Rep., 2019. [Online]. Available: `https://www.iea.org/reports/world-energy-outlook-2019`.

[34] IGU, *Wholesale gas price survery 2018 edition*, 2018.

[35] I. IGU, “World lng report”, *International Gas Union (IGU), Barcelona, Spain*, 2017.

[36] “Inventory of us greenhouse gas emissions and sinks: 1990–2017”, US Environmental Protection Agency, Tech. Rep., 2019.

[37] W. Jiang, “China’s global quest for energy security”, *Canadian Foreign Policy Journal*, vol. 13, no. 2, pp. 105–131, 2006.

[38] W. Lise and B. F. Hobbs, “Future evolution of the liberalised european gas market: Simulation results with a dynamic model”, *Energy*, vol. 33, no. 7, pp. 989–1004, 2008.

[39] A. Losz, “Recent trends in lng liquefaction costs and shipping”, *Columbia Center on Global Energy Policy*, 2018.

[40] C. M. Macal and M. J. North, “Tutorial on agent-based modeling and simulation”, in *Proceedings of the Winter Simulation Conference, 2005.*, IEEE, 2005, 14–pp.

[41] R. Mammadov, “Russia continues to grapple with multiple pipeline-to-china challenges”, *Eurasia Daily Monitor*, vol. 16, 141 2019.

[42] *Marketbuilder*, https://www.deloitte.com/us/en/pages/energy-and-resources/solutions/mark point.html, Deloitte.

[43] E. J. Moniz, H. D. Jacoby, A. J. Meggs, R. Armtrong, D. Cohn, S. Connors, J. Deutch, Q. Ejaz, J. Hezir, and G. Kaufman, “The future of natural gas”, *Cambridge, MA: Massachusetts Institute of Technology*, 2011.

[44] S. Moryadee, “One-and-two-level natural gas equilibrium models and algorithms”, PhD thesis, University of Maryland, 2015.

[45] D. M. Nesbitt, “The economic foundation of generalized equilibrium modeling”, *Operations Research*, vol. 32, no. 6, pp. 1240–1267, 1984.

[46] W. M. News, *Four lng carriers transit panama canal in one day*. [Online]. Available: https://worldmaritimenews.com/archives/261678/four-lng-carriers-transit-panama-canal-in-one-day/.

[47] PDVSA, *Transportation, distribution and commercialization of gas*. [Online]. Available: http://www.pdvsa.com/index.php?option=com_content&view=article&id=6549&Itemid=1178&lang=en.

[48] B. Petroleum, "Bp statistical review of world energy report", *BP: London, UK*, 2019.

[49] A. Pipeline, *Alliance pipeline*. [Online]. Available: https://www.alliancepipeline.com/Pages/default.aspx.

[50] G. plc., *Dolphin gas project, ras laffan*. [Online]. Available: https://www.hydrocarbons-technology.com/projects/dolphin-gas/.

[51] ——, *Turkmenistan-afghanistan-pakistan-india (tapi) gas pipeline project*. [Online]. Available: https://www.hydrocarbons-technology.com/projects/turkmenistan-afghanistan-pakistan-india-tapi-gas-pipeline-project/.

[52] Reuters, *Bolivias ypfb cleared by brazil to use gasbol pipeline independently*, Jan. 2020. [Online]. Available: https://www.reuters.com/article/brazil-gas-ypfb-idAFL8N29F4SS.

[53] C. Rühl, "Bp statistical review of world energy, june 2008", *London: BP*, 2008.

[54] Sea-Distances.org, *Voyage calculator*, https://sea-distances.org/.

[55] B. Songhurst, "Lng plant cost reduction 2014–18", 2018.

[56] *South midstream*, Kinder Morgan. [Online]. Available: https://www.kindermorgan.com/pages/business/gas_pipelines/south_midstream/default.aspx.

[57] TANAP, *Trans anatolian natural gas pipeline project*. [Online]. Available: https://www.tanap.com/tanap-project/why-tanap/.

[58] H. Technology, *Arab gas pipeline (agp), jordan, syria, lebanon*. [Online]. Available: https://www.hydrocarbons-technology.com/projects/arab-gas-pipeline-agp/.

[59] "Toll tariffs approved by cabinet council", Panama Canal Authority, Tech. Rep., April 1, 2016.

[60] "Tolls table", Suez Canal Authority, Tech. Rep., May 1, 2015. [Online]. Available: https://www.suezcanal.gov.eg/English/Tolls/Pages/TollsTable.aspx.

[61] U.S.E.I.A., "Natural gas information", U.S. Energy Information Administration, Washington D.C., Tech. Rep., 2020.

[62] USCG, "The president's fiscal year 2020 budget proposals for the coast guard", March 18, 2019.

[63] "Uscg projected lng inspector needs", United States Coast Guard Liquefied Gas Carrier National Center of Expertise, Tech. Rep., 2019, [Computer file].

[64] USEIA, *Annual energy outlook 2018 with projections to 2050*, 2018.

[65] ——, "Model documentation report:international natural gas model 2011", Tech. Rep., 2011.

[66] ——, "Performance profiles of major energy producers 2009", *United States Energy Information Administration*, February 25, 2011.

[67] Q. Wang, X. Chen, A. N. Jha, and H. Rogers, "Natural gas from shale formation–the evolution, evidences and challenges of shale gas revolution in united states", *Renewable and Sustainable Energy Reviews*, vol. 30, pp. 1–28, 2014.

[68] D. Welsby, "Modelling natural gas resource uncertainties and regional gas markets: A review of current models and an introduction to a new field-level gas production and trade model",

[69] D. A. Wood, "A review and outlook for the global lng trade", *Journal of Natural Gas Science and Engineering*, vol. 9, pp. 16–27, 2012.